Universidade de Aveiro
2016
Departamento de Engenharia de Materiais e Cerâmica

Tânia Sofia Oliveira Macedo

AUMENTO DA RESISTÊNCIA AO ENVELHECIMENTO DA ZrO_2 (2 MOL% Y_2O_3)

IMPROVEMENT OF AGEING RESISTANCE OF 2YSZ CERAMIC

Universidade de Aveiro Departamento de Engenharia de Materiais e Cerâmica
2016

Tânia Sofia Oliveira Macedo

AUMENTO DA RESISTÊNCIA AO ENVELHECIMENTO DA ZrO_2 (2 MOL% Y_2O_3)

IMPROVEMENT OF THE AGEING RESISTANCE OF 2YSZ CERAMIC

Dissertação apresentada à Universidade de Aveiro para cumprimento dos requisitos necessários à obtenção do grau de Mestre em Materiais e Dispositivos Biomédicos, realizada sob a orientação científica da Doutora Maria Margarida Tavares Lopes de Almeida, Professora Auxiliar do Departamento de Engenharia de Materiais e Cerâmica da Universidade de Aveiro, e dos Doutores Nuno Neves e Nuno Vitorino, supervisores da empresa INNOVNANO.

O júri

Presidente

Prof. Doutor Rui Ramos Ferreira e Silva
Professor associado no Departamento de Engenharia de Materiais de Cerâmica da Universidade de Aveiro

Doutor Duncan Paul Fagg
Equiparado a Investigador principal na Divisão de Investigação em Nanotecnologia do Centro de Tecnologia Mecânica e Automação da Universidade de Aveiro.

Prof.ª Doutora Maria Margarida Tavares Lopes de Almeida
Professora auxiliar no Departamento de Engenharia de Materiais e Cerâmica da Universidade de Aveiro

agradecimentos

Quero exprimir os meus sinceros agradecimentos a todos aqueles que contribuíram, direta ou indiretamente, para a elaboração da minha tese. O apoio e dedicação dessas pessoas constituíram de facto uma preciosa ajuda.

À empresa INNOVNANO, pela excelente oportunidade que me proporcionaram para levar a cabo este projeto e por terem posto ao meu dispor os equipamentos e materiais necessários. Agradeço ainda aos Engenheiros Cátia, Cristina e Daniel pelo seu apoio e disponibilidade ao longo destes meses.

À Professora Doutora Margarida Almeida pela orientação ativa ao longo deste percurso. Agradeço pela disponibilidade e generosidade no decurso destes meses bem como, pelo conhecimento científico, correções, sugestões e críticas relevantes fornecidas na realização deste documento.

Aos Doutores Nuno Neves e Nuno Vitorino, pelo seu acompanhamento ao longo destes meses, pela sua disponibilidade, conhecimento científico, sugestões, correções e recomendações dados durante o desenvolvimento deste trabalho.

Aos Engenheiros Nuno Silva e Alexandre Rocha pela sua enorme amizade, aconselhamento e apoio essencial.

À engenheira Ana Bastos, pela sua orientação no trabalho experimental, e pelo apoio generoso e amizade ao longo destes meses.

A toda a equipa técnica do DEMaC, pelo ensino na utilização dos equipamentos necessários e pela disponibilidade na caracterização das amostras.

Aos meus colegas do curso de mestrado que me acompanharam neste percurso, sobretudo ao meu colega de laboratório Luís Teixeira pela sua amizade, boa disposição e atenção e ainda ao Pedro Moreira pelo seu apoio e gentileza.

Ao Sérgio, pelo apoio indispensável, ouvinte atento, pela paciência no decurso deste trabalho nos bons e maus momentos.

Por último, porém não menos importante, gostaria de agradecer à minha família pelo apoio, compreensão, carinho e por me concederem a possibilidade de terminar este ciclo de estudos. Sem a sua ajuda, nada disto teria sido possível.

keywords Zirconia, 2YSZ, Low Temperature Degradation, Dopants, Mechanical Properties.

abstract

Zirconia is a widely studied ceramic and it is applied in several areas such as engineering (solid oxide fuel cells, thermal barrier coatings) and biomedicine, in areas such as orthopedic and odontology. This material can be applied with the purpose to restore a body function that was compromised by a degenerative disease (orthopedic implants), in dental area and sensors due to its excellent mechanical properties, aesthetic characteristics and biocompatibility. However, this ceramic is sensitive to ageing and has a low hardness. To overcome these limitations, samples of Yttria Stabilized Zirconia doped with different oxides were developed and the goal was to improve the ageing resistance and mechanical properties of un-doped 2 mol% Yttria Stabilized Zirconia (2YSZ).

A careful selection of the dopants and respective concentrations was performed. According to the literature, ceria (CeO_2), silica (SiO_2), alumina (Al_2O_3), lanthana (La_2O_3), ytterbia (Yb_2O_3) and manganese oxide (MnO_2) improve the ageing resistance and/or the mechanical properties of Yttria Stabilized Zirconia (YSZ). In this study, thirteen different doped 2YSZ compositions were developed. For each selected dopant, three to four compositions were performed with different dopant concentrations.

After a wet milling stage, the doped stabilized zirconia powders were obtained by spray-drying, from stabilized suspensions with a controlled nanometric particle size distribution. The obtained doped sprayed powders were characterized through several techniques, such as scanning electron microscopy (SEM), X-ray diffraction (XRD), X-ray fluorescence (XRF), density and specific surface area (SSA). Green bodies of all doped compositions were obtained by uniaxial pressing (70 MPa). High density ceramics (with relative density between 90% and approximately 99%) were achieved at low sintering temperatures (1350 °C and 1400 °C). The grain size of the sintered samples was measured by SEM images, and a dispersed microstructure with a nanometric grain size was observed for all 2YSZ doped samples. The crystallographic phases present in the doped samples were identified by XRD. In order to assess their thermal ageing resistance, the samples were subjected to a thermal treatment at low temperatures (200 °C) during a period of 36 hours.

After this treatment, the fracture toughness of the aged samples was evaluated. From all the starting samples, those with better resistance to thermal ageing and fracture toughness were afterwards selected: samples of 2YSZ doped with CeO_2 (0.50 wt%) and with SiO_2 (0.25 wt%) and La_2O_3 (1.07 wt%).

Cylindrical bodies of the selected doped 2YSZ compositions were obtained by two pressing stages - uniaxial and cold isostatic pressing - and sintered at 1350 ºC for 3 hours. The behaviour of the sintered samples was investigated in terms of hydrothermal ageing resistance, according to the specifications mentioned in ISO 13356:2008 (134 ± 2 ºC and 0.2 MPa), and mechanical properties: Vickers' hardness along with fracture toughness and flexural strength.

The amount of monoclinic zirconia, indicative of degradation, was determined by XRD after 5 hours of ageing test. Afterwards the mechanical behaviour (Vickers hardness, fracture toughness and flexural strength) of the aged samples was assessed.

The results obtained in the present study demonstrate that adequate doped 2YSZ samples, with improved hydrothermal degradation resistance (9.87 % of monoclinic zirconia for SiO_2 with La_2O_3 doped 2YSZ sample while un-doped 2YSZ presented a monoclinic phase higher than 15 %) can be obtained. The mechanical properties of the sample of 2YSZ doped with both oxides (SiO_2 and La_2O_3), before and after the hydrothermal ageing, were practically maintained (1159 vs 1141 HV (hardness), 9.68 vs 9.15 MPa.$m^{1/2}$ (fracture toughness) and 700 vs 698 MPa (flexural strength)). Nevertheless, a decrease of the mechanical properties was observed for both selected doped 2YSZ samples in relation to un-doped sample.

palavras-chave Zircónia, 2YSZ, Resistência à degradação, Dopantes, Propriedades Mecânica

resumo

A zircónia é um cerâmico amplamente estudado e aplicado em diversas áreas da engenharia (células de combustível, revestimentos de barreiras térmicas) e biomedicina, em áreas como a ortopedia e a odontologia. Este material tem sido aplicado com o propósito de restaurar funções corporais que foram comprometidas por uma doença degenerativa (implantes ortopédicos), na área dentária e em sensores, devido às suas excelentes propriedades mecânicas, características estéticas e biocompatibilidade. Atualmente, existe a necessidade de desenvolver novos dispositivos com elevadas taxas de sucesso para as aplicações médicas mencionadas. O aumento da longevidade dos dispositivos protéticos para uma população jovem, mais ativa, com maior esperança de vida, requer o desenvolvimento de novos produtos, com desempenhos e *designs* fiáveis. O uso de Yttria Tetragonal Zirconia Polycrystal (Y-TZP) abriu possibilidades para desenvolver novos e promissores implantes, com novas e mais complexas geometrias, que não eram possíveis com outros cerâmicos, como por exemplo a alumina (mais frágil). Contudo, a zircónia cerâmica apresenta algumas limitações de trabalho: é sensível ao envelhecimento e apresenta baixa dureza. Devido a estas limitações, foram desenvolvidas várias amostras de zircónia estabilizada com 2 mol% de ítria (2YSZ), dopadas com diferentes óxidos, com o objetivo de avaliar e melhorar a resistência ao envelhecimento e propriedades mecânicas, quando comparadas com as amostras não dopadas.

Para este efeito, foi realizada uma seleção criteriosa dos dopantes e respetivas concentrações. De acordo com a literatura, a céria (CeO_2), sílica (SiO_2), alumina (Al_2O_3), lantana (La_2O_3), íterbia (Yb_2O_3) e óxido de manganês (MnO_2) melhoram a resistência ao envelhecimento e/ou as propriedades mecânicas da zircónia estabilizada com ítria (YSZ).Neste estudo, foram desenvolvidas treze diferentes composições dopadas, de zircónia estabilizada com 2 mol% de ítria (2YSZ). Por cada dopante selecionado foram preparadas três a quatro composições.

Após uma etapa de moagem, os pós dopados de zircónia foram obtidos por atomização, a partir de suspensões estabilizadas, com uma distribuição de tamanho de partícula nanométrico controlado. Os pós atomizados foram caracterizados recorrendo a várias técnicas tais como microscopia eletrónica de varrimento (SEM), difração de raios-X (DRX), fluorescência de raios-X (FRX), densidade real, e área superficial específica (SSA).

Os corpos em verde de todas as composições foram obtidos por prensagem uniaxial (70 MPa). Foram obtidos corpos cerâmicos com densidade elevada (com densidade relativa entre 90% e aproximadamente 99%) a uma temperatura de sinterização relativamente baixa (1350 ºC e 1400 ºC).

O tamanho de grão das amostras sinterizadas foi medido através de imagens SEM, sendo verificado em todas as amostras de 2YSZ dopadas, uma microestrutura dispersa, com um tamanho de grão nanométrico.

As fases cristalográficas presentes nas amostras dopadas foram identificadas por DRX.

A fim de avaliar a resistência ao envelhecimento, as amostras sinterizadas foram submetidas a um tratamento térmico a baixas temperaturas (200 ºC) durante um período de 36 horas. Após este tratamento foi avaliada a tenacidade à fratura das amostras envelhecidas.

Com base nestes resultados selecionaram-se as amostras que apresentavam melhor resistência ao envelhecimento térmico e tenacidade à fratura: 2YSZ dopada com CeO_2 (0.50 wt%) e SiO_2 (0.25 wt%) com La_2O_3 (1.07 wt%).

Os pós das composições selecionadas foram sujeitos a prensagem uniaxial seguida de prensagem isostática a frio e sinterizadas a 1350 ºC durante 3 horas. Após sinterização, o comportamento destas amostras foi investigado em termos de resistência ao envelhecimento hidrotérmico e propriedades mecânicas: dureza de Vickers, tenacidade à fratura e resistência à flexão.

Os testes de envelhecimento hidrotérmico foram realizados de acordo com as especificações mencionadas na norma ISO 13356:2008 (134 ± 2 ºC e 0.2 MPa). A percentagem de zircónia monoclínica, indicador de degradação, foi determinada por difração de raios-X após 5 horas de teste de envelhecimento hidrotérmico. Posteriormente, avaliou-se o comportamento mecânico (dureza de Vickers, a tenacidade à fratura e resistência à flexão) das amostras envelhecidas.

O presente estudo demonstra que podem ser obtidas amostras cerâmicas de 2YSZ dopadas adequadas, com resistência à degradação hidrotérmico melhoradas (9.87 % de zircónia monoclínica para a amostra de 2YSZ dopada com SiO_2 e La_2O_3, enquanto que a amostra de zircónia não dopada apresenta uma percentagem de fase monoclínica superior a 15 %). As propriedades mecânicas da amostra dopada com ambos os óxidos (SiO_2 e La_2O_3), antes e após o envelhecimento hidrotérmico, foram praticamente mantidas (1159 vs 1141 HV (dureza), 9.68 vs 9.15 MPa.$m^{1/2}$ (tenacidade à fratura) e 700 vs 698 MPa (resistência à flexão)). Porém, uma diminuição das propriedades mecânicas foi observada para ambas as amostras dopadas de 2YSZ selecionadas em relação à amostra de zircónia não dopada.

Index

List of Figures

List of Tables

List of Abreviations

YSZ – Yttria Stabilized Zirconia

Y-TZP – Yttria Tetragonal Zirconia Polycrystal

Y-STZ – Yttria Stabilized Tetragonal Zirconia

SZ – Stabilized Zirconia

2YSZ – 2 mol% Yttria Stabilized Zirconia

3YSZ – 3 mol% Yttria Stabilized Zirconia

LTD – Low Temperature Degradation

XRD – X-ray Diffraction

XRF – X-ray Fluorescence

SEM – Scanning Electron Microscopy

HIP – Hot Isostatic Pressing

CIP – Cold Isostatic Pressing

UP – Uniaxial Pressing

MAJ- Mehl-Avrami-Johnson (law)

rpm – rotations per minute

Chapter 1

Introduction and Objectives

1. Introduction

Zirconia has been widely studied and applied in diverse fields such as engineering (solid oxide fuel cells and thermal barrier coating), medicine and dentistry. Due to its outstanding mechanical properties, esthetical characteristics and biocompatibility, this ceramic material has been getting the attention of the scientific community.

Crystalline dioxide of zirconium is well known as bioinert and inorganic oxide. This oxide exhibits good chemical stability, toughness, mechanical strength, Young's Modulus value similar to stainless steel alloys and long term biocompatibility, turning this ceramic into an excellent candidate to be used in a wide range of applications [1], [2]. According to its properties, zirconia becomes very attractive to the world of biomaterials, especially, to restore a body function that was compromised by a degenerative disease (orthopedic joints), in dental care and sensors.

In the 1980's, zirconia femoral heads were introduced to overcome the brittleness of alumina and the consequent potential failure of implants [3], [4]. The alumina devices presented a high fracture rate due to slow crack growth that led to failure [2]. Nevertheless, some efforts were taken in order to densify alumina, namely, using high purity raw powders with a narrow size distribution and the application of different sintering methods (hot isostatic pressing (HIP), for example) [5]. However, these alumina devices still presented brittleness and became unreliable for these medical applications. To overcome such brittleness and increase the reliability of these implants, zirconia ceramics were introduced. The first paper concerning the use of zirconia ball head for arthroplasty was published in 1988 [1]. Later, in 1989, the *Food and Drug Administration* approved the use of zirconia ball head for arthroplasty.

During the last 20 years, more than six hundred thousand zirconia femoral head implants have been implemented worldwide, predominantly in the US and in Europe [4], [5]. Biomedical grade zirconia exhibits the best mechanical properties of oxide ceramics, significantly better than the mechanical properties presented by alumina. Indeed, the fracture toughness of zirconia is practically the double that of alumina (6-8 $MPa \cdot m^{1/2}$ versus 3-4 $MPa \cdot m^{1/2}$) and the strength can achieve values around 2 GPa for a fine grain grade of zirconia [3]. These exceptional properties are related with the phase transformation toughening mechanism presented by zirconia, which highly increases its fracture toughness and strength, leading to an increase in the crack propagation resistance [1], [4], [6]. This mechanism consists in a stress induced phase transformation, where the metastable tetragonal grains are converted into monoclinic phase at the crack tip, which is

accompanied by volume expansion induced by compressive stress [4]. Nonetheless, due to this transformability, zirconia tetragonal grains can be very unstable and extensive transformation into the monoclinic phase can cause degradation of this ceramic. In order to maintain the tetragonal phase of zirconia, some suitable stabilizers, like yttrium oxide (Y_2O_3) are commonly added to this oxide. Frequently, biomedical grade zirconia (orthopedics and dental) contain, normally, 3 mol% of yttria.

Nevertheless, Yttria Stabilized Zirconia (YSZ) ceramics undergo Low Temperature Degradation (LDT) [7]. This effect causes serious limitation in stabilized zirconia, since it causes the formation of micro-cracking and loss of strength in presence of a moist environment, which occurs from room temperature up to 400 ºC [7], [8], [9]. There is a relevant concern in relation to degradation when devices are used in a moisture atmosphere, such as at body temperature and when they are autoclaved for sterilization. In 2001, *Food and Drug Administration* (FDA, USA) announced the recall of a series of Yttria - Stabilized Tetragonal Zirconia Polycrystal (Y-TZP) hip prostheses due to a fracture of zirconia femoral heads. The Saint Gobain Desmarquest, a major manufacturer of the zirconia implants, stopped with Prozyr®(femoral heads implants of zirconia) activities and requested a worldwide recall of some batches, because of their higher fracture rates *in vivo*, caused by their degradability [4], [7]. The cause of the fractures was due to the tetragonal to monoclinic phase transition detected on the surface of these implants. A cascade of implications, namely, micro-cracking, nucleation and growth, occurred in the low density parts originated by the presence of monoclinic phase of the zirconia. This monoclinic phase presents a lower value of density than tetragonal phase and is more susceptible to ageing, under exposure to physiological moisture environment and cycling loading [7], [10].

On the same year that zirconia was applied in orthopedics the dental community discovered the use of zirconia [3]. Since its introduction in the dental field, zirconia has been widely used to produce fixed partial dentures (FPDs), implant abutments and zirconia restorations (Figure 1). Moreover, zirconia can be processed, with precision, to complex geometries using CAD/CAM techniques. Zirconia properties are highly suitable for applications in the dental field because they exhibit excellent mechanical properties, natural tooth appearance, insolubility in water environment, no cytotoxicity, reduction of bacterial adhesion and low corrosion potential [11]. The tetragonal zirconia ceramic, when stabilized with yttria, achieves excellent mechanical and esthetical properties(colour, translucency) [3]. There is some evidence, in dental clinical practice, of two main problems which are chipping of porcelain veneering in single crowns and FDPs, and fracture of zirconia abutments. In particular, chipping of veneering has been appointed as the most common

problem of zirconia restorations [11]. However, the consequences of failure of a dental implant or dental restoration device are less problematic than that of an orthopedic implant.

Figure 1. Representation of an example of a zirconia dental bridge. Adapted from [12].

Although the success of zirconia's usage, due to enhanced strength implants, biocompatibility and its diverse applications, there are still problems to be solved such as the risk of degradation, low hardness and problems with manufacturing mechanisms.

The retention of tetragonal zirconia phase is crucial to obtain excellent mechanical properties and increase the ageing resistance, making zirconia a stable material that presents good properties. Zirconia stabilized with 2 mol% of yttria is more unstable compared to 3 mol% of Yttria Stabilized Zirconia (3YSZ), resulting in a stronger degradation of such ceramics [6], [7]. Although 2 mol% Yttria Stabilized Zirconia (2YSZ) exhibits excellent mechanical properties (strength and fracture toughness), it presents a higher degradation due to the spontaneous transformability of the zirconia phases (tetragonal to monoclinic phase). However, this problematic situation can be overcome by the addition of other stabilizers and dopants, such as CeO_2, CaO or MgO, as has been widely investigated [8]. These stabilizers and dopants will enhance the stability of the tetragonal phase, mechanical properties, and therefore, improve the stability of zirconia, resulting in an increase of the ageing resistance. Nevertheless, the ability to adjust the microstructure of this ceramic is crucial to achieve the requirements of biomedical devices (in order to produce very effective arthroprosthetic devices, with higher success rates that make their use adequate especially to younger population and more active patients) as well as in dental implants (to achieve reliable dental restorations).

1.1. Objectives

The main objective of the present study is to develop 2 mol% Yttria Stabilized Zirconia (2YSZ), provided by INNOVNANO, doped with different elements (and different percentages of each element) with improved thermal and hydrothermal ageing resistance and mechanical properties.

The2YSZ powders were doped with different types of oxides and different amounts of each oxide. Through the literature it was verified that ceria (CeO_2), silica (SiO_2), alumina (Al_2O_3), lanthana (La_2O_3), ytterbia (Yb_2O_3) and manganese oxide (MnO_2) present improvements in the ageing resistance and/or of mechanical properties of zirconia ceramics.

The various compositions of doped 2YSZ were defined on the basis of the results presented by several authors [45]-[59], [64].

Three different compositions of 2YSZ doped with ceria were defined:

- 2 mol% Yttria Stabilized Zirconia and 0.25 wt% of CeO_2
- 2 mol% Yttria Stabilized Zirconia and 0.5 wt% of CeO_2
- 2 mol% Yttria Stabilized Zirconia and 0.75 wt% of CeO_2

Concerning the 2YSZ compositions doped with silica were produced by adding another dopants, alumina and lanthana. Three different compositions were produced:

- 2 mol% Yttria Stabilized Zirconia and 0.25 wt% of SiO_2;
- 2 mol% Yttria Stabilized Zirconia, 0.25 wt% of SiO_2 and 0.25 wt% Al_2O_3;
- 2 mol% Yttria Stabilized Zirconia, 0.25 wt% of SiO_2 and 1.07 wt% La_2O_3.

Also, three compositions of 2YSZ doped with different concentrations of ytterbia were produced:

- 2 mol% Yttria Stabilized Zirconia and 13.12 wt% of Yb_2O_3;
- 2 mol% Yttria Stabilized Zirconia and 19.68 wt% of Yb_2O_3;
- 2 mol% Yttria Stabilized Zirconia and 26.24 wt% of Yb_2O_3.

Furthermore, four compositions of 2YSZ doped with manganese oxide were produced:

- 2 mol% Yttria Stabilized Zirconia and 0.025 wt% of MnO_2;
- 2 mol% Yttria Stabilized Zirconia and 0.05 wt% of MnO_2;
- 2 mol% Yttria Stabilized Zirconia and 0.25 wt% of MnO_2;
- 2 mol% Yttria Stabilized Zirconia and 0.75 wt% of MnO_2.

The characteristics of the obtained samples were analysed based on the ISO standard 13356:2008: *Implants for surgery – ceramic materials based on yttria-stabilized tetragonal zirconia (Y-TZP)* [13]. In order to evaluate the effect of the selected dopants on the resistance to degradation of the 2YSZ, the samples were submitted to thermal ageing tests. Thereafter, mechanical tests, namely fracture toughness, of the aged samples was measured. According to the obtained outcomes of thermal ageing resistance and fracture toughness tests, the doped 2YSZ samples with better properties were selected. In order to fully characterize these selected samples, hydrothermal ageing tests and mechanical tests (hardness, fracture toughness and flexural strength), before and after degradation tests, were performed.

1.2. Document Structure

This document is structured in five chapters. The first chapter synthesizes the current situation of the research theme and its interest, as well as the objectives of this project. The second chapter approaches the literature review about zirconia, in order to understand its properties and applications, and the dopants currently added to this oxide. In the third chapter, the experimental procedure describing all the characterization techniques and tests performed in this study are mentioned. The fourth chapter presents the experimental results and their analysis. Lastly, in the fifth chapter, the main conclusions are presented alongside with the plan for future developments and suggestions.

Chapter 2

Literature Review

2. Literature Review

2.1. Properties of Zirconia

Zirconia does not exist in nature in a pure state, but can be found as a free oxide (ZrO_2) with the mineral Baddeleyite [1], [8], [14]. This oxide presents an approximate density of 5.7 g/cm^3. This ceramic is a polymorphic material with three crystallographic forms: monoclinic, tetragonal and cubic. The monoclinic phase is the most stable form of zirconia and it is stable from room temperatures up to 1170 ºC. The tetragonal form is stable at temperatures of 1170-2370 ºC. The cubic form is stable at temperatures over 2370 ºC [1], [8], [14].

This ceramic exhibits notable changes in volume during the phase transformation, i.e., the tetragonal to monoclinic phase transformation [1], [14]. During cooling, the stress induced phase transformation at room temperature, ahead with a propagation crack, results in a 3-5 % volume expansion and approximately 7 % shear strain. On the contrary, upon heating, a decrease of 5 % in volume occurs (Figure 2) [1], [3], [7], [14]. These values may vary depending on grain size and concentration of stabilizer, as it will be demonstrated throughout this document.

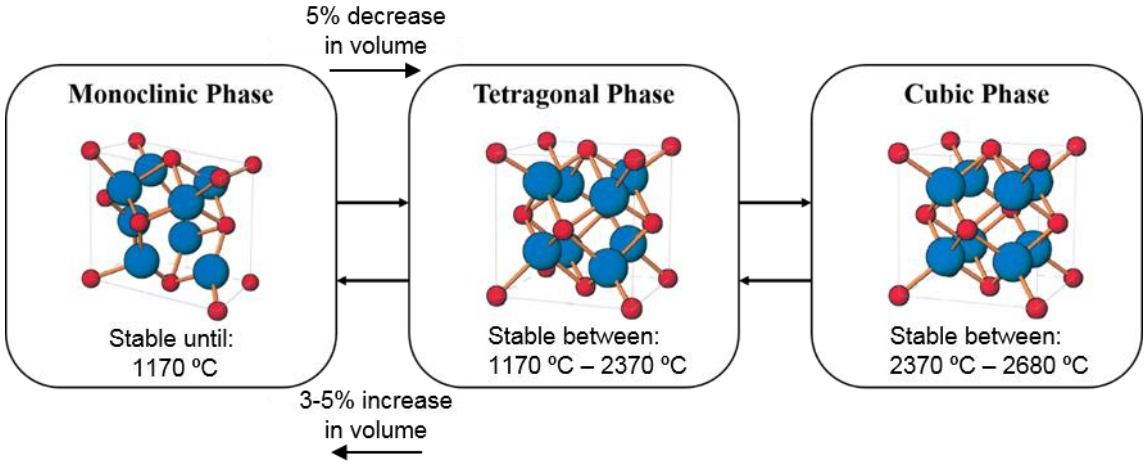

Figure 2. Temperature phase transformation of zirconia. Adapted from [14], [15].

The tetragonal to monoclinic transformation was identified in 1975, and it brought emerging knowledge for new applications of zirconia. Indeed, this phase transformation is a mechanism of transformation of the toughening of the ceramic material [8]. Furthermore, the mechanism of stress induced phase transformation which involves the transformation of metastable tetragonal grains to the monoclinic phase at the crack tip, accompanied by a volumetric expansion, induces compressive stresses [5], [7], [16]. In fact, these

compressive stresses, protect the crack tip from applied stress, enhancing the fracture toughness of zirconia [16].

This transformations of phases of zirconia is martensitic and it occurs during the sintering and for both heating and cooling [8]. It is accompanied by a shear strain and a large increase of volume, as previous mentioned, leading to occurrence of internal stresses on cooling. These developed internal stresses are so large that pure zirconia sintered above 1170 ºC disintegrates by cracking upon cooling [8]. Through this mechanism, the propagation of the fracture becomes more difficult, and toughness increase occurs in the material.

Nevertheless, it is fundamental to stabilize the tetragonal phase of zirconia, which presents higher density (around 6 g/cm^3) and better mechanical properties in relation to monoclinic zirconia [6], [14]. Zirconia in tetragonal phase presents good chemical and dimensional stability, good mechanical strength and toughness, and a Young's Modulus value similar to stainless steel alloy. This oxide exhibits resistance to traction that can be as high as 900-1200 MPa and its compression resistance is about 2000 MPa [17]. All these aspects originated an increased interest in using zirconia as a ceramic biomaterial. Table 1 shows the mechanical properties of tetragonal zirconia [1].

Table 1. Properties of tetragonal zirconia. Adapted from [1].

Property	Tetragonal Zirconia (TZP)
Young's Modulus (GPa)	210
Strength (MPa)	900-1200
Hardness (HV)	1200

The grain size and sintering process are two factors that affect zirconia's mechanical properties because higher temperatures and longer sintering time induce the formation of a larger grain size. Larger grain size makes zirconia less stable and more vulnerable to spontaneous tetragonal to monoclinic transformation than smaller grains (<1 μm). When grain size is below that of approximately 0.2 μm, the transformation is not possible, leading to a reduction in fracture toughness [11].

The zirconia phase transformation toughening mechanism begins in the presence of large tensile stresses around a crack and, as previously mentioned, a volume expansion occurs. This volume expansion of tetragonal grains can stop the crack propagation. Nevertheless, in the proximity of that crack, the grains will be destabilized, originating a transformation zone in the material [8]. A schematic representation of this phenomenon is given in Figure 3. The formation of the transformation zone in the material means that, when

volume expansion occurs, stresses are created in the surroundings of the tetragonal grains, leading them to transform too, trying to expand to the bulk of the material [8]. The tensile stresses created by this transformation may induce micro-cracking at the grain boundaries, facilitating the access to diffusion of the water species inside the bulk [7]. This transformability can cause loss of strength, low temperature degradation and consequent deterioration of the zirconia. Therefore, it is crucial to control this phenomenon of transformation, in order to obtain the improved crack resistance without losing the outstanding properties of tetragonal phase zirconia.

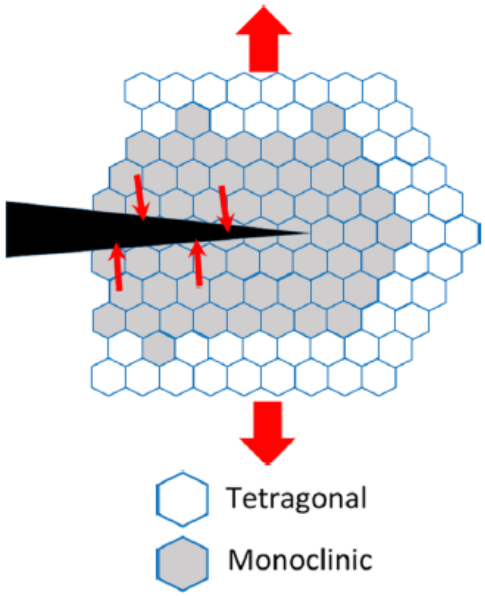

Figure 3. Schematic representation of phase transformation toughening. Adapted from [3].

The thermodynamics of the tetragonal to monoclinic transformation in this material is expressed in terms of different energy contributions to the overall energy of transformation [7]. The change of total free energy ($\Delta G_{t\text{-}m}$) per units of volume required for the transformation of zirconia can be expressed by equation (1) [7], [8]:

$$\Delta G_{t\text{-}m} = \Delta G_c + \Delta U_{SE} + \Delta U_S \quad (1)$$

where ΔG_c corresponds to the difference in the chemical free energy associated with the tetragonal to monoclinic phase transformation. This gradient is dependent on the temperature and composition, including the oxygen vacancy content. It presents negative values ($\Delta G_c<0$) for temperatures below the equilibrium temperature. The term ΔU_{SE} refers to the change in elastic strain energy associated with the transformation of particles, and it is usually a positive value. This variable is dependent on the modulus of the surrounding matrix, the size and shape of the particle and the presence of internal or external stresses. Lastly, the variable ΔU_S is the change in energy associated with the formation of new

interfaces upon the occurrence of the transformation, like micro-cracks. The value of the gradient is normally a positive value. In general, when the overall value ΔG_{t-m} is positive, the particles retention on tetragonal state is verified. On the other hand, when this value is negative, the particles are metastable and probably will be transformed into monoclinic [7], [8], [9].

In fact, by a decrease in ΔG_c and an increase in ΔU_{SE}, the addition of a stabilizer to zirconia decreases the driving force of the tetragonal to monoclinic phase transformation of zirconia. Stabilization of the tetragonal phase of zirconia is related with the elastic self-energy ΔU_{SE} (equation (1)). ΔU_{SE} is directly associated to the surrounding matrix modulus, where the high matrix modulus will increase the elastic self-energy, providing stabilization of tetragonal phase zirconia. However, ΔU_{SE} is also influenced by applied or internal stresses. These tensile stresses will act to reduce ΔU_{SE} and causing the destabilization of the tetragonal phase [7], [8], [9].

2.2. Low Temperature Degradation

Zirconia presents sensitivity to low temperature degradation making this the main concern regarding the utilization of this material.

Low Temperature Degradation (LTD) is a phenomenon that leads to ageing of zirconia and occurs in the presence of moisture [4], [7], [8]. This kinetic phenomenon consists in a slow transformation of the tetragonal to monoclinic zirconia, from room temperature to around 400 °C, through nucleation and growth processes [4], [8]. This phenomenon of degradation begins at the surface of the zirconia by a stress corrosion type mechanism that can be extended to the inner parts of this ceramic [4], [8].

Ageing of zirconia corresponds to Low Temperature Degradation, a phenomenon which is related with a spontaneous slow transformation of the crystals from the tetragonal phase to the less stable monoclinic phase, in absence of any mechanical stress [11].

An explanation of this ageing phenomenon is reported by *Schubert and Frey* [18], where the moisture species penetrate into the tetragonal lattice, leading to the formation of tensile stresses on the surface grains. This causes a destabilization of the tetragonal phase by reducing the value of the elastic self-energy of the transformation (ΔU_{SE}). Through a decrease of ΔU_{SE}, the rate of the phases transformation will increase, as previously mentioned [19]. According to *Fabris et al.* [20], these moisture species penetrate the tetragonal lattice and cause a destabilization of this lattice by eradication of the oxygen vacancies.

As it would be expected, the effects of LTD are loss of strength and micro-cracking, due to the lower density and thus lower hardness and resistance to crack formation presented by the monoclinic phase. This will lead to appearance of porosity on the surface of the material and consequently a path for the water or biologic fluids to penetrate into the material [7]. The nucleation of the transformation process leads to a cascade of events that occur neighbor to neighbor, as schematized in Figure 4.

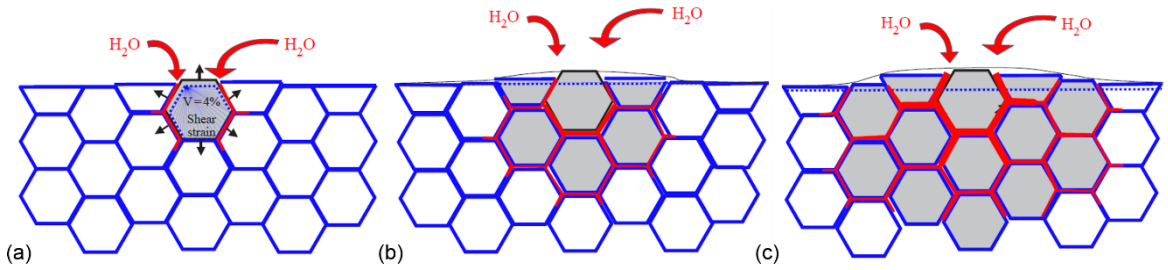

Figure 4. Schematic demonstration of the ageing process occurring in a cross section of a zirconia biomaterial. **(*a*)** Nucleation on a particular grain at the surface; **(*b*)** Growth of the transformed zone; **(*c*)** Penetration of water due to micro-cracks around the transformed grains (red path). Adapted from [4].

The diffusion of moisture species into the lattice via oxygen vacancies will cause a change of lattice parameters because this moisture species create tensile hydrostatic stress in the grains and change the oxygen configuration around the Zr^{4+} ions, leading to instability and consequent transformation. This is caused by stress accumulation and/or decrease of the difference in chemical free energy between tetragonal and monoclinic phases (ΔGc). Thus, the nucleation occurs in the most unstable grains subjected to the highest tensile stresses. This will lead to a volume increase of the grains that will induce the ocurrence of micro-cracking and will create stresses on the other grains, which will lead to a continous increase of the number of monoclinic nuclei. As a consequence, the growth of the transformed zone will lead to large micro-cracking and surface roughening, caused by volume expansion upon transformation [7]. Hence, transformation proceeds in the presence of the fluids (water or biological fluids) and stresses. The fluids will enter the lattice and will provide the prolongation of the monoclinic transformation through the bulk [4], [7], [8].

In Figure 5 a schematic representation of two alternatives ways of transformation of grains of zirconia is demonstrated. Basically, Low Temperature Degradation is an alternative to the resistance to crack propagation, caused by the stress induced transformation for the tetragonal to monoclinic transformation. On the other hand, when the transformation is initiated by a propagation crack, an improved toughening is achieved.

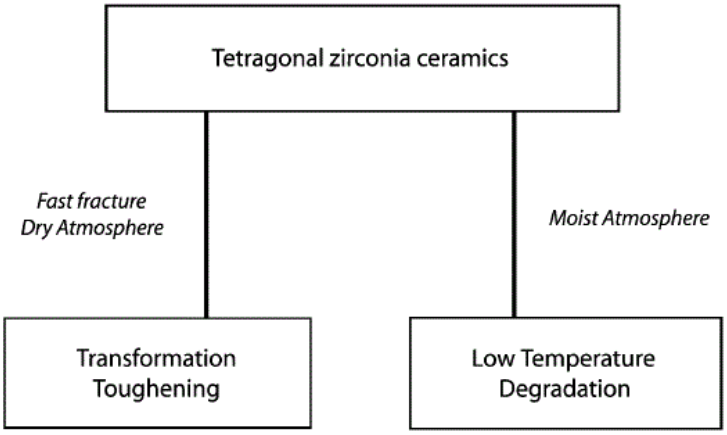

Figure 5. The scheme represents two alternative ways by which tetragonal phase can transform into monoclinic phase. In the left, the alternative corresponds to crack propagation induced transformation and the other (in the right) is intermediate temperature exposure to moisture. Adapted from [8].

The diffusion of water derived species from the surface results not only in undesirable transformations, but also on surface roughening resulting in several detrimental factors, such as micro-cracking, grain pull-out, wear debris, and loss of strength, as described on the scheme of Figure 6 [8]. The initial transformation of specific grains can be caused by several factors like their non-equilibrium state due to their size (large grains are more unstable), lower stabilizer content, a specific orientation on the surface, or the presence of residual stresses (compressive or tensile) [4], [21]. These aspects can lead to the fracture of the zirconia ceramic.

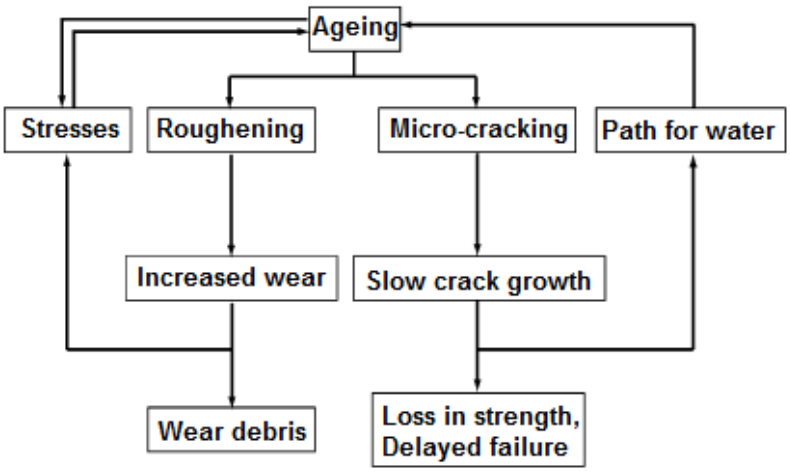

Figure 6. Potential consequences of ageing on zirconia materials. Adapted from [8].

Some cases of surface degradation (roughening and micro-cracking) caused by phase transformation were reported by *Haraguchi et al.* [4].Craters at contact regions were visible in zirconia that may correspond to monoclinic spots, but worn out, due to the large

amounts of removed grain induced by wear. Figure 7 schematically represents a scenario of surface degradation due to the combination of LTD and wear [4].

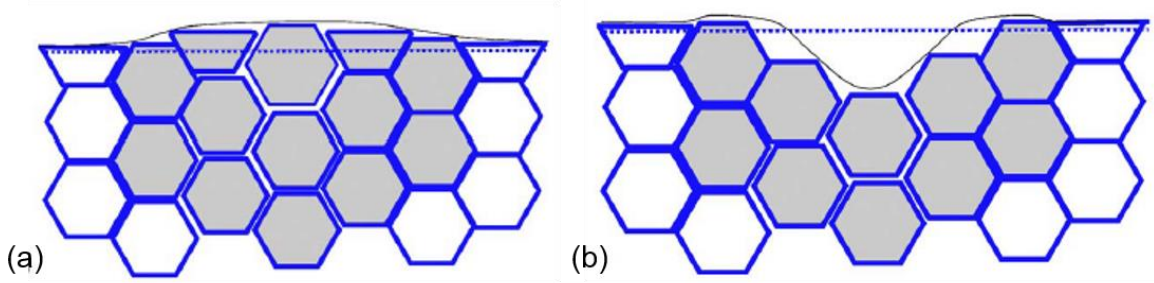

Figure 7. Illustration of the surface degradation of zirconia hip prostheses caused by the combination of ageing and wear. **(a)** Surface roughening and micro-cracking on the surface material. **(b)** Grain-out induced by wear, creating craters at the surface of the material. Adapted from [4].

In this sense, the hydrothermal degradation, an ageing phenomenon that affects the surface of zirconia ceramic when exposed to humid environments, becomes a crucial factor which affects the surface stability of zirconia. After long exposure to this environment degradation, grain boundary micro-cracks are formed and monoclinic uplifts appear on the surface producing an increase in roughness accompanied by grain pull-out, as previously mentioned. The extension of the transformed zone can be observed and eventually measured, in terms of fraction of monoclinic zirconia content from its first appearance on some isolated grains to the progression into the bulk through the sample of the first superficial layer and into the volume [7], [22]. A complete overview, from the early stages of degradation to the macroscopic consequences, is represented on Figure 8, which demonstrates the evolution of the monoclinic fraction versus time, measured by X-ray diffraction.

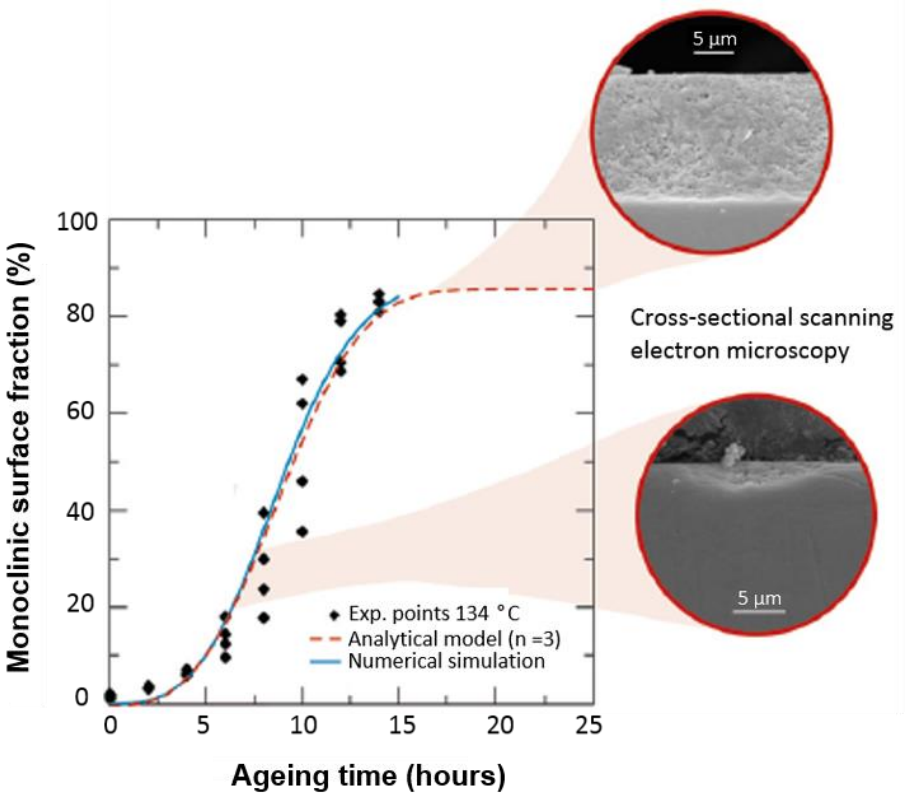

Figure 8. Representation of the evolution of the monoclinic fraction versus time measured by X-ray diffraction. The nucleation-growth process starts on the surface of the sample, in one grain and propagates to the rest of the grains. The growth into the bulk was observed by cross-sectional scanning electron microscopy. Adapted from [7].

The sterilization process on polished sections of zirconia, at 134 °C and 2 bar in autoclave, also led to the surface roughening of the material, causing grain removal induced by wear. This originated craters on the surface of the material such as the presented in Figure 9, which are related with the monoclinic nuclei formed by ageing, that will lead to their catastrophic degradation [4].

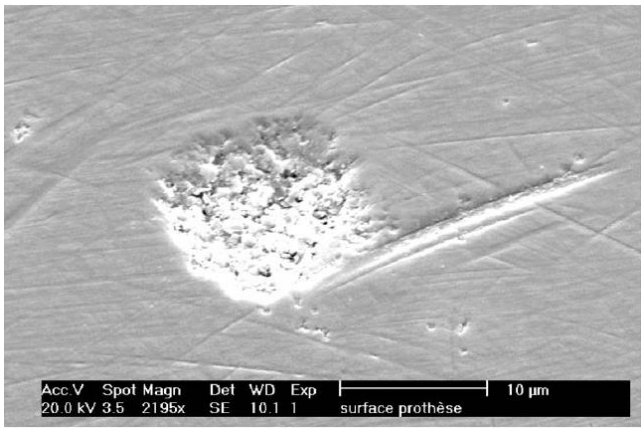

Figure 9. SEM picture of retrieved zirconia head for total hip replacement after 4.5 years *in vitro*. A large crater on the surface of zirconia head, induced by ageing associated to wear, is clearly seen. Adapted from [4].

In order to prevent the degradation of zirconia, an International Standard that specifies the characteristics and test methods for ceramics based on Yttria Stabilized Tetragonal Zirconia (Y-STZ) was established. The second edition of this ISO standard (ISO 13356) [13] was published in 2008, which specifies the material properties, namely, bulk density, chemical composition, microstructure, mechanical properties and the ageing tests.

According with the mentioned ISO standard, the Y-STZ ceramic for implant applications must be submitted to an accelerated hydrothermal ageing test. The samples of zirconia must be placed in a suitable autoclave and exposed to steam at 134 ± 2 ºC under a pressure of 0.2 MPa during a period of time of 5 hours. This is the standard period of time for ageing evaluation required by ISO 13356:2008 and it was chosen considering that this time is correspondent to the common prosthesis lifetime of 15 to 20 years old *in vivo* [7], [23]. After the procedure of the accelerated ageing test, the monoclinic fraction of the zirconia sample must be determined by X-ray diffraction analysis, and should be equal or below 25%. Regarding the residual biaxial and bending strength of the aged samples, it should not decrease more than 20 % and must be equal or greater than 500 MPa after this test.

The surface finish of the ceramic can benefit the resistance to aging, or decrease it. When the material is exposed to a degradation environment, the grains are transformed as a function of their disequilibrium state, since all the grains remain in a similar stress state [24].

When a scratch is formed on the material's surface by machining or polishing, it leaves a homogenous stress state on the surrounding area of the scratch [21]. The area affected by these stresses will be susceptible to transformation of the grains which will lead to ageing. According to *Deville et al.* [21], rough polishing can produce a compressive surface stress layer that is beneficial for the ageing resistance. Comparatively when a smooth polishing is applied, preferential transformation nucleation around scratches is produced due to tensile residual stresses. The material polished with 6 µm finish produces compressive stresses that appear on the surface of zirconia, and this compressive stress is less favorable for transformation when compared to tensile stresses. On the other hand, a smooth finish from 1 µm to 3 µm creates an elastic/plastic zone that leads to the formation of a region for nucleation. Hence, during the ageing treatment these regions can change the stability of the zirconia ceramic [21].

The ageing resistance of zirconia can also be affected by the sintering temperature [25], [26], [27]. *Kawai et al.* [26], reported that through the increase of sintering temperature, the fraction of monoclinic phase of zirconia increases in Y-TZPs. It was observed that for a Y-TZP sintered at a temperature higher than 1400 ºC, the monoclinic zirconia content was

approximately 80 % with a penetration depth of 17.6 µm. The excessive grain growth promoted by the sintering temperature and increasing time, can reduce the protection against degradation [28], [29]. This is in agreement with Equation (1), which refers that smaller grains present higher values of ΔU_S, leading to a higher stability of the material.

In order to understand and quantify the progress of the zirconia transformation kinetics, X-ray diffraction is mostly used. Several studies have reported that LTD kinetics follow sigmoidal laws related with the nucleation-growth process [30]–[32]. The surface transformation (tetragonal to monoclinic zirconia) induced by the ageing process can be expressed according to a modified Mehl-Avrami-Johnson (MAJ) law (equation 2) [8], [31]–[34].

$$V_m = 1 - (1 - V_m^0)\exp\left[-(bt)^n\right] \quad (2)$$

In this equation, V_m^0 corresponds to the initial monoclinic phase fraction in the material before being submitted to ageing tests, b is a parameter that represents the temperature dependence of the ageing effect, t is the ageing duration, and n is the MAJ exponent (or time exponent, which is a constant independent of temperature). From the literature, the exponent n can vary between 0.3 and 4 [31], [34]. According to *Christian* [35], the n constant is different according with the ageing mechanism, reflecting the proportion of nucleation and growth during these deleterious transformations [31], [35] and it depends on the microstructure and chemical composition of the material in analysis [36]. The n exponent can be derived from the logarithmic form, as represented in equation (3).

$$\ln\left(\ln\left(\frac{1 - V_m^0}{1 - V_m}\right)\right) = n\ln(b) + n\ln(t) \quad (3)$$

Through MAJ law,n can be determined from the slope of the best regression line of the plot $\ln\left(\ln\left(1 - \frac{V_m^0}{1} - V_m\right)\right)$ versus $\ln(t)$. A small value of n represents a higher contribution of the nucleation phase to the ageing process, i.e., an accelerated nucleation occurs. On the other hand, a n value close to 4 represents a homogeneous nucleation and a three-dimensional growth mechanism is dominant [34], [36], [37]. For values of $n$between 1 and 2 a decelerated growth rate of monoclinic phase zirconia is observed [37], being also a one-dimensional process [32], [34]. Therefore, the nucleation process is only present on the surface of the material and a growth into the bulk does not occur.

Hence, this MAJ law became widely used to investigate the degree of degradation present in the sample submitted to the ageing process and it can be divided into three successive stages. In the initial stage, the single and isolated tetragonal grains or nuclei at

the surface begin to transform into the monoclinic structure; in the second stage, there is an exponential increase in the monoclinic phase, which is normally interpreted as a three-dimensional growth of the monoclinic phase into the volume. In the last stage, a "saturation phenomenon" occurs, as described by *Nakajima et al.*, being this phenomenon associated with the maximum transformable tetragonal zirconia content [38].

2.3. Stabilized Zirconia

Zirconia behaviour is influenced by the selection of the starting powders, composition and size of the grains, which affects the mechanical parameters and the ageing resistance of this ceramic.

Developing stabilized tetragonal zirconia ceramics with good mechanical properties, namely, high fracture toughness and flexural strength was always the priority with this ceramic. The addition of a stabilizer to zirconia was studied with the purpose of enhancing the stability of the tetragonal zirconia phase, improving the stability of the material itself [39]. In 1975, *Garvie et al .*[40] published the first study related with the stabilization of zirconia's tetragonal phase. This study is relative to a test of magnesia partially stabilized zirconia. From this publication, various stabilizers added to zirconia were analyzed.

Regarding the addition of the stabilizer to zirconia, the oxygen ions around Zr^{4+} cations will stabilize, making the tetragonal or even the cubic phase stables and preventing an undesirable transformation of the tetragonal zirconia to monoclinic phase during cooling at low temperature. In order to maintain the tetragonal zirconia phase at low temperature and control the transformability of these ceramics, several stabilizers, such as calcia (CaO), ceria (CeO_2) and yttria (Y_2O_3), have been added to ZrO_2 [1], [8], [41]. These multiphase materials are known as Partially Stabilized Zirconia (PSZ) [1]. Some of these stabilizers contain undersized and oversized trivalent ions (as the yttria (Y^{3+})), as well as oversized tetravalent ions (like ceria (Ce^{4+})). *Li et al.* [8], verified that the stabilization of tetragonal zirconia with oversized trivalent cations, such as Y^{3+} , is twice as efficient than undersized trivalent cations, since they are more efficient in relieving the oxygen overcrowding (by both oxygen vacancies generation and dilatation of the cation network).

Yttria is the stabilizer that presents the best characteristics since it allows the attainment of a system with only tetragonal phase and it improves the material's ageing resistance, making it the most used stabilizer for zirconia. This stabilized zirconia is designed Yttria-Stabilized Tetragonal Zirconia Polycrystal ceramic (Y-TZP) [42]. This composition decreases the driving force of the transformability at room temperature and

retains the metastable tetragonal grains in dense bodies, when the content is around 3 mol% of yttria [1]. Thus, the yttria content will increase the value of ΔU_{SE}, mentioned in equation (1). In the case of Y-TZP, many oxygen vacancies are created by the trivalent cations (Y^{3+}), causing the water diffusion rate to be higher when compared with other stabilized zirconia with tetravalent cations, like ceria stabilized zirconia (Ce-TZP), in which Ce^{4+} does not induce vacancies [3]. Unfortunately, the content of yttria can also trigger Low Temperature Degradation, once that with yttria doping the water species can locate the oxygen vacancies site present on the surface of the zirconia [18]. According to *Schubert et al.* [3], the penetration of OH^- leads to a lattice concentration, causing tensile stresses on the surface of the grains, which destabilizes the tetragonal phase and provides the martensitic tetragonal to monoclinic phase transformation. The presence of yttria (Y^{3+}) as a stabilizer for zirconia (Zr^{4+}) creates oxygen vacancies in Yttria Stabilized Zirconia according to the equation (4) [42]:

$$Y_2O_3 \xrightarrow{ZrO_2} 2Y'_{Zr} + V_{\ddot{O}} + 3O_O^{\times} \quad (4)$$

where Y'_{Zr} represents the negatively charged yttrium ion that will substitute the zirconium ion, Vö indicates the positively charged oxygen vacancies and $3O_O^{\times}$ represents the lattice oxygen [42]. Similarly, cations such as Mg^{2+}, Ca^{2+} have lower valence comparatively with zirconium ion (Zr^{4+}), inducing the formation of oxygen vacancies (Vö). The substitution of Zr^{4+} ion by the Y^{3+} will create a negative charge in the lattice, and in order to replace the charge neutrality, an oxygen vacancy is created for each mol of yttria incorporated in the lattice [43]. Therefore, two yttrium ions are necessary to electrically balance just one oxygen vacancy [43].

Magnesia-Stabilized Zirconia (MgO-SZs) presents residual porosity and bigger grain size (30-40 μm), what have discouraged the use of this composition for biomedical applications, since these factors together can lead to degradation of the implant. Moreover, the reinforcement by phase transformation toughening is less pronounced in magnesia stabilized zirconia when compared to yttria stabilized zirconia [14].

Ceria can be used to stabilize zirconia and it presents many similarities with Yttria Stabilized Zirconia. Ceria Stabilized Zirconia also presents an equivalent value of fracture toughness relative to the Y-TZP, but the grain sizes must be larger [43]. While for a Ce-TZP, to achieve a K_{IC} of 12 $MPa.m^{1/2}$ it needs a grain size of 8 μm, Y-TZP achieves this value with a grain size of 2 μm [43]. Table 2 shows the values of typical mechanical properties presented by yttria and ceria stabilized tetragonal zirconia (Y-TZP and Ce-TZP).

Table 2. Values of typical mechanical properties presented by Y-TZPs and Ce-TZPs. Adapted from [43].

	Y-TZP	**Ce-TZP**
Stabilizer (mol%)	2-3	12-15
Hardness (GPa)	10-12	7-10
Fracture toughness, K_{IC} (RT, MPa.m$^{1/2}$)	6-15	6-30
Young's modulus (GPa)	140-200	140-200
Bend strength (MPa)	800-1300	500-800

By analyzing the table, it is possible to verify that a higher amount of ceria is necessary to achieve similar mechanical properties than those of Y-TZP.

The exact yttria amount, in yttria stabilized tetragonal zirconia, plays a crucial role in the transformability of zirconia and consequently in the toughness properties. The toughness of Y-TZPs is strongly influenced by the grain size of the zirconia [43]. In fact, to control the volume expansion due to the transformation occurrence, it is necessary to limit the zirconia grain size [9]. Indeed, the zirconia grain size must be between two critical values, i.e., the lower value (D_c') and the higher value (D_c). Below the D_c' value the transformation is hindered (the tetragonal phase is stabilized because of its very small size), and above the D_c value a spontaneous transformation occurs. These critical sizes depend on the content of oxide stabilizer present in zirconia [3]. Figure 10 shows that with a concentration of 2 mol% Yttria Stabilized Zirconia (2YSZ) the critical size is approximately 0.2 μm, while for 3 mol% of yttria it increases to approximately 1 μm [1].

Therefore, as previous mentioned, smaller and fine grain sizes are important factors in order to achieve better mechanical properties and ageing resistance. The lower the grain size obtained by 2YSZ is, a higher increase of toughness of the zirconia is expected. The toughness increases mostly due to the decrease of the stabilizer, i.e., lesser stabilizer will imply a higher toughness. Increasing the amount of yttria to about 3 mol% Yttria Stabilized Zirconia (3YSZ), leads to a superior critical size of the grains, leading to a decrease in the mechanical properties, in terms of the fracture toughness. Hence, the amount of zirconia stabilizer is an important factor to attain when selecting a zirconia grain size. Nevertheless, this grain size should be able to trigger and maintain the toughening mechanism presented by the tetragonal phase of the zirconia.

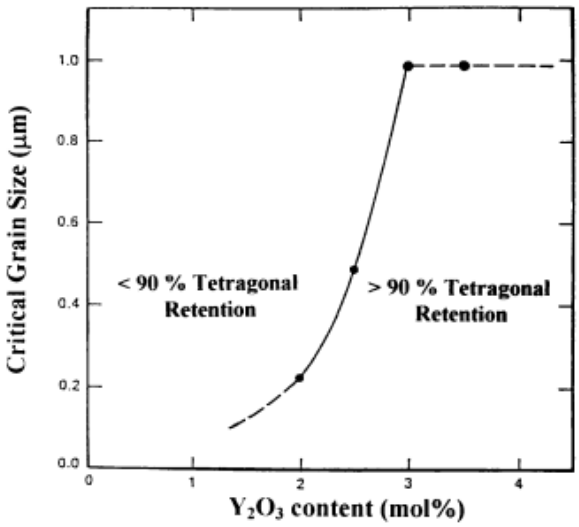

Figure 10. Critical grain size against yttria content in tetragonal zirconia. Adapted from [1].

Investigations of the effect of yttria content in ZrO_2 concluded that 2 mol% of this stabilizer is an optimum concentration that contributes to stability and to an increase in the mechanical properties. Table 3 demonstrates that 2YSZ has excellent properties, exhibiting a highest fracture toughness of 8.1 MPa.m$^{1/2}$ while the other samples present a fracture toughness that did not exceed 6 MPa.m$^{1/2}$ [6].

Table 3. Density and mechanical properties of samples with different concentration of yttria. Adapted from [6].

Sample	Yttria (molar ratio)	Tetragonal phase (vol. % of zirconia)	Cubic phase (vol. %)	Fracture toughness (MPa.m$^{1/2}$)
AZ38	2Y	100	0	8.1 (±) 0.1
AZ60	2.5Y	94.6	5.4	5.6 (±) 0.2
AZ35	3Y	98.7	1.3	6.0 (±) 0.1

Through the zirconia-yttria phase diagram represented in Figure 11, it is possible to verify that in zirconia with contents higher than 3 mol% of yttria, the fraction of transformable tetragonal phase decreases. Thus, the decrease of tetragonal phase will affect the mechanical properties, such as the toughness and hardness of the material [6].

In order to prevent the spontaneous transformability of zirconia, 3 mol% Yttria Stabilized Zirconia (3YSZ) is used, retaining the stable tetragonal zirconia phase. However, with this reduction of the transformability of zirconia at room temperature there are consequences at the level of mechanical properties, as previously mentioned. Although, 2YSZ presents superior mechanical properties, such as strength and fracture toughness, it is more susceptible to degradation. This brittleness of 2YSZ can be overcame through other

stabilizers and dopants addition, with the purpose of enhancing the ageing resistance and thus, avoiding the degradation.

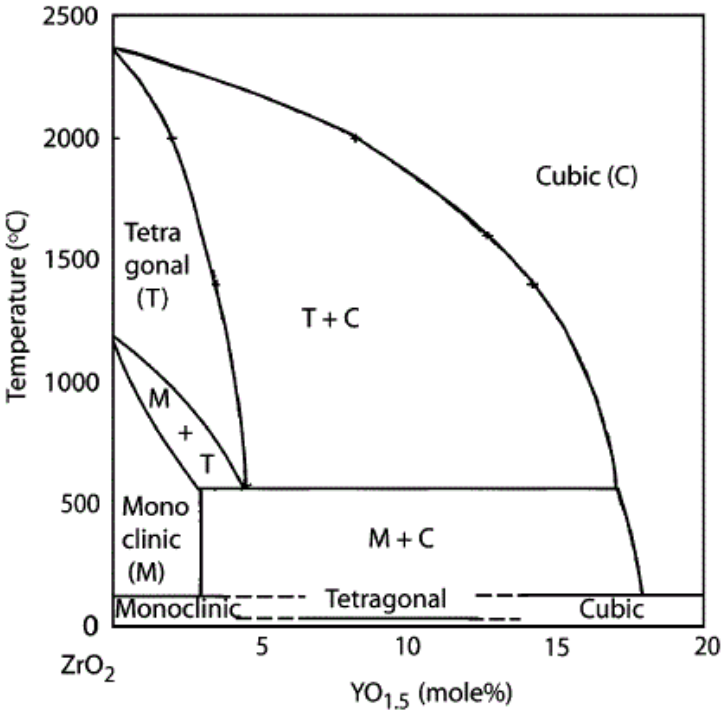

Figure 11. The zirconia-yttria phase diagram, in which T=tetragonal, C=cubic, M=monoclinic and L= liquid phase of zirconia. Adapted from [44], [45].

2.4. Dopants

In order to provide an increase of the ageing resistance and/or enhance the mechanical properties of tetragonal zirconia, the addition of different dopants and different percentages of each element have been tested. In this topic some examples of these dopants will be presented, alongside with the reported effects on the characteristics of tetragonal zirconia.

2.4.1. Ceria

Ceria is usually tested as a stabilizer, although it has also been tested as a dopant, in order to improve the mechanical properties of Y-TZP. Ceria (CeO_2) is added to completely stabilize zirconia in its tetragonal phase and it has been verified that its addition increases the fracture toughness of Y-TZP [46]. Nevertheless, the amount of ceria must be carefully controlled, since higher amounts tend to increase the material's porosity which decreases the bulk density and material's strength [47], [48].

According to the study of *Ragurajan et al* .[47], an addition of 0.5 wt% of ceria to 3 mol% of Yttria Stabilized Zirconia, sintered at 1400 ºC, achieved the best results for fracture toughness, reaching 6.4 $MPam^{1/2}$, against 5.3 $MPam^{1/2}$ for the un-doped samples. With this composition, the sample presents the most homogeneous microstructure, with a smaller grain size. At this sintering temperature (1400 ºC), this sample also achieved the highest value of density (5.9 g/cm^3), being this value of density the probable explanation for the enhanced value of hardness. For the samples containing 0.5 wt% ceria at a sintering temperature of 1400 ºC the highest value for the Vickers Hardness was achieved, 1346 HV (~13.2 GPa). Retaining this composition but with a sintering temperature of 1450 ºC, the achieved Young's Modulus was approximately 211 GPa [47].

As mentioned, in section 2.3., ceria has been also used as a tetragonal zirconia stabilizer, and some authors reported that the monoclinic phase content decreases with the increasing amount of ceria. *Hernandez et al*. [49] observed that 3Y-TZP with more than 2 mol% of ceria prevented the formation of monoclinic phase during hydrothermal treatment (at 160 ºC), while the same material without ceria presented 80 % of monoclinic phase after the treatment.

2.4.2. Manganese Oxide

The inclusion of transition metal oxides, such as manganese oxide (MnO_2), can improve the densification of zirconia and its resistance to degradation without grain growth [50], [51]. According to Duh and Hwung [50], small contents of manganese oxide increased the densification rate for Y-TZP. The densification of zirconia through the addition of manganese is related with the decrease of diffusion activation energy caused by the solid solution of MnO_2 in the ZrO_2 crystal. Upon sintering, the zirconia sites, that will cause fast diffusion paths within single grains, are replaced by manganese cations [51]. Through the addition of MnO_2 a compact surface of the material is achieved.

In a study reported by *Ramesh et al.* [50], [51], it was observed that the addition of an amount of manganese oxide higher than 0.05 wt% to a 3 mol% Yttria Stabilized Zirconia (3YSZ) significantly improved the bulk density at lower sintering temperatures (below 1400 ºC). On the other hand, when 1 wt% of MnO_2 was added, the bulk density led to the opposite result. In particular, the lower bulk density presented by samples with 1 wt% of MnO_2 for temperatures above 1300 ºC occurs due to the formation of cubic zirconia in the tetragonal matrix (Figure 12) [51].

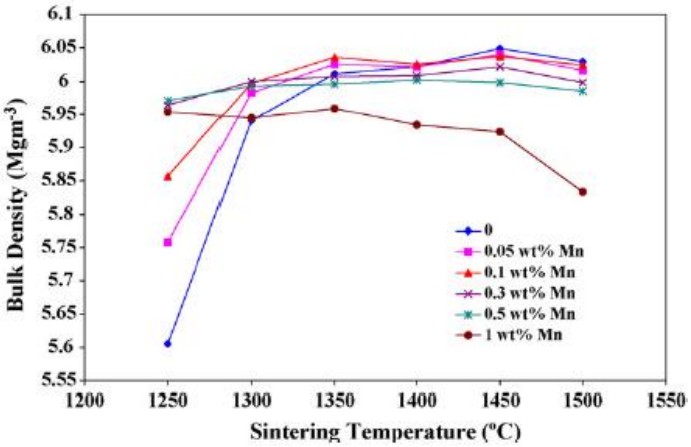

Figure 12. Representation of the effect of the sintering temperature and manganese oxide addition on the bulk density of Y-TZP. Adapted from [51].

In relation to the Young's Modulus, higher values are reached at lower sintering temperatures. The Young's Modulus value varied linearly with increasing density. The addition of MnO_2 presents the beneficial effect of improving the hardness of 3YSZ at low sintering temperatures (below 1350 ºC). The doped samples reached higher values in relation to the un-doped ones. The maximum value of hardness (~13.7 GPa) was observed at a sintering temperature of 1400 ºC with the addition of 0.05 wt% of MnO_2 [51]. Similar results of hardness are achieved between the doped samples with 0.5 wt% and 0.3 wt%, where both materials exhibited very high hardness of 13.2 GPa (0.3 wt%) and 13.6 GPa (0.5 wt%), when sintered at 1250 ºC. Furthermore, the biggest difference was observed in the values of hardness achieved between the un-doped and the sample doped with 0.5 wt% of manganese oxide when sintering at 1250 ºC: the un-doped samples achieves 9.7 GPa while the doped sample reaches 13.6 GPa although, the hardness of all samples decreased above 1400 ºC. The fracture toughness of the un-doped and of the 0.5 wt% manganese doped zirconia did not present significant variations with the temperature, except for the 1 wt% MnO_2 doped zirconia which resulted in an increase from 4.8 MPa.$m^{1/2}$ at 1400 ºC to 5.3 MPa.$m^{1/2}$ at 1450 ºC and then rapidly to 7 MPa.$m^{1/2}$ at 1500 ºC. This phenomenon is related with a quick response of the metastable tetragonal zirconia grains to the induced stresses created during indentation, i.e., the enhanced transformation toughness effect [51].

The ageing resistance of the stabilized tetragonal phase was studied and it was verified that the doped sample with 0.5 wt% did not undergo phase transformation during the ageing experiments (180 ºC/10 bar for 24 hours). These results demonstrate that the addition of manganese oxide can be beneficial in order to slow down the kinetics of ageing by preventing the hydroxyl reaction from zirconia near grain boundary regions (Figure 13) [51].

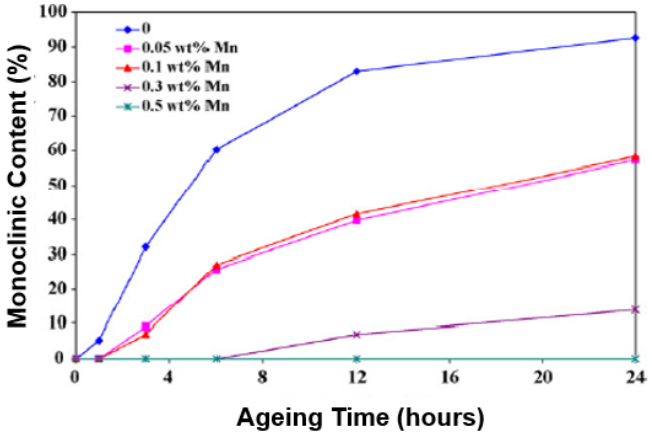

Figure 13. Effect of hydrothermal ageing on the monoclinic phase development in Y-TZPs sintered at 1350 ºC. Adapted from [51].

Other published study by *Zhou et al*. [52], also showed that the relative density of 8 mol% yttria stabilized zirconia (8 YSZ) was significantly improved by the addition of manganese oxide. During the sintering process, the Mn cations replace the Zr sites, leading to fast diffusion paths within the single grains. As a result of the formation of this faster diffusion path, the grain growth with manganese oxide additions enhanced, since the average grain size of the doped sample with 1 wt% of MnO_2 was 0.3 µm and 2.5 µm for the sample with 5 wt% of MnO_2. The results reported that for addition of an amount of 0-3 wt% MnO_2, the monoclinic zirconia fraction present in the bulk sample decreases significantly (53.8% to 12.5%), which confirms that additions of the manganese is beneficial to the tetragonal phase stability of 8YSZ sample. The surfaces of the sintered samples were compact and pores and second phases were not observed. The bending strength and hardness of the sintered samples improved with addition of these dopants to zirconia. Higher values were achieved at lower temperatures (from 1200 ºC to 1300 ºC), as reported by *Ramesh et al.* [50], [51]. The maximum value of Vickers hardness was approximately 1800 HV for the 5 wt% MnO_2 added to 8YSZ sample sintered at 1400 ºC, while the highest strength was approximately of 230 MPa for the sample doped with 3 wt% MnO_2 sintered at 1300 ºC.

2.4.3. Lanthana

To overcome the Low Temperature Degradation, which causes the martensitic transformation from tetragonal to monoclinic phase, lanthana in dopant amounts was also analyzed [53]. There is a clear evidence that the addition of ternary oxides (such as Y^{3+}, La^{3+}) can promote an effective deceleration of the transformability of zirconia once that

these cations with a lower valence than Zr^{4+} produce oxygen vacancies that maintain the charge balance. Ternary additions also influence the grain growth and grain boundary segregation on tetragonal zirconia polycrystal due to a difference in ionic radius which delays the degradation [53], [54].

In the work of *Zhang et al.* [55], it was observed that when lanthana is used as a dopant, the cation segregation occurs on grain boundaries in YSZ ceramics. This segregation of trivalent cation promotes a stronger binding of the oxygen vacancies at the grain boundary and highly contributes to maintain the stability in detrimental conditions. In order to slow down the ageing kinetics, larger oversized cations are preferred. Lanthana inhibits the grain growth of zirconia which is concomitant with a higher degradation resistance. So, it was reported that the addition of 0.2 mol% to 0.4 mol% of lanthana led to the highest ageing resistance of zirconia (Figure 14) [55]. However, above this value the ageing resistance starts to decrease. A secondary phase ($La_2Zr_2O_7$) precipitates for contents higher than 1 mol%, which can enhance the ageing of zirconia due to the accompanied volume expansion and even more detrimental is that the formation of a new phase is followed by a decrease in density [55]. The samples of lanthana with an amount of 0.02 mol% were not fully densified after sintering (1500 ºC for 2hours) resulting in pieces with residual porosity causing the decrease of its hardness. It was reported that with the addition of 0.1-0.4 mol% of lanthana and 0.1-0.25 wt% of alumina to 3 mol% Yttria Stabilized Zirconia, the samples can be fully densified when sintered for 2 hours at 1450 ºC or 1500 ºC [55].

In terms of hydrothermal stability, translucency and good mechanical properties, were achieved with a combination of 0.2 mol% of lanthana and 0.1 to 0.25 mol% of alumina in a 3 mol% Y-TZP, when compared to a commercialized zirconia [55].

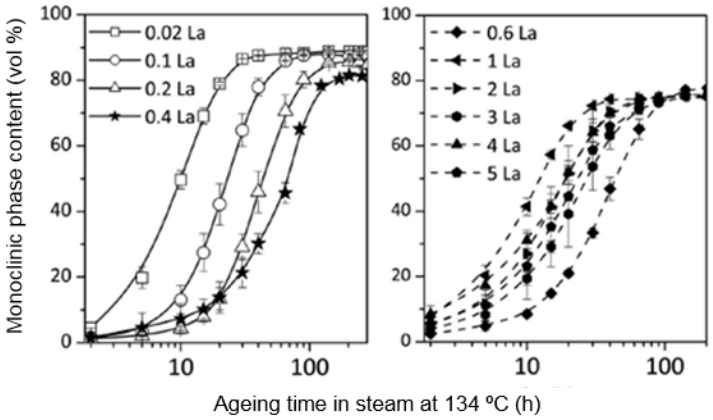

Figure 14. Representation of the monoclinic phase content of lanthana doped zirconia samples as a function of ageing time in steam at 134 ºC. The transformation rate decreased when the amount of lanthana increased from 0.02 mol% to 0.4 mol% (left) but increased when the amount of La_2O_3 was greater than 0.4 mol%. Adapted from [55].

In another study of *Nogiwa-Valdez et al.* [53], the addition of lanthana (1 wt%) and alumina (1 wt%) to 3 mol% Yttria Stabilized Zirconia (3YSZ) was investigated. The zirconia doped with two elements did not present significant variations in the mechanical properties, density or grain size. Regarding hydrothermal degradation resistance, good results were achieved. After the samples were exposed to hydrothermal conditions (heated steam at 180 ºC, ~90 kPa), the first detection of hydrothermal degradation was observed by Atomic Force Microscopy (AFM), which revealed that individual surface grains displayed monoclinic symmetry. The degradation proceeded in adjacent grains, which formed monoclinic clusters that grew in the radial direction and circular shape on the surface. The surface of the un-doped sample allowed the penetration of water species after 24 hours of exposure (leading to surface delamination) and after 72 hours, the degradation had progressed, fracturing the sample. With addition of alumina and lanthana the degradation progress was prevented, delaying the surface saturation, and therefore the failure of the material. Therefore, the addition of these dopant elements substantially reduced the nucleation rate and growth of monoclinic clusters (Figure 15).

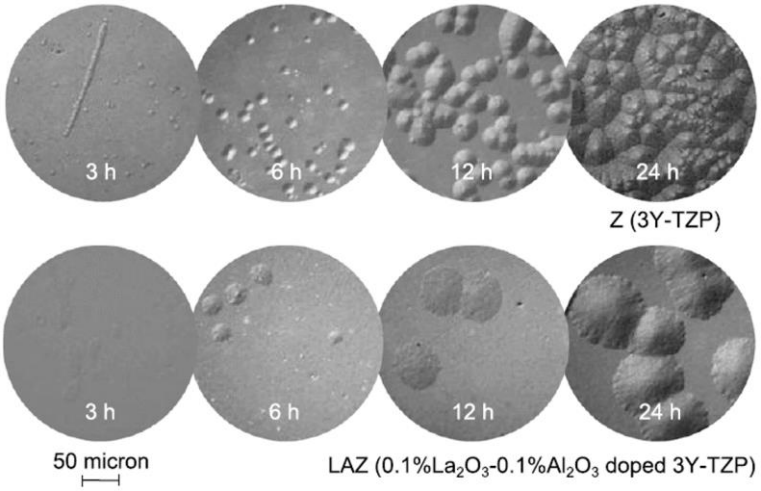

Figure 15. Group of images obtained by optical microscopy of Z sample (3Y-TZP) and LAZ sample (lanthana and alumina doped zirconia) exposed for 3, 6, 12 and 24 hours to hydrothermal tests. Adapted from [53].

Cross-section of those samples were observed to identify the degradation propagation rate into the bulk. Through Figure 16 it is possible to assume that the addition of both oxides considerable reduced the bulk propagation. After 72 hours of exposure, the sample with the ternary dopants presented a monoclinic layer with only 4.6 µm in comparison with the control sample (un-doped zirconia) which showed 41 µm of transformed layer. With addition of lanthana a modification in the transformation kinetics

was reported (since the grains were only partially transformed), leading to a reduction of the surface micro-cracking.

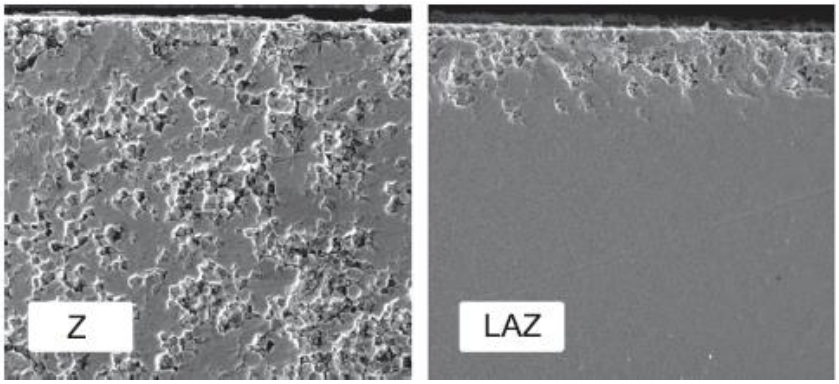

Figure 16. Images obtained by SEM of cross-section of the surface of the samples exposed for 48 hours to hydrothermal environment. The sample Z corresponds 3Y-TZP (control sample) and lanthana/alumina doped zirconia (LAZ). Adapted from [53].

2.4.4. Silica

Silica in small quantities is an attractive dopant for yttria stabilized zirconia and has been reported that it improves the resistance to Low Temperature Degradation without compromising its resistance to slow crack growth. Some authors reported that the addition of silica reduces the lattice strain resulting in a stabilized tetragonal zirconia [56]–[59]. The occurrence of the internal stresses can facilitate the growth of monoclinic clusters, promoting an extension of the transformation to their vicinity. Through the addition of silica to zirconia an amorphous phase at triple junctions appears. This makes the grains rounder leading to a reduction of stresses at the grain corners. Silica can limit the growth of monoclinic nuclei and thus, slowing down the ageing process preventing its propagation [56], [60].

Samodurova et al. [60] reported that the addition of SiO_2 did not change the densities, grain size or mechanical properties of 3 mol% Yttria Stabilized Zirconia (3YSZ), however the resistance to degradation was significantly improved. It was observed that the addition of silica (0.05 wt% and 0.025 wt %) resulted in the appearance of an amorphous silica phase at multiple grain junctions making the grains rounder. When silica or alumina are added to tetragonal zirconia, the rate of tetragonal to monoclinic transformation is highly improved causing a decrease of monoclinic phase nucleation. After 24 hours of ageing tests (at 134 ^{o}C) the formation of both layers of monoclinic zirconia was observed. These layers were thinner in comparison to those presented by the un-doped zirconia samples under the same conditions, and less amounts of micro-cracking in the grain boundaries appeared [60]. The

addition of silica and alumina causes the deceleration of Low Temperature Degradation of YSZ. Furthermore, good results were achieved when these two dopants were combined because they present improvements in the resistance to ageing without reducing the fracture toughness of the zirconia (before and after ageing tests) [60].

Gremillard et al. [57], [59], obtained results similar to the ones of *Samodurova et al*. [60]. It was reported that the addition of silica did not cause modifications in the fracture toughness, but this dopant highly improved the resistance to degradation. After exposing the samples in a steam environment (at 134 ºC) for 15 hours, the control sample achieved a maximum transformation of monoclinic zirconia of approximately of 75 %, while the doped zirconia with 0.5 wt% of SiO_2 only reached 30 % of monoclinic content, for the same period of the time exposed to the degradation environment. In terms of ageing kinetics of the doped zirconia appears to be nearly constant with the time, being the result of a random transformation of grains, without inducing the transformations to neighbors [57].

Concerning the flexural strength parameter, a study of *Nakamura et al*. [56] reported that this mechanical property increases in doped samples (3YSZ doped with 0.2 mol% SiO_2) when compared with the control sample of stabilized zirconia, for all three tested sintering temperatures (1400 ºC, 1450 ºC and 1500 ºC). The results of the flexural strength, after 50 hours of the ageing tests, revealed that the samples doped with silica only weakened by less than 20 %, while the stabilized zirconia samples have damaged surfaces (weakened by 50 to 60 %). Significant differences in the flexural strength of doped zirconia samples when measured before and after the ageing time were not verified (Figure 17).

After subjecting the sample to 40 hours of ageing, it was observed that the monoclinic formation rate was slower for the doped samples, both in surface and bulk. The thickness of the degraded layer was only 12 µm to doped samples while 36.7 µm for the un-doped samples, indicating that the doped sample had higher resistance to degradation than the un-doped YSZ samples.

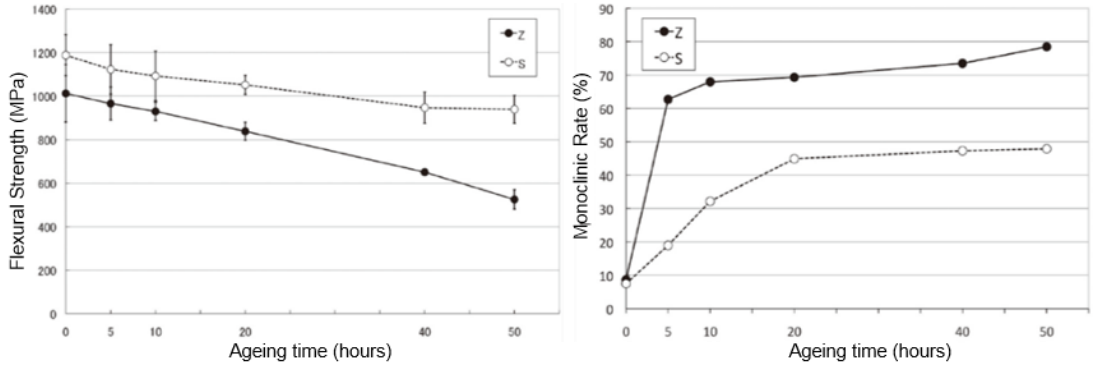

Figure 17. Results of flexural strength and monoclinic rate by zirconia doped with silica samples (S) and un-doped zirconia (Z) as a function of ageing time. Adapted from [56].

2.4.5. Titania

Titania has been tested as a dopant that can have a stabilizing effect in tetragonal zirconia, once that its addition leads to a decrease of cubic zirconia formed during the sintering stage and also lowers the sintering temperature [61]. Concerning Y-Ti-TZP, these systems have been developed in order to improve the resistance to low temperature ageing and destabilization of the tetragonal phase, while TiO_2 additions have been mostly interesting in the improvement of the electrical properties of stabilized zirconia by reduction in the mobility of oxygen vacancies [61].

Hodgson et al. [61] reported that the addition of TiO_2 causes no modifications in grain size or morphology of the samples, except in the samples sintered at temperatures above 1650 ºC. From x-ray diffraction analysis, the samples showed the presence of tetragonal, cubic and monoclinic zirconia phase. The presence of titania (0 -1 wt%) causes small modifications in the phase composition of the sintered material. It was observed a notably increase in the tetragonal zirconia content and a corresponding decrease in the amount of cubic phase formed during the sintering, being this difference more significant with the increase of the sintering temperature (1650 ºC). The mechanical properties of the Y-TZP un-doped samples and titania doped samples in relation to sintering temperature were studied (Figure 18). In relation to hardness, a decrease associated with the addition of TiO_2 at lower sintering temperatures occurs which is related with lower densities achieved for these samples. Although for sintering temperatures above 1650 ºC this difference becomes insignificant. However, a small increase in fracture toughness with the addition of titanium oxide is observed, which can be associated to the stability of tetragonal phase present in the microstructure promoting the transformation toughening mechanism [61].

In the studies of *Zhao et al.* [62] with TiO_2 doped yttria stabilized zirconia, it was reported that no monoclinic phase were detected through X-ray diffraction and Raman spectra after being exposed to tests at longtime hydrothermal ageing. In that work, the mechanical properties were also investigated. The Vickers hardness showed no higher variations while the fracture toughness was significantly enhanced by the addition of titanium oxide.

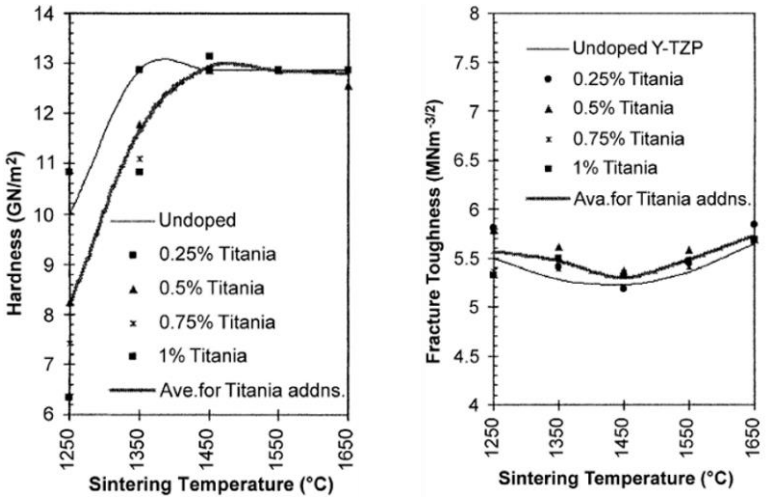

Figure 18. Vickers hardness and fracture toughness as a function of sintered temperature of the un-doped and TiO_2 doped samples. Results presented by *Hodgson et al.* [61].

2.4.6. Copper Oxide

This transition metal oxide has been used to densify at considerable low temperatures, to enhance mechanical properties, to suppress grain growth and to enhance ageing resistance in Y-TZP [63]. It has been reported that the bulk density and fracture toughness of copper oxide doped yttria stabilized zirconia improves when compared to those of the un-doped samples [64].

In a study of *Ramesh et al.* [64], copper oxide (0.05, 0.1 and 0.2 wt%) were added to 2.5 mol% of yttria stabilized zirconia. In this study all samples were submitted at the same sintering temperature (1300 ºC), identified as the optimum temperature for this composition. After sintering, it was demonstrated that all samples had a tetragonal zirconia structure, and grinding and polishing did not modify the tetragonal phase. So, the addition of copper oxide was beneficial to enhance the densification of zirconia samples [64].

In terms of ageing resistance, the un-doped yttria stabilized zirconia presents poor resistance to degradation when compared to the 0.05 wt% copper oxide doped Y-TZP (Figure 19). The samples doped with 0.05 wt% CuO presents the best ageing resistance because less than 40 % monoclinic content was obtained after being submitted to 200 hours of exposure tests [64].

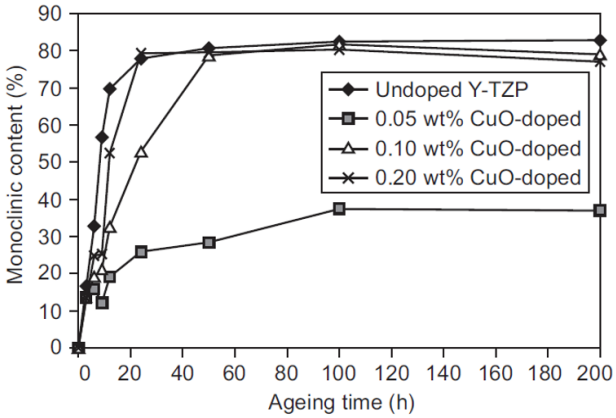

Figure 19. Effects of copper oxide additions on the ageing resistance behaviour (180 ºC and 10 bar) in zirconia. Adapted from [64].

The un-doped samples shows a catastrophic effect of Low Temperature Degradation, causing severe micro-cracks within the sample, as represented in Figure 20 [64].

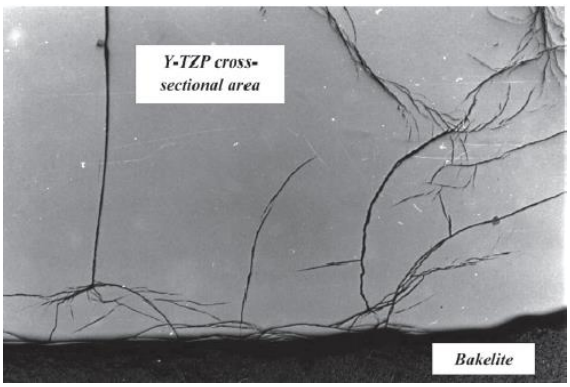

Figure 20. Optical micrograph representation revealing catastrophic micro-cracking of a polished cross section area of un-doped zirconia due to monoclinic phase formation after exposure for 24 hours (180 ºC and 10 bar). Adapted from [64].

At the level of bulk density, the best results were achieved for the composition of 0.05 wt% copper oxide doped YSZ, significantly higher than that for un-doped zirconia samples. All doped samples showed higher bulk density than 6 mg/m^3, as shown in Figure 21 [64].

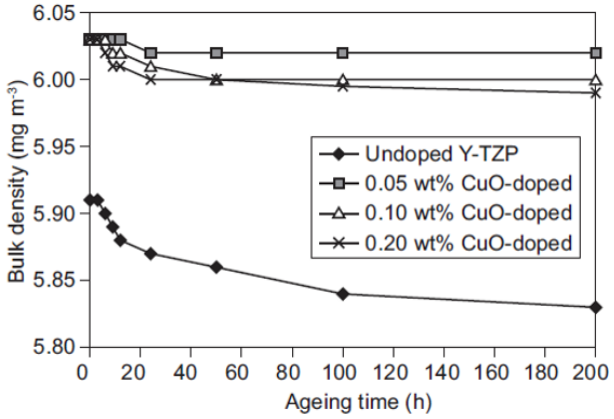

Figure 21. The effect of bulk density with the ageing time. Adapted from [64].

This oxide increases the transformability of zirconia, which explains the enhanced mechanical properties. Although, the monoclinic content may be a concern in the addition of copper oxide, since this phase could lead to the degradation of the zirconia ceramic. For this reason, the amount of this oxide should be carefully selected in order to obtain the enhanced mechanical properties without affecting the ageing resistance [64].

The un-doped zirconia samples present the poorest corrosion resistance, which can be due to attack near grain boundary regions causing the destabilization of the tetragonal phase and thus inducing the phase transformation. Other possibility is related with ageing resistance, in which hydroxyl groups react with yttria along grain boundary regions causing the formation of Y-OH bonds. For this reason, the copper oxide doped yttria stabilized zirconia sample presents an enhanced corrosion resistance due to grain boundaries preventing the OH group reaction with Y [64].

The samples that achieved the less monoclinic layer propagation were the 0.05 wt% CuO doped Y-TZP, achieving a very thin layer (4 μm) in relation to 740 μm thickness in the case of un-doped zirconia [64].

2.4.7. Ytterbia

The inclusion of ytterbia has been reported to increase the mechanical properties and stability of the tetragonal zirconia phase. In a study of *Kan et al.* [65] the effect of adding different amounts of Yb_2O_3 (1, 2, 3 and 4 mol%) to 1 mol% Yttria Stabilized Zirconia was analyzed. The bulk density increases linearly with the addition of Yb_2O_3 and with a sintering temperature reaching full density at 1450 ºC. In order to know which phase was present for 1 mol% Y_2O_3 stabilized zirconia with different contents of Yb_2O_3 at diverse sintering conditions (1400 ºC/1hour, 1450 ºC/1hour and 1450 ºC/4hours) a XRD analysis was realized (Figure 22). In general, only tetragonal or tetragonal plus cubic phases are present, except for the composition of 1 mol% Yb_2O_3 sintered at 1450 ºC during 4 hours where small amounts of monoclinic zirconia were observed [65]. Regarding the referred work [65], the fully polycrystalline tetragonal zirconia phase was achieved by an amount of 1 mol% Yttria Stabilized Zirconia with 1 and 2 mol% Yb_2O_3. In other hand, the fully stabilized cubic zirconia phase was obtained with 4 mol% Yb_2O_3 [65].

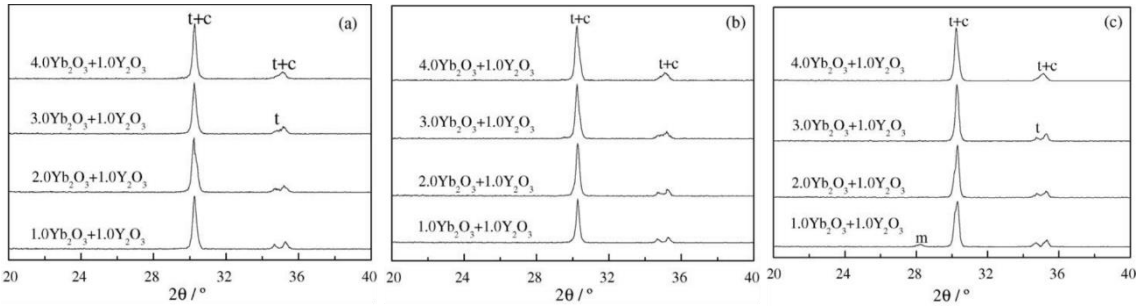

Figure 22. XRD analysis of polished Yb_2O_3 and Y_2O_3 stabilized zirconia sintered under different conditions: (a) 1400 ºC/1hour; (b) 1450 ºC/1 hour and (c) 1450 ºC/4 hours. Adapted from [65].

The mechanical properties of the ceramics with different grades of ytterbia, sintered at different conditions as a function of the ytterbia content was analyzed (Figure 23). It was verified that the Vickers hardness increases with the increase of Yb_2O_3 and it decreases with a longer sintering time at 1450 ºC, which is a consequence of grain growth and of the increase of cubic zirconia content. The composition of 1 mol% Yb_2O_3 sintered at 1450 ºC for 4 hours exhibit a lower hardness resulting in the transformability of the tetragonal grains to monoclinic and the presence of micro-cracks. This study confirms that the fracture toughness decreases with the increase of ytterbia amount, being more predominant upon increasing from 1 mol% to 2 mol% of Yb_2O_3. An excellent value of mechanical properties was achieved with the composition of 1 mol% Y_2O_3 and 1 mol% Yb_2O_3 sintered at 1450 ºC during 1 hour, with a fracture toughness of 8.5 MPa.$m^{1/2}$ and hardness of 12 GPa [65].

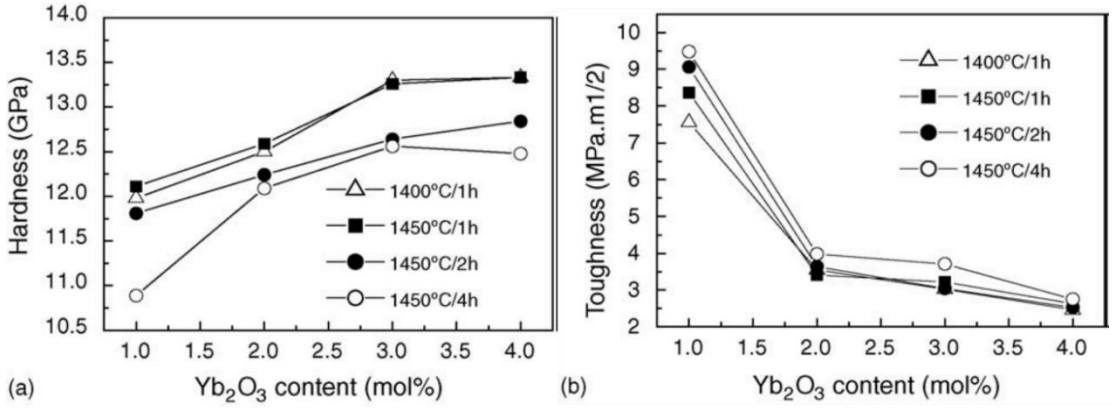

Figure 23. Mechanical properties of the different ceramic grades, sintered at different conditions as a function of the Yb_2O_3 content: (a) Vickers hardness and (b) fracture toughness. Adapted from [65].

2.4.8. Pentavalent Oxides

The addition of pentavalent oxides, such as niobium oxide (Nb_2O_5) and tantalum oxide (Ta_2O_5), has been tested with Yttria Stabilized Zirconia. The alloys of these pentavalent

oxides present lower number of cations coordinated to oxygen ions, leading to an increase in the stability of the tetragonal phase of zirconia [66].

Through the addition of these oxides the samples showed a tendency to increase the bulk density, and consequently the decrease of porosity in the bulk material. In fact, with this increased of density, the mechanical properties of yttria stabilized zirconia are enhanced. It was reported that the Vickers Hardness, fracture toughness and flexural strength increased with the addition of these oxides in Y-TZP [67]. In particular, through the addition of either Nb_2O_5 or Ta_2O_5 the problem of ageing can be compensated [66].

According to *Zhao et al.* [68], the addition of niobium into Yttria Stabilized Zirconia causes destabilization of the tetragonal zirconia phase and leads to the appearance of small amounts of monoclinic zirconia. Similar results can be observed with the addition of tantalum dopants. Moreover, with the increase of the amount of both dopants the transformability of zirconia also increases, resulting in a decrease of the tetragonal phase, increasing the metastable phase in the material. This phenomenon can be due to the addition of the dopants into zirconia causing the extinction of oxygen vacancies and consequently overcrowding of the oxygen in tetragonal zirconia, leading to an increase of strain in the tetragonal structure. The addition of these dopants increases the transformability of zirconia, being responsible for the enhanced mechanical properties. Nevertheless, the presence of monoclinic phase in zirconia is a concern, since this transformability phenomenon leads to premature degradation of the ceramic [68].

In order to obtain enhanced mechanical properties without affecting the ageing resistance it is crucial to carefully select the amount of these pentavalent oxides.

Cho et al.[66] reported that zirconia stabilizers niobium (Nb_2O_5) and tantalum (Ta_2O_5) are not toxic to cells and when added to Yttria Stabilized Zirconia both are considered biocompatible materials. Several studies have reported that $Nb_2O_5$and Ta_2O_5 have a good biocompatibility and are viable for their applications as biomaterials [69], [70]. Niobium oxide has demonstrated a short and long term biocompatibility, and this material provides mechanical strength to other materials (Titanium alloy) [71]. It was reported that the samples of Nb_2O_5 presented cell proliferation, mitochondrial activity and cell volume similar or superior to that of titanium and stainless steel samples, respectively. Tantalum oxide material has gained interest for orthopedic implant applications due to its osteoinductive properties [72] and the fact that this materials are to be used as a porous trabecular-like structure for hard tissue generation [73].

Table 4 present the summarized researched dopants for zirconia, alongside with the produced effects on both mechanical properties and ageing resistance.

Table 4. Dopants added to zirconia.

Dopant	Composition	Fracture Toughness ($MPa.m^{1/2}$)	Hardness (HV)	Flexural Strength (MPa)	Ageing Resistance	*Obs.*
Ceria	YSZ (3 mol% yttria) + 0.5 wt% CeO_2 [47]	6.4	1346	-	-	Density decrease at higher sintering temperature
Manganese Oxide	YSZ (3 mol% yttria) + 0.05-1 wt% MnO_2 [51]	5-7.1	1366 -1397	-	Increase with the amount of MnO_2	At lower sintering temperature the bulk density increases
	YSZ (8 mol% yttria) + 1- 5 wt% MnO_2 [52]	-	1400 – 1800	200 – 235	High tetragonal zirconia retention	
Lanthana	YSZ (3mol% yttria) + 0.2 mol% La_2O_3 + 0.25 mol% Al_2O_3 [55]	6.02	1331	690	Ageing resistance increase until 0.4 mol% La_2O_3	Hydrothermal stability and mechanical properties similar to a control product
	YSZ (3mol% yttria) + 0.1 wt% Al_2O_3 + 0.1 wt% La_2O_3 [53]	5.7	1305	-	Enhance protection against ageing	Was not observed considerable modifications on mechanical properties
Silica	YSZ (3mol%yttria) + 0.25 wt% SiO_2 + 0.25 wt% Al_2O_3 [60]	4.6	1489	1244	Significantly improved resistance	Does not affect the density, grain size and mechanical properties
Titania	YSZ (8 wt% yttria) + 4-16 wt% TiO_2 [62]	2.28-3.23	1002 - 1039	-	-	Increase fracture toughness at lower sintering temperature
Copper oxide	YSZ (2.5 mol% yttria) + 0.05 wt% CuO [64]	-	1122	-	Ageing resistance is better for 0.05 mol% of CuO	The density slightly decreases with addition of CuO
Ytterbia	YSZ (1 mol% yttria) + 1.0-2.0 mol% Yb_2O_3 [65]	8.5	1224	-	Ageing resistance increase with Yb_2O_3 (1.0-2.0 wt%)	Bulk density increase with amount of Yb_2O_3
Niobia	YSZ (3 mol% yttria) + 0.05-1 wt% Nb_2O_5 [74]	7.01 – 7.13	1346 – 1356	-	Increase with Nb_2O_5 content sintered at 1500 ºC	With increase of sintering temperature the density decreases

2.5. Biological Behaviour

Biocompatibility of a material has been defined as the ability of the material to perform an appropriated host response without causing any undesirable local or systemic effects in a specific body application [75]. Reaction of bone, soft collagenous tissues and blood are involved in the host response to ceramic implant. Thus, interfacial reaction between these materials and body tissue both *in vitro* and *in vivo* must be considered in order to evaluate the biocompatibility of zirconia biomaterial.

The biocompatibility of zirconia has been widely evaluated, since as already referred this ceramic is commonly used as a femoral ball head in total hip replacement and in the dental field. So, aspects like biocompatibility, intrinsic mechanical properties, before *in vivo* contact with soft tissue and blood must be strictly evaluated [1], [14].

Curiously, the results of biocompatibility studies in zirconia were first obtained *in vivo* in 1969, and only after the results of *in vitro* were published in 1990 [1], [17]. In relation to *in vitro* tests, several authors concluded that zirconia has no cytotoxic effects in fibroblasts cells cultures, using different tests, as viability of cells and MTT assays (Figure 24) [1], [17]. Studies of i*n vitro* tests demonstrated that zirconia does not elicit either mutagenic or transforming effects on fibroblasts [76].

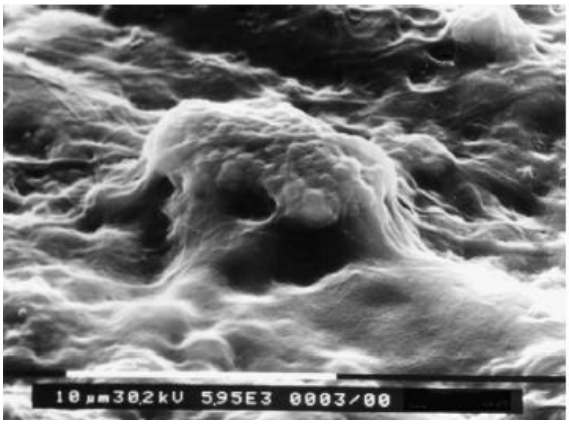

Figure 24. SEM image of fibroblast culture on zirconia (magnification 7400 x). Cells grown on all zirconia surface, covering it with a cellular layer. Adapted from [17]**.**

In relation to dental area, according to several studies it was confirmed that the inflammatory infiltrate, micro-vessel density and vascular endothelial growth factor appeared higher around the titanium crowns samples than around the zirconia ones [14], [17]. At cellular proliferation, it has been verified that fewer bacteria accumulates around the tetragonal zirconia when compared with other material such as titanium [14], [17]. *Warashina et al.* [77]*,* reported that zirconia induce less proinflammatory mediators (IL-1β, IL-6 and TNF-α) in comparison to titanium or polyethylene. Regarding biocompatibility of

this ceramic there is no evidence of cases of gingival inflammation or periodontitis [14]. According to *Kobayashi E. et al.* [78], zirconia and titanium dentistry implants do not inhibit the bone forming cells, osteoblasts, allowing the osseointegration process to occur.

Therefore, these results suggest that zirconia may be a suitable material for manufacturing implant abutments with a low bacterial colonization capacity [14].

In the presence of Yttria Stabilized Zirconia (Y_2O_3- ZrO_2), *Dion et al.* [79]verified the cell viability and MTT assays of 3T3 fibroblasts and HUVEC. The conclusion was that this ceramic and its products have no toxic effects on culture cells and also when in contact with the blood cells. *Satoh and Niwa* [1], performed *in vitro* carciogeneticity and teratogeneticity tests regarding Yttria Stabilized Zirconia, and they observed that in both tests the results were negative. According to the results of genotoxicity tests, the absence of aberration in chromosomic patterns in cells culture on zirconia was noticed [1], [4], [76]. According to *Li et al.* [80], the release of yttrium ions *in vitro* tests was an indicator of material degradation. Nevertheless, it was verified that this effect was not reported in *in vivo* tests.

Table 5 describes studies of *in vitro* culture of osteoblasts in zirconia substrates [81].

Table 5. Synthesis of cell culture studies involving zirconia substrates. Adapted from [81]**.**

Reference	Material	Cell type	Test	Main conclusions
Josset et al.	Zirconia, Alumina, Glass	Primary human osteoblast	Cell proliferation; Total protein synthesis; Cell morphology; Evidence of osteoblastic proteins; Carcinogenicity (DNA image cytometry Ag-NORs quantification).	No adverse response
Carinci et al.	Zirconia	Osteoblast cells (MG63 cells)	Gene expression analysis (DNA microarray).	Modulation of immunity, vesicular transport, and cell regulation.
Hao et al.	Zirconia* (MgO-PSZ)	Human fetal osteoblast cells (hFOB 1.19)	Surface analysis; Cell proliferation; Cell adhesion.	Increase of cell attachment and spreading by surface treatment.
Hao et al.	Zirconia* (Y-PSZ)	Human fetal osteoblast cells (hFOB 1.19)	Surface analysis; Cell adhesion.	Increase of cell attachment by surface treatment.
Bächle et al.	Zirconia (Y-TZP)	Osteoblast cells (CAL72 cells)	Cell proliferation; Cell morphology; Cell-covered surface area.	No adverse response Similar cell proliferation of different substrates.

*Carbon dioxide laser irradiation.

Ag-NOR, argyrophilic nuclear organizer region; MgO-PSZ, magnesia partially stabilizer zirconia.

In relation to *in vivo* tests, the biocompatibility of zirconia material was investigated by implanting in bone and in soft tissue. The first *in vivo* study, carried out by Helmer and Driskell [1], in which Yttria Stabilized Zirconia ceramic was implanted in a monkey's femur, reported the absence of adverse tissue reaction. Various *in vivo* tests were executed using different species of animals, and it was observed, at a general level, the absence of any local or systemic adverse reaction nor carcinogenic effects after the implantation of zirconia ceramics into muscles or bones [1].

2.6. Applications of Zirconia

Zirconia ceramic exhibits advantages over other ceramic materials due to its higher mechanical strength and fracture toughness. It can be used for functional as well as structural applications. Nowadays, zirconia has been proposed for clinical applications like arthroplasty and dental devices, where they are mainly applied as replacements for hip, knee and teeth. It presents a reduced wear rate and excellent long-term biocompatibility, that can increase the longevity of the prosthetic joints, being this feature clinically important for replacements (especially for hip and knee) because it is increasingly applied in young and active patients [3]. Zirconia has benefic ceramic properties offering diverse possibilities for technological applications such as sensors, solid oxide fuel cells (SOFC) and thermal barrier coatings (TBCs).

These applications are reported, alongside with benefits and restrictions of this ceramic on these applications respectively.

2.6.1. Body Implants

Currently, biomedical implants are being widely used to restore a body function that has been deteriorated by a disease or a trauma. A ceramic implant has to resist wear and cyclic fatigue for several million cycles under high loads. Furthermore it has to be biocompatible and chemically inert (both mandatory requirements) for ten years *in vivo* [8].

The increase of the lifetime durability of the *in vivo* arthroplasty procedure is a crucial step for the advancement of the human beings quality of life. Actually, the lifetime of artificial hip joint usually ranges from 12 to 15 years [82]. Nevertheless, due to the improvement of these bioceramics through the past years it is expected that the lifetime of biomedical devices reaches the 20 years [83].

The lifetime performance of zirconia orthopedic prosthetics and dental devices can be lead to undesirable implications on quality of human life, due to the consequences related with ageing process. In fact, these biomedical implants are subjected to constant wear, leading to the appearance of debris, this factor being a major issue, since debris leads to relevant health problems, such as aseptic loosening, periprosthetic osteolysis [82], reduce the expression of type I collagen [84], osteocalcin, alkaline phosphatase and osteopontin by osteoblasts [85]. The extension of micro-cracks will also generate defects on transformed zone (tetragonal to monoclinic transformation), due to defects generated in stressed regions of the implant which may grow with the transformed zone until a threshold size that slows

down the crack propagation to proceed, leading to consequential implant failure as is schematically described in Figure 25.

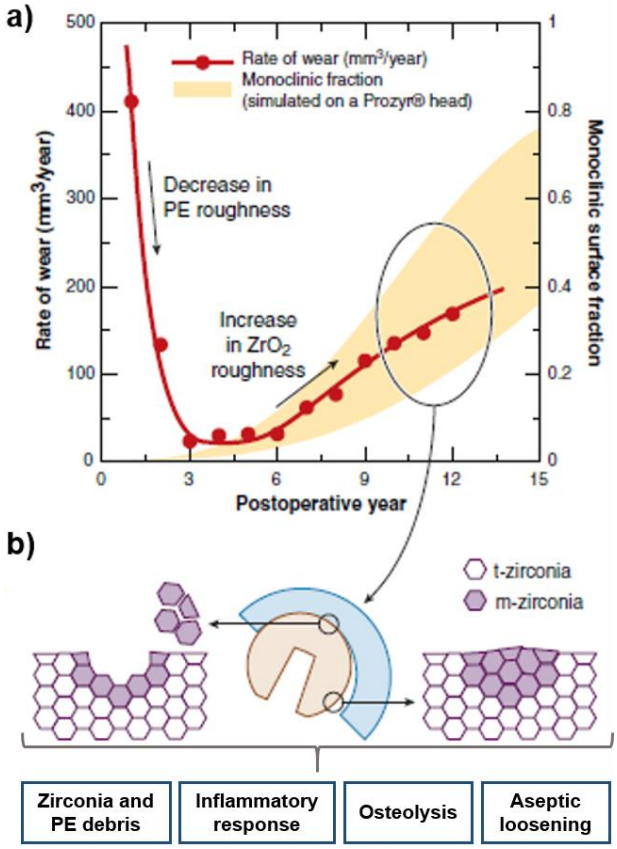

Figure 25. Illustration of aseptic loosening triggered by ageing process of zirconia implant (ball head). (a) Plot of monoclinic fraction zirconia and wear rate vs time (years), (b) scheme of a polyethylene (PE) cup-zirconia ball head after a few years *in vivo*. Adapted from [7]**.**

After the early decrease of wear rate due to polyethylene (PE) polishing by the femoral head, a significant increase in wear rate occurs, that is correlated with the increase in monoclinic content and roughness of the ball head that appear throughout ageing mechanism [7], [86]. Hence, the zirconia grain pullout in the bearing region and polyethylene debris may lead to the appearance of premature osteolysis [7].

Therefore, in order to overcome the problem of wear, nanosized particles (alumina, zirconia) have been used. In 1970, alumina become the most widely used ceramic in total hip arthroplasty, however this ceramic presented a higher fracture toughness [87]. To overcome this brittleness, and the consequent potential failure presented by alumina ceramics, in 1990 zirconia was introduced in the field of orthopedics [1], [8]. Zirconia implants allows a great corrosion resistance, due to the ion *in vivo* release which is significantly smaller in comparison to metallic biomaterials. Metallic prosthetics materials

are more prone to corrosion, thus releasing ions, leading to adverse reaction in the surrounding tissue of the patient [53].

In 1997, the U.S Food and Drug Administration (FDA) announced that the standard steam sterilization procedure (134 ºC, 2 bars) led to the occurrence of surface roughening of temporal head implants and consequently degradation of the material, being the origin of failures due to an accelerated Low Temperature Degradation (LTD) of zirconia [4], [8]. Since then, the LTD degradation has a critical role in zirconia implants. So, diverse studies were done with zirconia implants, demonstrating that even the implants processed under the best conditions could present a certain degree of degradation *in vivo*. Depending on analyses of the results, it was verified that the extent of degradation ranged from roughening (due to surface uplifts), hardness decrease (due to micro-cracking) to failure (slow crack growth), represented in Figure 26 [8].

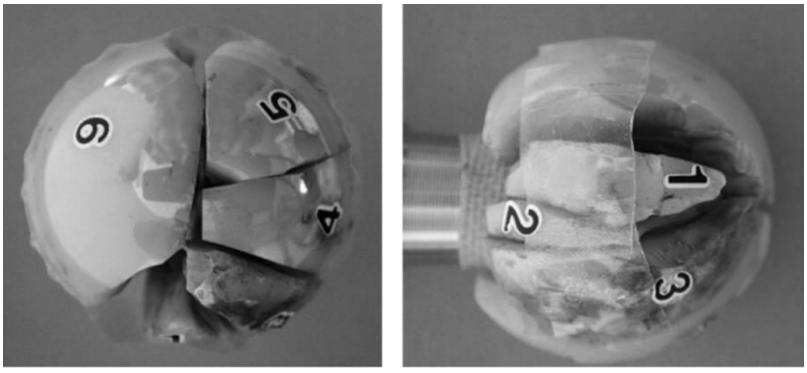

Figure 26. Example of representation of reconstitution of the fractured ball head stabilized with 3% mole of yttria. **a)** Top view and **b)** lateral view. Adapted from [10].

The increase in wear rate caused by the tetragonal to monoclinic phase surface transformation of the zirconia femoral heads, related with roughness, became critical due to the biological interaction with small particles resulting in wear debris. The wear particles created at the contact surfaces penetrate the periprosthetic tissues triggering a macrophage reaction and leading to osteolysis and eventual loosening of the prosthesis and thus, an eventual need for replacement of the implant [8].

2.6.2. Dental Applications

The success of zirconia in orthopedic implants encouraged the development of applications in the dental area. Over the last decade, new dental ceramic materials (like glass ceramics, polycrystalline alumina and zirconia ceramics) with the aid of the new processing technology (computer-assisted fabrication systems (CAD/CAM)) have been

successfully introduced in the dental area. Due to the diversity of dental materials it is possible to produce dental prostheses such as crowns, fixed dental prostheses (FDPs), abutments and removable dental prostheses [8], [16], [81].

Nowadays, titanium and titanium alloys are the materials usually used in implant manufacturing and became the most used material for tooth replacement in dental implantology. These materials present excellent biocompatibility and favorable mechanical properties [88], [89]. The main disadvantage of titanium utilization is associated with esthetic problems, since this material presents dark grayish color [90]. It was described that galvanic side effects were noted after this material become in contact with saliva and fluoride [90]. Even though allergic reactions to titanium are very rare, cellular sensitization has been reported [90]. Due to these disadvantages, the application of others materials was crucial to dental field. Alumina ceramic was used to prepare ceramic crowns, however this ceramic showed failures in the preparation of post crown and implanting abutments, in consequence of its poor bending strength and wear resistance [91]. In general, ceramics are sensitive to shear and tensile loading, and its surface can lead to premature fracture. The introduction of high strength zirconia ceramics as restorative dental materials has created interest in the dental community [41]. The increased worldwide acceptance and interest in using the zirconia ceramic in abutment implants is especially due to aesthetic reasons. They cause a good color response when translucent, metal free restorations are possible and in case of soft tissue recession no metal is exposed. Another interesting characteristic of zirconia abutments is that it avoids the grayish color that appears in the titanium abutments through the soft tissues [11]. In addition, ceramics particles induces less inflammatory response and bone resorption than titanium particles [77], [92].

Zirconia restorations exhibit superior fracture resistance when compared to other materials as was verified by *Luthy* [17], which reported that zirconia restorations presents 755 N of measured load bearing capacities, followed by alumina with 518 N and ceramic reinforced with lithium disilicate with 282 N. In comparison to alumina, the enhanced strength of zirconia can be associated to microstructural differences, such as higher density, smaller particle size and polymorphic mechanism against flaw propagation [81]. Yttria Stabilized Zirconia (YSZ) provides advantages for dental implants in terms of mechanical properties, namely, higher fracture resistance and higher flexural strength, when compared to aluminum oxide [93].

While other ceramics only allow the construction of structures that are resistant to chewing stresses on anterior teeth, the zirconia FPDs demonstrates the capacity to be also applied in molars. Zirconia restorations have been applied in FPDs supported by teeth or

implants. Due to mechanical reliability of zirconia ceramic it is possible to realize single tooth restorations and fixed partial dentures with a single bridge element on both anterior and posterior elements. *Albrektsson et al*. [94] reported that the quality of the implant surface is one major factor that influences wound healing at the implantation site and consequently affects the osseointegration process. Hence, diverse chemical and physical surface modifications have been developed in order to improve the osseous healing [88]. Smooth implant surfaces are not favorable for osseointegration process due to poor interaction with tissues [90].

Zirconia ceramic has been considered a suitable dental implant due to its mechanical properties, biocompatibility and its toothlike color [88]. In order to obtain excellent aesthetic results some physical characteristics of zirconia should be considered, because zirconia not only has a color similar to the teeth but a crucial factor is that this material is opaque [17], [95]. This opacity is an advantage because when a dischromic tooth or metal must be covered, the utilization of zirconia core allows occult this unfavorable aspect, as is showed in Figure 27 [17], [90].

Figure 27. a) Intraoral view of prepared discolored non-vital teeth and of the soft tissue morphology; **b)** Intraoral view of try in of zirconia frameworks on the opacity of the zirconia framework masks the dischromic abutment on the left second premolar. Adapted from [17].

One fragility of zirconia is the core-veneer interface, which can result in ceramic chipping or cracking. The factors that can influence veneer cracking are several, such as differences in thermal expansion coefficients between core and ceramic, firing shrinkage of ceramic, flaws on veneering and poor wetting by veneering on core. So, nowadays, in order to minimize these aspects unfavorable, special ceramics were developed. After veneering and finishing, cementation occurs as represented in Figure 28 [17].

Figure 28. Cemented zirconia-ceramic restorations on left second premolar and first molar. Adapted from [17].

In terms of ageing of zirconia, this can have prejudicial effects on its mechanical properties, where the mechanical stress and moisture environment can accelerate this process of ageing [95]. Through *in vitro* tests, it was observed that the ageing reduces the mechanical characteristics of zirconia ceramics, however the decreasing of the mechanical properties are still into clinical acceptable values, which makes this material promising for dental restorations [95].

In a study of *Butz et al.* [17],diverse characteristics were analyzed, like the survival rate, the facture strength and the failure mode of this type of abutment, and it was verified that after a chewing simulation and fracture loading, zirconia abutments tend to behave like those of titanium (281 N versus 305 N).

According *Scarano et al.* [17], the bacterial adhesion to zirconia is not very significant, being observed that a degree of coverage bacteria from 12.1 % in zirconia to 19.3 % in titanium occurred. These results were analyzed through an *in vivo* study, confirming that zirconia accumulated fewer bacteria in comparison with titanium in terms of the total number of bacteria and by the presence of pathogens (*Rimondini et al*. [96]).

Through clinical studies published [17] to date it is referred that zirconium oxide restorations can be considered reliable for clinic use because this material demonstrates a good tolerance and resistance. However, more biological and mechanical studies are necessary for a total understanding of the behaviour of zirconia in a long time period. In order to indicate the zirconia as a suitable material for prosthetic restorative ceramic it is crucial to evaluate the ceramic bonding, ageing and wear zirconia abutment.

2.6.3. Solid Oxide Fuel Cells (SOFC)

The use of Yttria Stabilized Zirconia (YSZ) materials in applications as an ionic electrolyte in solid oxide fuel cells (SOFC) and sensors (like oxygen sensors) technology has been create a great interest [8].

SOFCs offer many advantages over traditional energy conversion systems including a clean, quiet operation and low pollution technology, i.e., emit very low levels of emissions of CO_2, CO, NO_X and SO_x to generate electricity at high efficiencies [97], [98]. SOFC system, water is generated as a result of the electrochemical reaction [8]. These fuel cells are useful in large and high power applications, such as in electricity generating stations at large-scale.

In recent years, the most studied SOFCs system are based in YSZ, because of its chemical stability, low thermal conductivity, high ionic conductivity and mechanical strength [8]. In the majority of instances, the zirconia ceramic is used in its cubic crystalline form and at high temperatures in order to maximize the ionic conductivity. Commonly, zirconia is stabilized with a high concentration of yttria (typically 8 mol% of yttria (8YSZ)) [8]. SOFC systems based in YSZ normally operate at high temperature (usually above 600 ºC). Under such operating conditions, with both temperature and concentration of stabilizer sufficiently higher, transformation and ageing phenomenon of zirconia are not a problem [99], [8].

There are two situations where the degradation of the zirconia fuel cells may occur under restrictive conditions. One of the situations is due to the utilization of zirconia with lower concentration of yttria, with the purpose of achieve superior fracture toughness. Even though the highest ionic conductivity is achieved by cubic zirconia, inferior fracture toughness properties are obtained. For this reason, some studies have been done to understand the behaviour of tetragonal zirconia with a concentration of 7.6 mol% fraction of yttria as an alternative. As these compositions are metastable, they are susceptible to phase transformation, that will depend if the operating temperature of the fuel cell is above or below of the T_0 (tetragonal to monoclinic transformation) temperature for the chosen yttria concentration. The second situation refers to the development of thinner zirconia electrolytes produced by deposition processes (like sputtering), where these thinner electrolytes show lower impedance resulting on lower cell operating temperatures and some reduced problems related with metal electrode oxidation [8]. It has been demonstrated that the peak of ionic conductivity occurs in thin sputtering zirconia films at 6.5 mol% of YSZ rather than 8 mol% Y_2O_3. As with the other studies, the crucial issue is whether the operating temperature is below the pertinent T_0 (tetragonal to monoclinic transformation) temperature [8].

2.6.4. Thermal Barrier Coating (TBCs)

Zirconia has also been applied as thermal barrier coatings (TBCs) due to its characteristics such as its high melting temperature (2700 ºC), its excellent low thermal conductivity (2 W/mK) and the ability to be plasma sprayed on complex shapes like blades [8]. The function of a TBC is to provide thermal protection to metallic engine components with a thermal gradient, enabling them to be used with other hotter gases for long periods of time [8], [100]. The main applications of TBCs involves the protection of gas turbine blades, vanes, combustors for both aerospace and power generation turbines, cylinders of diesel engines and other applications that involves high temperature insulation [8]. The utilization of TBCs have improved the fuel efficiency and also facilitated the increase in turbine inlet temperatures.

The selected composition was 4 mol% of Yttria Stabilized Zirconia (4 YSZ) due to performed tests after introducing TBCs into gas turbine jet engines. According to recent works [8] it was reported that this metastable composition presents the highest fracture toughness which can be associated with ferroelastic toughening. Through deposition by plasma spraying or electron beam physical vapor deposition, the 4YSZ TBCs are retained in metastable tetragonal zirconia phase material [8], [100].

It has been verified that at high temperatures a slow separation of metastable zirconia into two phases occurs, tetragonal and cubic phase, which presents equilibrium compositions depending on the temperature. When 5 mol% of Yttria Stabilized Zirconia (5 YSZ) is submitted to a high temperature for longer periods of time, as for example after 350 hours at 1425 ºC, it occurs the separation in equilibrium conditions of the tetragonal and cubic phases. These phases can be cooled until room temperature without occurring the transformation to monoclinic phase. Although, when the coating is performed at an intermediate temperature in air, a fraction of the zirconia is transformed into monoclinic phase, being this transformation related with the phenomenon of ageing of the sintered ceramics. This suggests that there is a relation between the size of grains of tetragonal region and its susceptibility to transformations [8].

Chapter 3

Experimental Procedure

3. Experimental Procedure

This chapter summarizes and describes the materials and experimental work developed. The experimental work that was done can be divided in four main parts:

- production and characterization of the 2 mol% Yttria Stabilized Zirconia (2YSZ) doped with different oxides by spray-drying;
- pressing and sintering in a laboratory furnace of the doped 2YSZ samples;
- thermal ageing tests and implementation of mechanical tests (fracture toughness) on the sintered pieces;
- selection of the doped 2YSZ samples with improved resistance to ageing and mechanical properties;
- mechanical (Vickers hardness, fracture toughness and biaxial strength) and hydrothermal ageing resistance tests of the selected doped 2YSZ samples.

The characterization techniques performed to the powders throughout the experimental work are detailed. The purpose of the utilizations of these characterization techniques was to characterize the produced materials in terms of their composition, microstructure, degradation and mechanical behaviour. From the raw materials up to the final characterization of the aged samples, several production and characterization techniques were applied. A general schematisation of the experimental work is displayed in Figure 29.

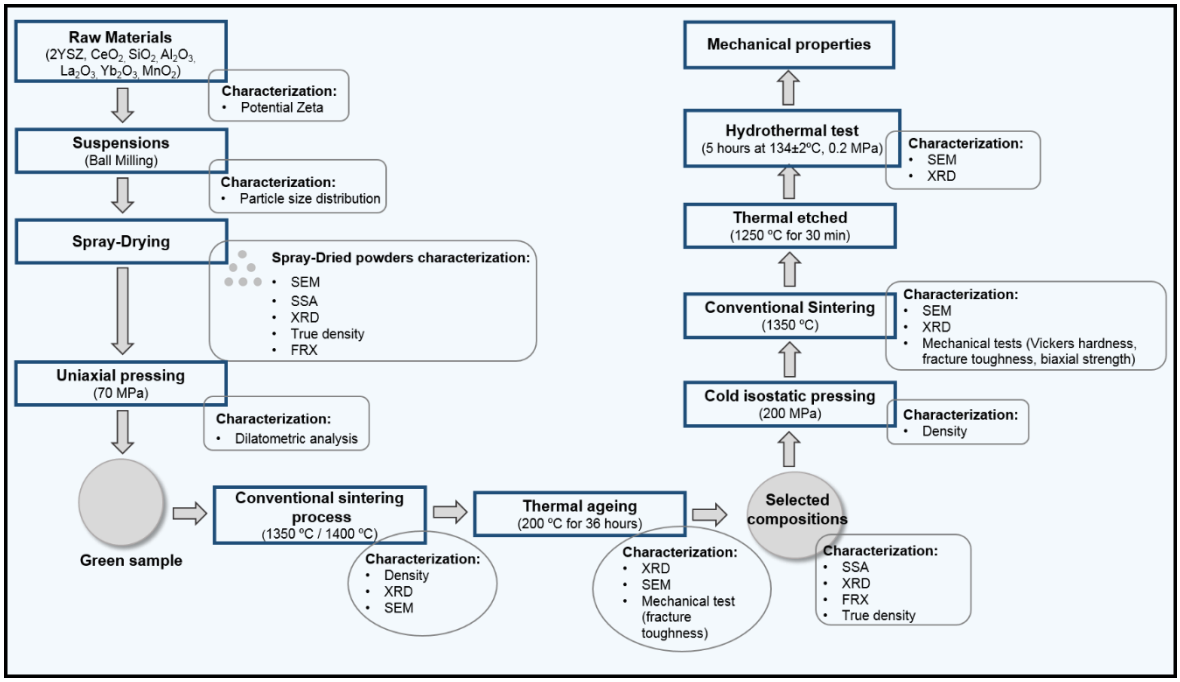

Figure 29. Synopsis of the manufacture process and characterization of doped 2YSZ ceramic on present study.

3.1. Materials

The commercialized 2 mol% Yttria Stabilized Zirconia (2YSZ, INNOVNANO) powder used in the experimental work presented a mean particle size of ~ 50 nm. Ceria, silica, alumina, lanthana, ytterbia and manganese oxides were used as dopants in order to improve the resistance to ageing and mechanical properties of 2YSZ samples.

Ceria (Cerium (IV) Oxide, Sigma Aldrich, > 99.95 %) with a mean particle size of less than 50 nm; Silica (Silicon Dioxide, Sigma Aldrich, 99.5 %), with mean particle size of 10-20 nm; Alumina (Aluminum Oxide, ABSCO Limited, Batch 11612, 99.99 %) provided by INNOVNANO, with mean particle size of ~50 nm; Ytterbia (Ytterbium (III) Oxide, Sigma Aldrich, ≥ 99.7 %), with mean particle size of less than 100 nm; Lanthana (Lanthanum (III) Oxide – for AAS, Sigma Aldrich, ≥ 99.9 %); and Manganese Oxide (Manganese Oxide (IV) Oxide, Sigma Aldrich, ~85 %), with mean particle size of less than 10 μm), were used as dopants to the produced suspensions of 2YSZ.

In order to adjust the pH of the suspensions accordingly to the results obtained from the zeta potential measurements, NaOH (0.5 M and 1 M) and HCl (0.5 M) solutions were used.

3.2. Preparation Methods

Aqueous suspensions of 2YSZ were prepared according to the defined compositions using different dopants (ceria (CeO_2), silica (SiO_2), alumina (Al_2O_3), lanthana (La_2O_3), ytterbia (Yb_2O_3), and manganese oxide (MnO_2)), represented in Table 6. According to the literature [45]-[59], [64], the selected dopants provide an enhanced stability of the tetragonal phase, resulting in an increased ageing resistance and/or mechanical properties of Yttria Stabilized Zirconia (YSZ). For each dopant added to 2YSZ three or four compositions were developed, being the selected amounts based in the results published in literature [45]-[59], [64].

Table 6. Defined compositions for the 2YSZ doped with different oxides.

	Compositions
CeO_2	2 mol% Yttria Stabilized Zirconia and 0.25 wt% of CeO_2
	2 mol% Yttria Stabilized Zirconia and 0.5 wt% of CeO_2
	2 mol% Yttria Stabilized Zirconia and 0.75 wt% of CeO_2
SiO_2	2 mol% Yttria Stabilized Zirconia and 0.25 wt% of SiO_2
	2 mol% Yttria Stabilized Zirconia, 0.25 wt% of SiO_2 and 0.25 wt%Al_2O_3
	2 mol% Yttria Stabilized Zirconia, 0.25 wt% of SiO_2 and 1.07 wt%La_2O_3
Yb_2O_3	2 mol% Yttria Stabilized Zirconia and 13.12 wt% of Yb_2O_3
	2 mol% Yttria Stabilized Zirconia and 19.68 wt% of Yb_2O_3
	2 mol% Yttria Stabilized Zirconia and 26.24 wt% of Yb_2O_3
MnO_2	2 mol% Yttria Stabilized Zirconia and 0.025 wt% of MnO_2
	2 mol% Yttria Stabilized Zirconia and 0.05 wt% of MnO_2
	2 mol% Yttria Stabilized Zirconia and 0.25 wt% of MnO_2
	2 mol% Yttria Stabilized Zirconia and 0.75 wt% of MnO_2

3.2.1. Preparation of the Suspensions

Before preparing the suspensions, zeta potential measurements were performed in order to determine the stability range of each material. The pH value was adjusted with the purpose to achieve a stabilized initial suspension for each composition.

In order to control the particle size, the suspensions were submitted to a stage of ball milling. Ball milled doped 2YSZ were spray dried. The parameters of the spray drying were optimized in preliminary stages of this study.

3.2.1.1. Zeta Potential

The zeta potential of zirconia and dopant powders was measured in order to characterize the electrochemical equilibrium of the particles in suspension, in accordance to the stabilized suspension.

The magnitude of this parameter gives an indication of the stability of the colloidal system. If the particles in suspension present a large negative or positive potential they tend to separate and the suspension is stabilized. On the other hand, if the particles have a low zeta potential value, i.e., near zero (isoelectric point), they will be agglomerated [101]. At this point the suspension is highly unstable. To prevent agglomeration of the particles in the suspension, the adequate pH value of the medium was determined.

This parameter was determined in a Zetasizer Nano ZS (Malvern Instruments), with a zetasizer nano series 6.00 software (Figure 30). This equipment analyses the mobility of the particles in a liquid medium when an electrical field is applied to the suspension. The velocity of the particles is proportional to their zeta potential. The velocity of the movement of the particles is measured by laser electrophoresis which allows to calculate the electrophoretic mobility (zeta potential) [102].

Figure 30. The measurements of zeta potential was performed on Zetasizer Nano ZS from Malvern, Available at the University of Aveiro.

In order to ensure a constant ionic strength of all materials, a solution of KCl (10^{-3} M) was used as the dispersing medium. To adjust the pH value of the suspensions, HCl (0.001 M - 0.1 M) and NaOH (0.001 M - 0.1 M) were added. Measurements of zeta potential were performed in the pH range of 2 to 11.

3.2.1.2. Ball Milling

In accordance with the amounts of zirconia and dopant powders defined for each composition (wt%), the aqueous suspensions were prepared. Preliminary tests allowed to adjust the spray drying conditions. For the compositions of doped 2YSZ the aqueous suspensions should have a solid content of 3 % with the objective of taking advantage of the maximum yield rate of the atomizer.

The aqueous suspensions were submitted to a deagglomeration process with the aim to achieve a controlled size distribution of the powders. Distilled water was added to the

powders, on adequate proportion, on a micrometric bead mill at 3500 rpm for 15 minutes, Dispermat®- SL12-nano (VMA) (Figure 31).

Figure 31. Micrometric bead mill Dispermat® SL12-nano, available at INNOVNANO.

After milling of the powders the particle size distribution of the particles in aqueous medium was measured in a Mastersize 2000 (Malvern) (Figure 32). This process was important to verify if the particles were well deagglomerated. After obtaining the particle size distribution, the buckets containing the suspensions were stored, to be used in a spray drying equipment.

Figure 32. Malvern Mastersizer 2000, available at INNOVNANO.

3.2.2. Spray Drying Process

Before submitting the suspension to the spray drying process, the pH of the suspensions was measured, under stirring, and adjusted with a NaOH solution (0.5 M and 1 M) to achieve an appropriate value (approximately 10 - 11) defined from the zeta potential measurements. The several compositions of doped 2YSZ granules were then obtained on a laboratorial spray dryer, Büchi Mini Spray Dryer B-191, with a 73 µm nozzle (Figure 33-(b)).

Spray drying is a technique based on the transformation of aqueous solutions or emulsions into a dry powder by atomization. This process became widely used in the chemical industry, in research, from pharmaceutical up to nanotechnology areas [103], [104]. The principle of this method consists in the evaporation of moisture from an atomized feed which occurs in a drying chamber, by mixing the droplets of the spray and the hot drying air. The contact between the droplets of the suspension and the intense heat causes the solvent in the droplets to evaporate, resulting into an efficient drying powder process. Figure 33 illustrates the spray drying process and the laboratorial equipment that was used.

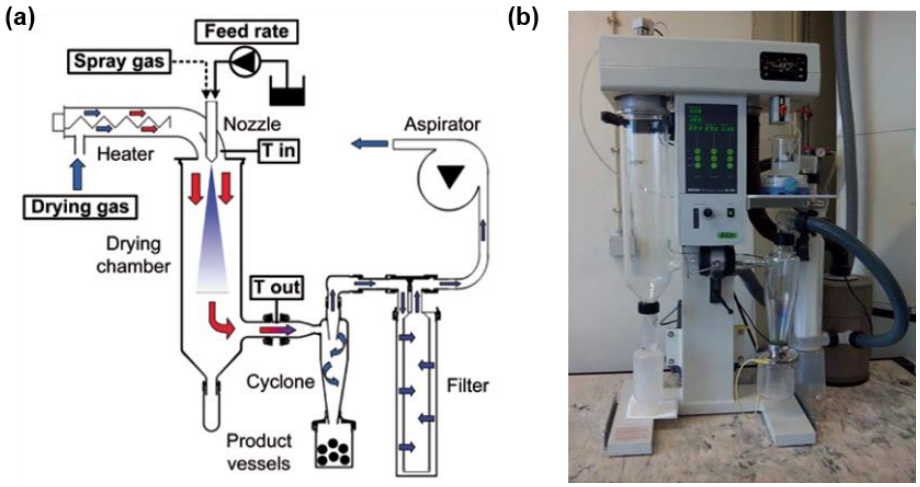

Figure 33. Spray drying process. **(a)**: Representation schematics of the spray drying process from [105]; **(b)**: Laboratorial Büchi Mini Spray-dryer B-191 available at the University of Aveiro.

Regarding the final powders features, such as grain size, morphology and microstructure, this process can be controlled by changing some adjustable parameters such as the inlet and outlet temperature, the feed rate of the peristaltic pump, the flow rate of both spray and drying gases, and the nozzle diameter. The inlet temperature is understood as the temperature of the heated drying air and it is measured prior to the suspension flow into the drying chamber. The outlet temperature is the temperature of the air containing the solid particles outside the entrance of the cyclone. This last parameter is the result of the intense heat and mass transfer in the drying cylinder and it cannot be regulated but it is influenced by other parameters such as the peristaltic pump performance (feed rate), aspirator flow rate, and the concentration of the suspension being atomized. All these parameters can influence the residual moisture present in the product, the particle size and morphology, the yield rate of the process and the temperature load [106].

In order to obtain the maximum yield of this process, the equipment was submitted to a set of optimization tests in order to adjust the operation (Table 7).

Table 7. Established parameters for Büchi Mini Spray-dryer B-191.

Parameter	Value
Inlet Temperature (ºC)	170 ºC
Outlet Temperature (ºC)	~90 ºC
Aspirator Flow Rate (%)	95 %
Pump Performance (%)	25 %

The established parameters were followed and then the obtained powders were stored. In this study, the defined 2YSZ doped suspensions were spray-dried without the use of binders or any dopants.

3.2.3. Processing of green and sintered bodies

The spray dried powders were submitted to uniaxial cold pressing in a hydraulic press(Specac's Laboratory Hydraulic Press), at 70 MPa (Figure 34), and cylindrical green bodies with approximately 2 cm of diameter were obtained.

Figure 34. Specac's Laboratory Hydraulic Press, available at INNOVNANO.

The thermal ageing resistance and the fracture toughness of the samples have been evaluated and the best compositions were selected. After this selection, the obtained powders were submitted to uniaxial pressing (in the same conditions of the previous samples) and cold isostatic pressing (CIP).The uniaxially pressed bodies were subjected to CIP at 200 MPa, for ten minutes on a Wet Bag Cold Isostatic Press from Autoclave Engineers Press (available at University of Aveiro). Through this additional stage of pressing (CIP), an increase of the density of the green bodies was expected.

The sintering temperature was selected from dilatometry results of the samples. The green bodies were sintered at 1350 ºC and 1400 ºC (only for ytterbia doped 2YSZ sample)

for three hours, performed in air, in a laboratory furnace (Termolab MLR, with a maximum operating temperature of 1700 ºC).A sintering cycle with a heating rate of 2 ºC/min and a cooling rate of 5 ºC/min was applied for all samples as schematic representation can be seen in Figure 35.

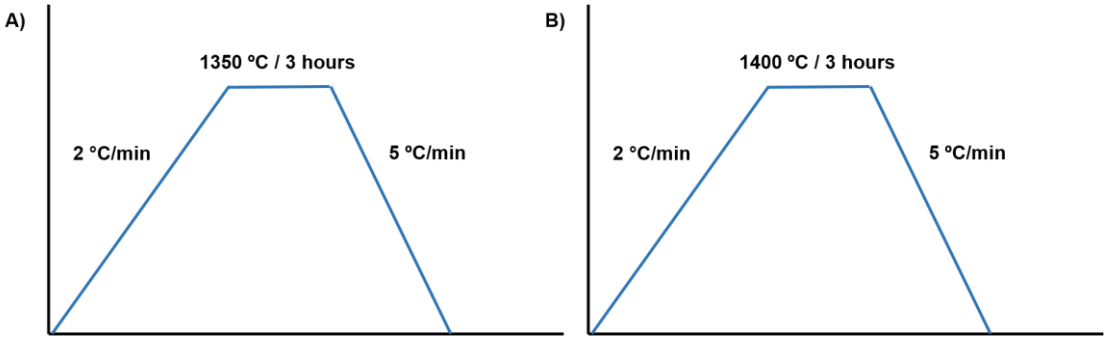

Figure 35. Schematic representation of sintering cycle applied on samples: **(A)** all green doped samples except **(B)** samples 2YSZ doped with Yb_2O_3.

3.3. Thermal ageing tests

In order to evaluate the degradation behaviour of zirconia, the stability of its tetragonal phase under ageing conditions was analyzed by a thermal ageing test performed in a laboratory furnace available at INNOVNANO. As previously mentioned, the ageing of zirconia, also called as Low Temperature Degradation (LTD), is a process caused by the progressive spontaneous slow transformation of the tetragonal phase into the monoclinic phase in absence of any mechanical stress [4], [7], [8], [11]. Since this phenomenon starts from the surface of the zirconia, loss of density, reduction in strength and toughness are observed. The fracture toughness of Yttria Stabilized Zirconia (YSZ) is significantly decreased at low temperatures, due to the formation of micro-cracking accompanied with the tetragonal to monoclinic phase transformation on the surface of the sintered ceramics [107]–[109]. The most critical temperature range for ageing development is around 200 ºC to 300 ºC [110]–[112]. According to *Masaki T.* [113], when the ageing is performed at temperatures around 200 ºC, a thermodynamic contribution that promotes the enhancement of the content of monoclinic phase occurs.

Before performing the ageing tests, the surface of the sintered pieces was polished. Firstly, a rough polishing with abrasives (MD-Piano #220, MD-Piano #1200) was performed and after that, a fine polishing was carried out using 9, 3 and 1 µm diamond paste. One piece of each composition was used to be tested at different times of degradation, being the samples exposed to a temperature of 200 ºC for 12 and 36 hours in a laboratory furnace at INNOVNANO, with both heating and cooling rates of 10 ^{0}C/min. X-ray diffraction was

performed on each aged sample in different time stages and the phase quantification with Diffract^{Plus} TOPAS software from Buker AXS was analyzed

3.4. Mechanical tests

Mechanical tests were performed in order to fully characterize the mechanical behaviour of the obtained sintered samples. Enhancement of the mechanical properties of 2YSZ ceramic is important for its wide range of applications, as already mentioned. Three different parameters were measured, namely, biaxial flexural strength, Vickers hardness and fracture toughness. Each one of these mechanical parameters was measured using equipment at INNOVNANO (Figure 36, 37).

3.4.1. Biaxial flexural strength

Biaxial flexural strength or bending strength is an important analysis to take in consideration when working with these ceramics. This test consists in placing the sample between two coaxial rings of unequal diameter and applying a compressive force, allowing a determination of the maximum stress and deflection of the material before its fracture. The ISO 13356:2008 standard [13] imposes strict requirements for this parameter in terms of mechanical testing equipment (compressive load applied, calibration), preparation of test piece (test pieces must have circular shapes, the diameter and thickness of the test pieces must be measured before performing the mechanical test), the value for YSZ samples must be equal or greater than 500 MPa and a minimum of ten samples must be used.

Before performing this test, the sintered pieces were submitted to a fine polishing on both surfaces. Ten pieces of each selected samples were subjected to this test.

The flexural strength was determined by a 3-point test (piston-on-three-ball). The equipment used for this test was a Testing Machine Zwick/Roell Z020 (Universal Materials) as displayed in Figure 36.

Figure 36. Biaxial flexural strength equipment: Testing Machine Zwick/Roell Z020 from Universal Materials, available at INNOVNANO.

For each selected composition of doped 2YSZ, the flexural values were obtained from five different measurements. Thereafter, the average value was calculated.

3.4.2. Vickers Hardness

The Vickers hardness test is one of the most used indentation hardness tests. Indentation hardness of a sample expresses its capacity to resist to deformation caused by a constant compression load from a sharp object (indenter). The Vickers hardness test utilizes a square-based diamond pyramid indenter with an angle of 136 º between the opposite faces at the vertex. This indenter is pressed against the surface of the test sample using a predefined force (F). This charge is maintained for 10 to 15 seconds. After the removal of the indenter, the diagonal lengths of the indentation are measured and the arithmetic mean is calculated. The Vickers hardness value (HV) is obtained by the equation (5),

$$HV = \frac{F}{A_{ind}} \tag{5}$$

where F corresponds to the applied force in kgf and $A_{ind}$is the surface area (mm^2) of the resulting indentation measured from the following equation,

$$A_{ind} = \frac{d^2}{2sin\left(\frac{136°}{2}\right)} \approx \frac{d^2}{1.8544} \tag{6}$$

where d represents the average length of the diagonal in millimetres resulting from the indentation. The Vickers Hardness (HV) can be calculated from the equation (7).

$$HV = \frac{F}{A_{ind}} \approx \frac{1.8544F}{d^2} \quad (7)$$

Where HV value can be obtained by multiplying *F* by the standard gravity value (9.807 m/s^2) and by converting millimetres to meters (d (m)).

The hardness of the sintered samples was characterized using the WIKI 100B system (Affri) with Affri Fully Automatic System software (Figure 37). The analysed surfaces of the selected doped 2YSZ samples were subjected to a fine polishing. Ten Vickers indentations were measured in different pieces and surface points of each sample, using a load value of 9.806 N. For each indentation, the test force was applied during 15 seconds. The values of each analysis were obtained by software and then an average value was calculated from the referred ten different measurements.

Figure 37. Vickers Hardness equipment: WIKI 100B Vickers Hardness Tester, available at INNOVNANO.

3.4.3. Fracture Toughness

The fracture toughness (K_{IC}) of the compositions was measured using the method of crack indentation. Regarding the indentations left from the hardness tests, the determination of the fracture toughness was performed. When the crack is developed only at the corners of the indentation, it is designed by Palmqvist (type Pq). The fracture toughness values of the samples was calculated based on Niihara equation [114], commonly used for the determination of this mechanical parameter in zirconia ceramic. Equation (8) was used:

$$3K_{IC} = 0.035 \left(Ha^{\frac{1}{2}}\right)\left(\frac{3E}{H}\right)^{0.4}\left(\frac{d}{a}\right)^{-0.5} \quad (8)$$

where *H* represents the Vickers hardness, *a* (m) is half distance of indent diagonal, *E* (MPa) is the Young's Modulus, and *d* (m) is the crack length. The value of the applied Young's Modulus was 210 MPa [1].

In order to determine the values of the fracture toughness the samples were subjected to a fine polishing (9, 3 and 1 µm diamond paste). Five indentations were performed in different surface points of each initial sample and an average value was calculated and taken in consideration.

The selected compositions were submitted to ten measurements and an average value of this parameter was calculated and selected. An optical microscopy was used in order to measure the crack length.

3.5. Accelerated ageing test

The selected doped 2YSZ compositions were submitted to ageing tests according to the International Standard ISO 13356:2008 [13], with the purpose of evaluating the stability of the tetragonal phase, when exposed to aggressive ageing conditions.

The accelerated ageing tests were executed at CTCV Materials, Coimbra. The samples were placed in an autoclave where they were exposed to steam under specified conditions of temperature and pressure, i.e., 134 ± 2 ºC and 0.2 MPa. For this test, ten pieces of each selected samples were submitted to 5 hours of ageing as specified by the ISO standard [13]. Before submitting the samples to ageing tests, they were polished using a 9, 3 and 1 µm diamond paste on a Struers TegraPol-25 polishing machine available at INNOVNANO and afterwards, these same samples were thermal etched in air at a temperature 100 ºC lower than the sintering temperature during 30 minutes, with both heating and cooling rate of 10 ºC/min.

3.6. Characterization Techniques

The produced materials were fully characterized through several characterization techniques. Firstly, the powders of 2YSZ doped with different dopants obtained from spray drying were characterized. With the implementation of conformation, sintering, ageing resistance and mechanical properties, diverse characterization techniques were performed. Throughout this section, the most important details about the characterization techniques used during different stages of this experimental study are described.

3.6.1. Characterization of the spray dried powders

Particle size distribution, content of crystalline phases, morphology, specific surface area, density, chemical compositions and thermal behaviour of the obtained spray dried powders were evaluated.

3.6.1.1. Particle size distribution

A Malvern Mastersizer 2000 (Figure 32) was used to measure the particle size distribution of the particles. This equipment uses laser diffraction to measure the size of the particles present in a well dispersed suspension. The intensity of the light scattered by the particles is determined considering a wide number of angles and converted to the size of the analysed particle through an algorithm of appropriate refraction model [115].

3.6.1.2. X-ray diffraction

X-ray diffraction is a non-destructive technique crucial to characterize the materials, since it allows to identifying and quantifying their crystalline phases. Through this technique, other structural properties can be analysed, namely, the crystallite size, degree of crystallinity and lattice parameters [116]. The emission of a monochromatic X-Ray beam towards a sample material, with regularly spaced atoms, makes each atom to become a source of radiation. This phenomenon will cause constructive and destructive interference of the waves emitted by the atoms. A diffracted beam results from the constructive interferences, because only the constructive interference waves correspond to maximums of diffraction [117]. The condition of the constructive interference is obtained by Bragg's Law (equation (7)). This law describes the phenomenon of X-ray diffraction, i.e., the relation between the diffraction angle and inter-planar spacing necessary to create constructive interfaces. The illustrative representation of this theory can be observed in Figure 38 – (a).

$$n\lambda = 2dsin\theta \quad (7)$$

In equation (7), *n* corresponds to a whole number, i.e., it is the diffraction order (*n* = 1,2,3 ...), λ is the wavelength of the incident radiation, d is the inter-planar spacing for the set of planes hkl (Miller indices) of the crystal structure, and θ is the incident angle of the beam in the material [117]. By varying the diffraction angle (2θ) and measuring the diffracted beam intensity, a diffractogram can be obtained. In order to identify the sample structure,

the obtained diffractograms were compared with the Powder Diffraction Files (PDF files) from the International Centre for Diffraction Data (ICDD).

The identification of the crystalline phases was determined by X-ray diffraction, on a Bruker D8 Advance X-ray diffractometer (XRD) with Cu Kα radiation (λ = 1.5406 Å) in the 2θ range from 5 ° to 80 ° at room temperature (Figure 38 - (b)).

The detected phases were thereafter quantified on Diffrac^{Plus} EVA software from Buker AXS, using the Rietveld refinement and matching with ICDD files. Rietveld refinement uses a least squares approach to refine a theoretical result until it corresponds to the measured profile. In order to analyse the amount of monoclinic and tetragonal zirconia phase, the Diffrac^{Plus} TOPAS software from Buker AXS was used.

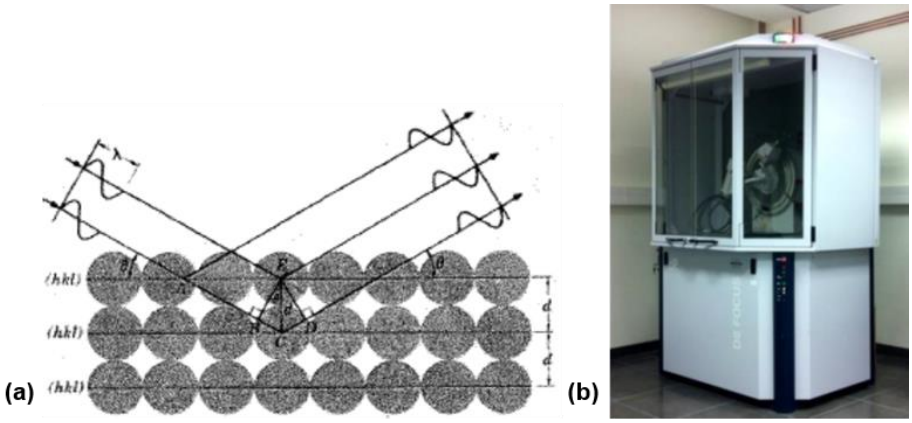

Figure 38. Illustrative representation of Bragg´s Law **(a)** (adapted from [61]) and the XRD equipment: Bruker D8 Advance X-ray diffractometer, available at INNOVNANO **(b)**.

3.6.1.3. Scanning electron microscopy

Scanning electron microscopy (SEM) can supply high resolution images of the surface of a sample at the nanometer scale. In order to obtain an image by SEM a highly energetic electron beam is emitted to the sample and several interactions can occur, such as absorption, reflection and emission of electrons [118]. SEM images are formed by the detection of secondary electrons emitted by the sample, which are detected by the equipment creating contrast and thus, an image is formed.

The spray dried granules morphology was observed by SEM, on HITACHI S-4100 microscope, available at University of Aveiro (Figure 39). The equipment presents an electron emission system tungsten filament with 25 kV of acceleration and 15 Å of maximum resolution. The powders were deposited on an aluminium sample holder, with carbon tape, and then covered by carbon thin film, on a EMITECH K950 carbon sputter equipment.

Figure 39. SEM used for observation of the spray dried granules morphology: HITACHI S-4100 microscope, available at University of Aveiro.

3.6.1.4. Specific surface area

Specific surface area (SSA) is defined as the ratio A/m (m^2/g) between the absolute surface area of a solid *A* and its mass, *m*. The SSA can be evaluated by a gas adsorption method, where a nonreactive gas (N_2) is adsorbed on the particles surface at the temperature of the N_2 boiling point (77 K), at a single or at multiple pressures. The amount of gas molecules required to cover the entire surface (external and the accessible internal pores surface) of a solid with a monomolecular layer is determined using the Brunauer-Emmett-Teller (B.E.T.) adsorption isotherm method [119]. This monolayer capacity can be determined using equation (9) [120].

$$\frac{P}{V_a(P_0 - P)} = \frac{c-1}{V_M c} \times \left(\frac{P}{P_0}\right) + \frac{1}{V_M c} \quad (9)$$

P and P_0 correspond respectively to the equilibrium and the saturation pressure of the gas at the temperature of adsorption, V_a is the adsorbed gas volume, V_M represents the volume of adsorbed gas monolayer and c is the B.E.T. constant that is associated to the enthalpy of adsorption of the adsorbed gas on the sample material.

The adsorptive gas is only physically adsorbed by van der Waals forces, and it can be desorbed when a decrease of pressure occurs at the same temperature.

The specific surface area of the commercial and of the doped 2YSZ powders were determined using the multipoint Brunauer-Emmett-Teller (B.E.T.) isotherm in a Quantachrome Nova 1000e Series System, with NovaWin software, available at INNOVNANO (Figure 40).

Figure 40. Specific surface area equipment: Nova 1000e Series System (Quantachrome) equipment, available at INNOVNANO.

3.6.1.5. True density

Gas pycnometers are the most commonly used equipments to determine the truedensity (or more specifically the volume) of the powders and bulk materials. The density is calculated using the measured drop in pressure when a determined amount of gas is allowed to expand into a chamber where the sample is contained. This parameter also excludes the presence of any pore volume accesible to the gas, i.e., presents closed porosity in the measured volume. In this analysis, a known mass of powder is placed into a cell of known volume. Then, the gas is introduced into the cell (in vacuum) and occupies the entire volume of this cell that is not occupied by the sample. The volume of the sample is determined, and thus the true density of the sample powder can be obtained. Helium is the most used gas because it presents a high diffusivity, and therefore can penetrate the finest pores [121].

The doped 2YSZ powder density was determined in vacuum using a AccuPyc II 1340 pycnometer (Micromeritics) and helium as measurement gas, available at INNOVNANO (Figure 41). The results of the true density of each sample were obtained by the mean value of ten different cycles.

Figure 41. Helium pycnometer: Accupyc II 1340 picnometer from Micrometrics, available at INNOVNANO.

3.6.1.6. X-ray Fluorescence

X-ray fluorescence (XRF) is a technique that allows qualitative and quantitative elemental analysis of powder samples. It consists of an intense X-rays beam collision with an atom from the sample that will become unstable, producing an ejection of an electron from the low energy level. Then, this vacant space will be filled by an electron from a higher energy level. These changes in energy levels cause differences of energy resulting in the release of secondary X-rays, which are characteristic of the element and allows to perform the chemical composition analysis [122].

XRF is an accurate method with fast acquisition of data, i.e., just few minutes, and it can be done in air (it does not demand a vacuum medium). Furthermore, it has the advantage of being a non-destructive technique and the samples to be analysed do not require any special preparation [123].

To evaluate the chemical composition of each sample a Buker-AXS S4 Pioneer X-ray Fluorescence with a rhodium X-ray source was used, being controlled by the SpectraPlus software, available in INNOVNANO (Figure 42).

Figure 42. Equipment of X-ray Fluorescence Spectrometer (Bruker-AXS S4 Pioneer), available at INNOVNANO.

3.6.1.7. Thermal analysis - Dilatometry

Dilatometry is a technique used for precise measurement of dimension changes in a sample throughout a specific temperature cycle, which allows the evaluation and selection of an adequate sintering cycle of the materials. Through this analysis, the information about the linear thermal expansion/shrinkage (Y=$\Delta L/L_0$) and respective shrinkage rate (dY/dt) as function of temperature (ºC) can be obtained.

The dilatometric tests were realized on a vertical dilatometer Linseis L-75 Platinum Series in air (Figure 43) where the cylindrical powder compacts were nonisothermal sintered up to 1600 ºC with a constant heating rate of 2 ºC/min and a cooling rate was maintained constant at 10 ºC/min.

Figure 43. Vertical dilatometer (Linseis L-75 Platinum Series), available at INNOVNANO.

3.6.2. Characterization of the green and sintered bodies

The conformation stage was performed after obtaining and characterizing the doped 2YSZ powders. In the following section all the techniques used for the characterization of the green and sintered pieces throughout this study are indicated and described.

3.6.2.1. Density measurement

The density of the green pieces was geometrically measured and determined by the ratio between the weight and the geometric volume of the samples (geometric density), as expressed in equation (10),

$$GD = \frac{m}{\pi \left(\frac{d}{2}\right)^2 h} \quad (10)$$

, where m, d and h correspond respectively to the mass, the diameter and the height of the sample. The green density of the selected doped 2YSZ samples was determined considering a mean value achieved from ten samples of each composition, pressed under the same conditions.

The density of the sintered samples (final density, ρ_f) was determined by the Archimedes liquid immersion technique considering the equation (11),

$$\rho_f = \frac{m_d}{m_s - m_i} \times \rho_{liq} \quad (11)$$

where m_d corresponds to the mass of the dried sample, m_s is the mass of the soaked sample, m_i is the mass of the immersed sample and ρ_{liq} is the density of the immersion liquid. In this measurement, distilled water was used. The final correspondent density values of thirteen initial composition were determined by the average of five different samples for each tested composition. In the selected doped samples, the final density value was obtained using ten samples of each composition.

3.6.2.2. X-ray diffraction

To investigate the presence of monoclinic zirconia phase in the sintered pieces, X-ray diffraction was also performed, on Bruker D8 Advance X-ray diffractometer (INNOVNANO) with Cu Kα radiation (λ=1.5406 Å) under the same diffraction angle (2θ) range as described in section 3.6.1.2. The same analysis was carried out in samples of each composition subjected to different hours of ageing resistance tests. Phase quantification was performed on Diffrac^{Plus} TOPAS software from Buker AXS by means of Rietveld refinement.

3.6.2.3. Scanning electron microscopy

The morphology and grain boundaries of each doped zirconia sample were evaluated by scanning electron microscopy (SEM). Posteriorly to sintering process, the sintered pieces were polished on a Struers TegraPol-25 polishing machine, at INNOVNANO. This last procedure is important because the sintered ceramic pieces surfaces always present surface irregularities, being thus necessary a fine polishing after sintering. In order to remove scratches until the desired surface finishing, a rough polishing with abrasives was

performed. Afterwards, a fine polishing was performed using 9, 3, and 1 μm diamond paste. To properly observe the microstructure and grain boundaries, the selected samples were thermal etched in air at low temperature (100 ºC lower than the sintering temperature for 30 minutes, with heating and cooling rates of 10 ºC/min). A HITACHI S-4100 microscope (University of Aveiro) was used and the samples were placed on an aluminium sample holder with carbon tape, being covered with a carbon thin film, on a EMITECH K950 carbon sputter.

By the stereology's line interception method, the grain size of each sample was measured with the obtained micrographs, using the image processing tool ImageJ 1.48v. In Figure 44 is represented the used method.

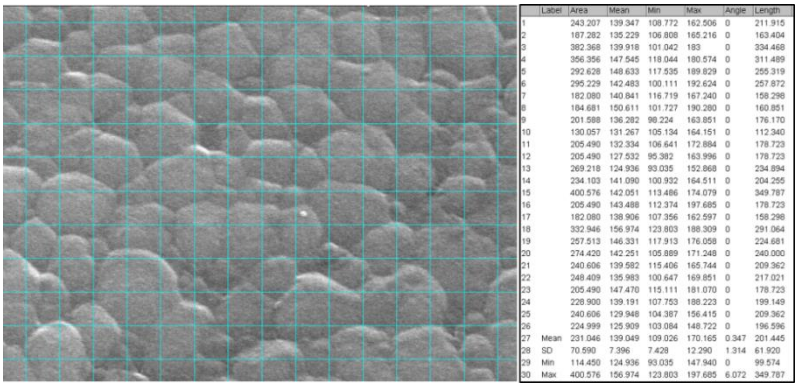

	Label	Area	Mean	Min	Max	Angle	Length
1		243.207	139.347	108.772	162.506	0	211.915
2		187.282	135.229	106.808	165.216	0	163.404
3		382.368	139.918	101.042	183	0	334.468
4		356.356	147.545	119.044	180.574	0	311.489
5		292.628	148.633	117.535	189.829	0	255.319
6		295.229	142.483	100.111	192.624	0	257.872
7		182.080	140.841	116.719	167.240	0	158.298
8		184.681	150.611	101.727	190.280	0	160.851
9		201.588	136.282	98.224	163.851	0	176.170
10		130.057	131.267	105.134	164.151	0	112.340
11		205.490	132.334	106.641	172.884	0	178.723
12		205.490	127.532	95.382	163.996	0	178.723
13		269.218	124.936	93.035	152.868	0	234.894
14		234.103	141.090	100.932	164.511	0	204.255
15		400.576	142.051	113.486	174.079	0	349.787
16		205.490	143.488	112.374	197.685	0	178.723
17		182.080	138.906	107.356	162.597	0	158.298
18		332.946	156.974	123.803	188.309	0	291.064
19		257.513	146.331	117.913	176.058	0	224.681
20		274.420	142.251	105.889	171.248	0	240.000
21		240.606	139.582	115.406	165.744	0	209.362
22		248.409	135.983	100.647	169.851	0	217.021
23		205.490	147.470	115.111	181.070	0	178.723
24		228.900	139.191	107.753	188.223	0	199.149
25		240.606	129.948	104.387	156.415	0	209.362
26		224.999	125.909	103.084	148.722	0	196.596
27	Mean	231.046	139.049	109.026	170.165	0.347	201.445
28	SD	70.590	7.396	7.428	12.290	1.314	61.920
29	Min	114.450	124.936	93.035	147.940	0	99.574
30	Max	400.576	156.974	123.803	197.685	6.072	349.787

Figure 44. Illustration of grain size measurement by the line interception method, by ImageJ software.

It was assumed that the grains were spherical using the correction factor given by Fullman [124], and thus proceed to measuring each grain of each compositions of doped 2YSZ. Through measuring of length of random interceptions, the average grain size can be determined using equation (12),

$$\bar{\mathrm{G}} = K\,\frac{\sum L}{N} \tag{12}$$

where $\bar{\mathrm{G}}$ corresponds to the mean grain size, K means the correction factor (1.5 for spherical grains [124]), L is the length of the line interception and N is the total number of line interceptions. For each sample two micrographs with the same magnification were acquired. Several measurements were performed in each micrograph used for each composition of doped 2YSZ.

3.6.3. Characterization of the aged samples

To evaluate the ageing resistance, the doped 2YSZ samples were submitted to two different ageing tests. In order to select the compositions with improved ageing resistance, one piece of each defined compositions was submitted to thermal ageing tests during 36 hours. After testing, the fracture toughness of aged samples was measured. Fracture toughness parameter is the first step in predicting the clinical performance of dental and orthopedic zirconia. Even though zirconia presents a higher hardness (1200 HV), the fracture toughness is the most relevant property in the study of degradation. This mechanical property is defined as the level of critical stress at which a particular defect at grain starts to grow. It indicates the material piece ability to resist to crack propagation, avoiding the catastrophic fracture [125]. The increase of the fracture toughness occurs when a sample is submitted to stress (internal or external), developing a micro-crack. This micro-crack starts to propagate at the surface of the material and a phase transformation of zirconia occurs, decreasing the propagation velocity of the micro-crack. As mentioned, this mechanism increases the fracture toughness which consequently toughens zirconia ceramic.

After the ageing test and the assessment of mechanical properties (fracture toughness) of all samples, the best compositions were selected. Therefore, only the selected composition samples were subjected to hydrothermal ageing tests. The recovered samples from ageing tests were characterized by the techniques described below.

3.6.3.1. X-ray diffraction

In order to evaluate the degradation of both samples submitted to thermal and hydrothermal ageing tests, X-ray diffraction was performed on the polished surface of each sample piece using the same Bruker D8 Advance X-ray diffractometer (INNOVNANO) with the same previous used conditions. The zirconia phase quantification of each sample was performed with Diffrac^{Plus} TOPAS software from Buker AXS.

3.6.3.2. Scanning electron microscopy

To evaluate the extension of the bulk degradation, a cross sectional view of all initial compositions which were submitted to thermal ageing tests was performed by scanning electron microscopy (SEM) using a HITACHI S-4100 microscope, in which the samples were covered with carbon using a EMITECH K950 carbon sputter. The selected samples,

i.e., the samples that presented improved resistance to ageing degradation and better mechanical properties were then subjected to hydrothermal ageing. These samples were also observed by SEM in the same way.

3.6.3.3. Mechanical tests

After hydrothermal ageing tests for a period of 5 hours, required by ISO 13356:2008 [13], the mechanical properties of the best selected samples were investigated. The Vickers hardness, fracture toughness and biaxial flexural strength were determined in the same conditions as those of the initial samples. These tests had the purpose of comparing the mechanical properties before and after the ageing test and to observe the influence of the oxides addition to zirconia on the mechanical properties of the different doped samples.

Chapter 4

Results and Discussion

4. Results and Discussion

4.1. 2YSZ Compositions

In this chapter the results obtained for the synthesis and characterization of the doped 2 mol% Yttria Stabilized Zirconia (2YSZ) bodies are presented and discussed. The chapter is divided in two sections:

- In the first section the results obtained for the several tested doped 2YSZ compositions are presented from which the ones with improved LTD resistance and/or mechanical properties have been selected.

- The second part covers the study of the selected compositions.

4.1.1. Suspensions Stability

The zeta potential of 2YSZ and of the various oxides used as dopants (ceria (CeO_2), silica (SiO_2), alumina (Al_2O_3), lanthana (La_2O_3), ytterbia (Yb_2O_3) and manganese oxide (MnO_2)) were measured in order to determine the appropriate pH range to ensure a good electrochemical balance between the different particles present in suspensions. In the following figures (45-50) the variation of the zeta potential of the oxides with 2YSZ for each composition is presented.

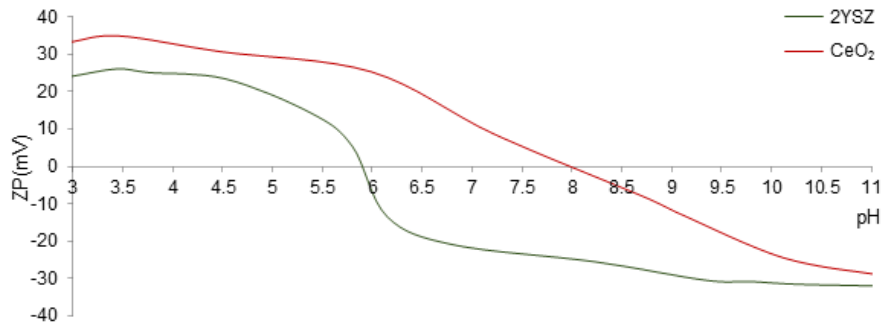

Figure 45. Zeta potential variation of 2YSZ and CeO_2.

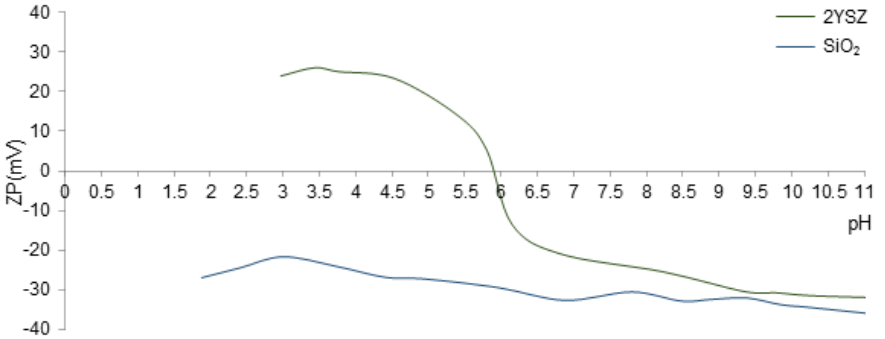

Figure 46. Zeta potential variation of 2YSZ andSiO_2.

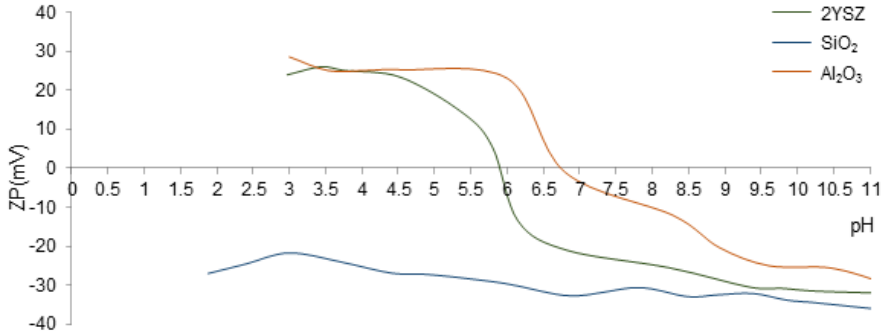

Figure 47. Zeta potential variation of 2YSZ, SiO_2 and Al_2O_3.

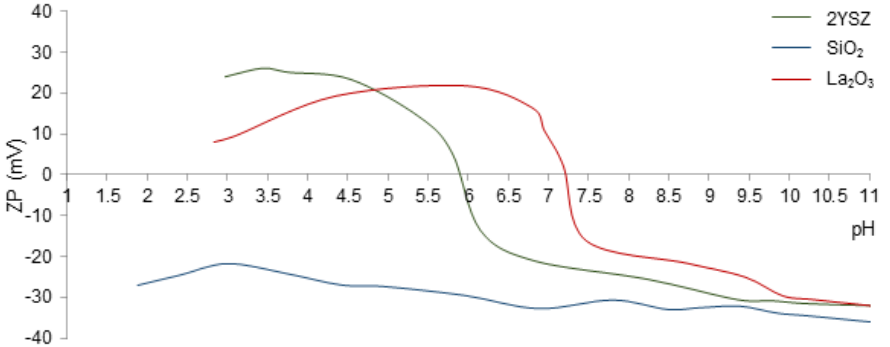

Figure 48. Zeta potential variation of 2YSZ, SiO_2 and La_2O_3.

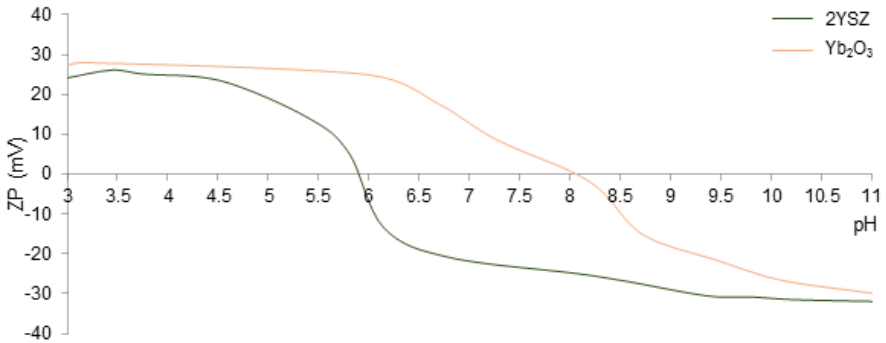

Figure 49. Zeta potential variation of 2YSZ and Yb_2O_3**.**

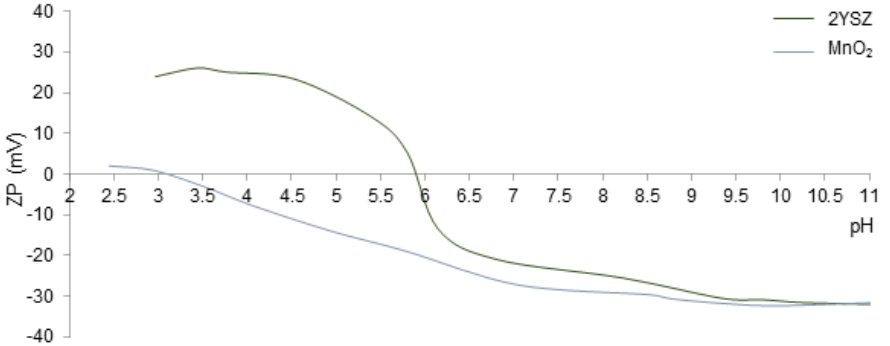

Figure 50. Zeta potential variation of 2YSZ and MnO_2**.**

According to the isoelectric points presented by 2YSZ and by the dopant oxides, the chosen pH value to adjust the different suspensions was approximately 10, except for the composition with silica and alumina where the selected pH value was 11 (Figure 47). At this pH value, the suspensions are stable and a good phase distribution of the powders is expected.

4.1.2. Particle size distribution

The particle size distribution of the powders used to synthesize the 2YSZ doped compositions was determined and adjusted, with the purpose to assure that the milling process leads to an efficient deagglomeration of the initial particles. The obtained size distribution and the mean diameter of the commercial powders (Figure 51) and of the different suspensions obtained after ball milling are presented in Figures 52, 53 and in Table 8.

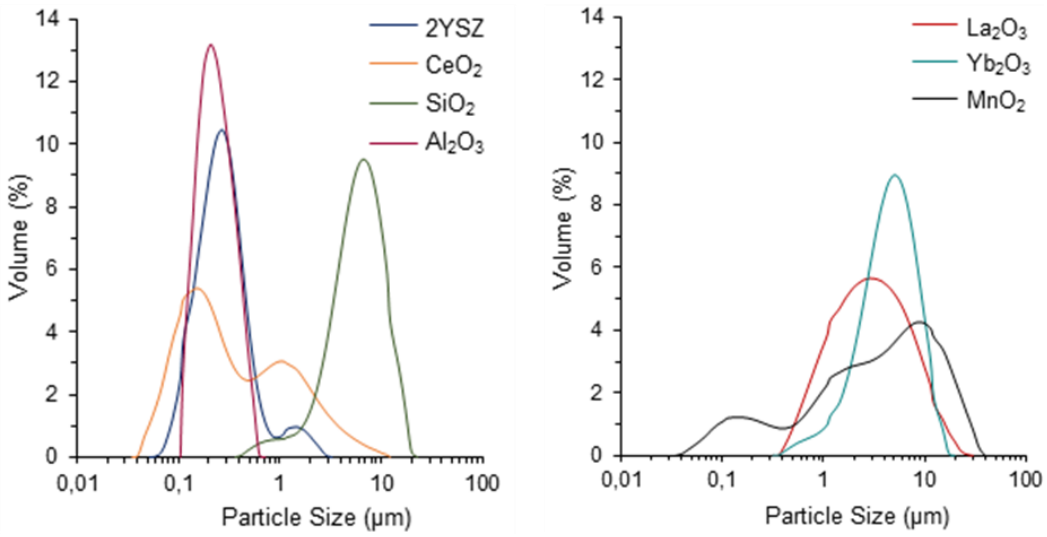

Figure 51. Particle size distribution of the commercial powders.

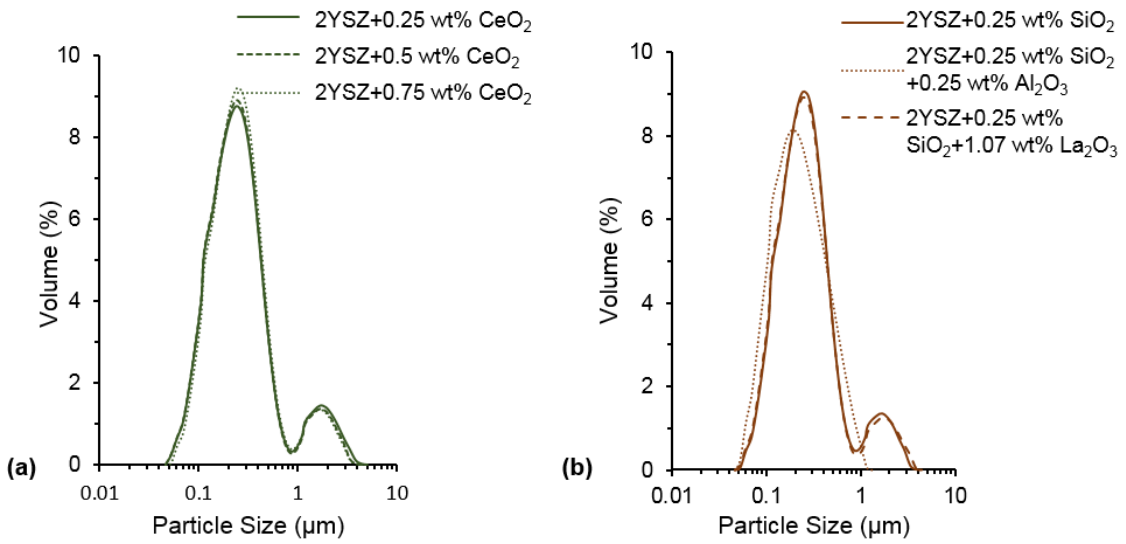

Figure 52. Particle size distribution of the particles after milling in suspension of **(a)** 2YSZ doped with CeO_2; **(b)** 2YSZ doped with: SiO_2; SiO_2plus Al_2O_3 and SiO_2 plus La_2O_3.

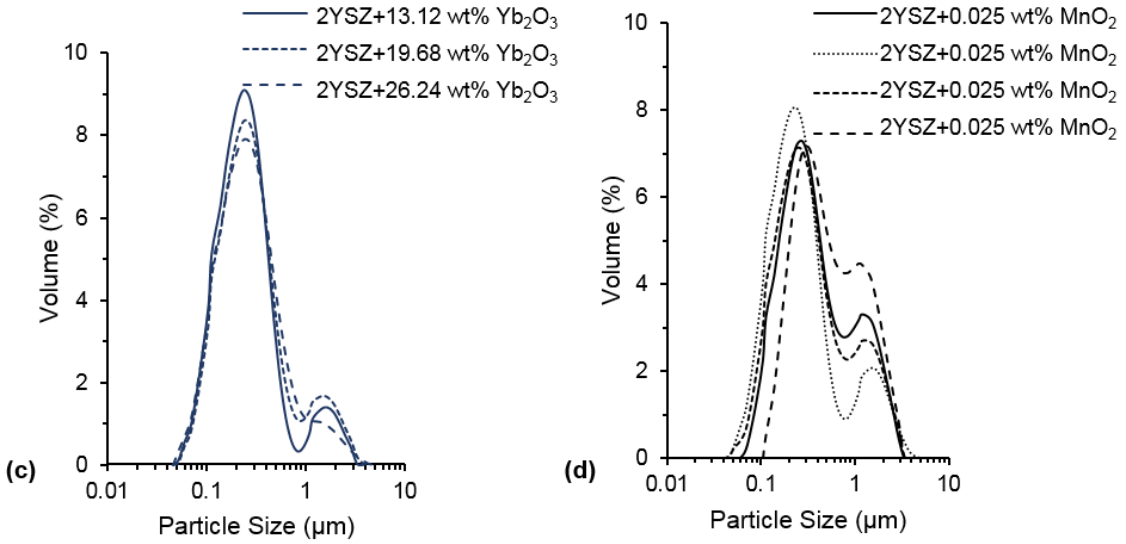

Figure 53. Particle size distribution of the particles after milling in suspension: **(a)** 2YSZ doped with Yb_2O_3; **(b)** 2YSZ doped with MnO_2.

From those results it can be concluded that all the particles show a bimodal distribution. The addition of manganese oxide to 2YSZ presents a higher proportion of the longer size fraction which explains the increase in the mean diameter of the particles in comparison with other dopants.

Table 8. Mean particle diameter of the commercial and doped powders.

		Composition	Mean diameter (d_{50}) (μm)
Commercial powders		2 mol% YSZ	0.247
		CeO_2	0.265
		SiO_2	5.721
		Al_2O_3	0.216
		La_2O_3	2.724
		Yb_2O_3	4.295
		MnO_2	3.543
Doped powders	CeO_2	2YSZ + 0.25 wt% CeO_2	0.224
		2YSZ + 0.5 wt% CeO_2	0.221
		2YSZ + 0.75 wt% CeO_2	0.230
	SiO_2	2YSZ + 0.25 wt% SiO_2	0.231
		2YSZ + 0.25 wt% SiO_2 + 0.25 wt% Al_2O_3	0.198
		2YSZ + 0.25 wt% SiO_2 + 1.07 wt% La_2O_3	0.228
	Yb_2O_3	2YSZ + 13.12 wt% Yb_2O_3	0.223
		2YSZ + 19.68 wt% Yb_2O_3	0.243
		2YSZ + 26.24 wt% Yb_2O_3	0.239
	MnO_2	2YSZ + 0.025 wt% MnO_2	0.308
		2YSZ + 0.05 wt% MnO_2	0.228
		2YSZ + 0.25 wt% MnO_2	0.276
		2YSZ + 0.75 wt% MnO_2	0.439

From the results presented in Table 8 it can be verified that the milling process effectively deagglomerated the suspension particles. The process of deagglomeration was a crucial factor in order to avoid the presence of a heterogeneous particle size after the spray drying process. Therefore, it was important to acquire a controlled size distribution of the particles in the suspensions before spray drying. With this milling process a good homogeneity of the particles with a narrow particle size distribution was achieved.

4.1.3. Characterization of the spray dried powders

4.1.3.1. Morphology

Ideally, from the spray drying process, agglomerates of spherical morphologies with a homogenous packing of the primary particles of the different materials should be

achieved, containing a defined agglomerate size distribution and porosity, but they must not be hollow. According to the literature, solid spheres are mentioned to be the ideal morphology for ceramic systems [126]. The solid spheres morphology provides a better packing of the granules during the pressing process, promoting a better densification. An efficient densification is important in order to achieve ceramic materials with better mechanical properties. As mentioned in the third chapter, a diverse number of variable parameters should be controlled in during the spray drying process in order to guarantee the desired granules characteristics after the atomization process. The morphology of the granules obtained are presented on Figure 54. It can be observed that they present a micrometric size and are formed by agglomerates of nanometric particles, according to the granulometric size distribution (Figure 52, 53 and Table 8).

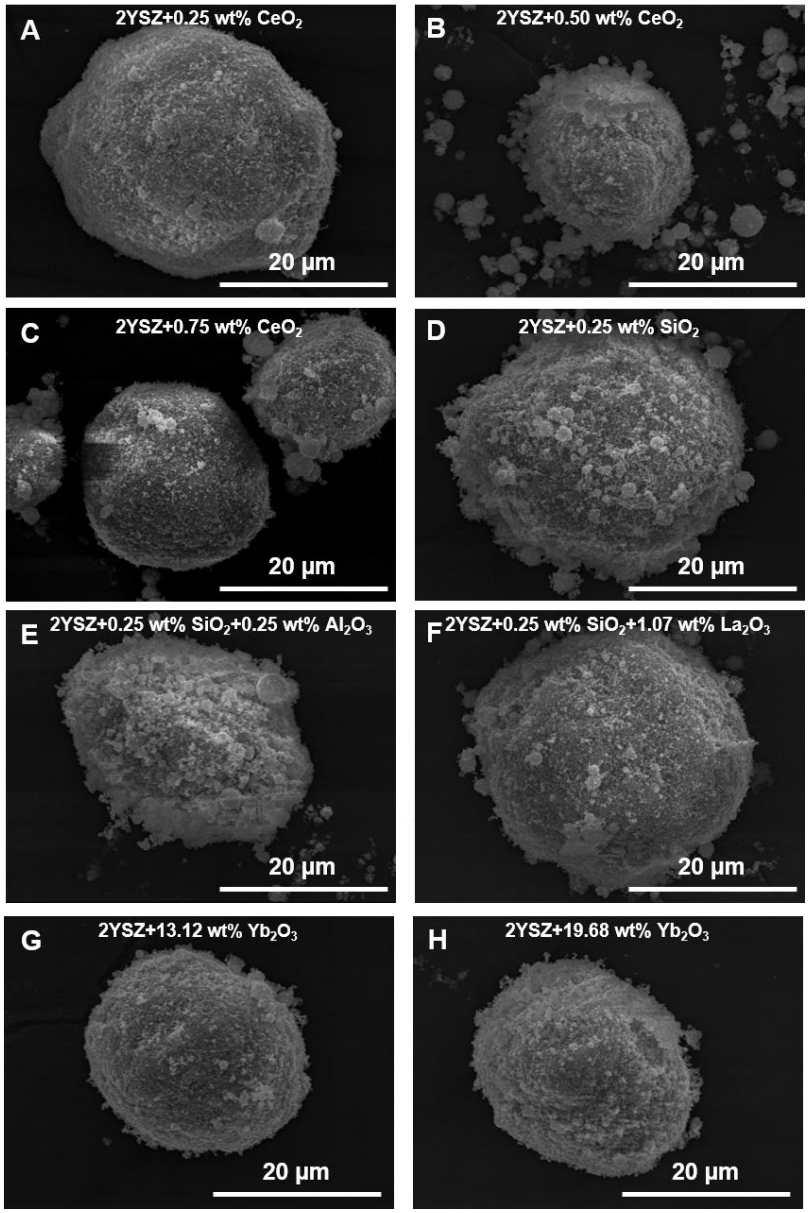

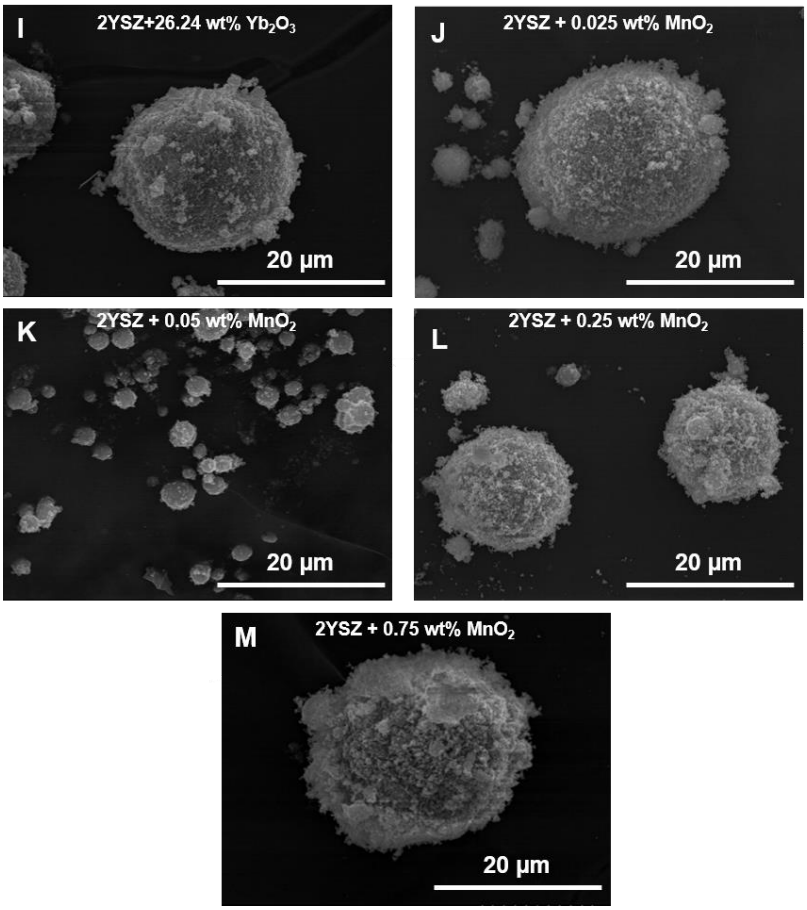

Figure 54. SEM images of the granules of each doped 2YSZ composition after spray drying.

All compositions present a granule diameter within the range of 5 µm to 62 µm. The nanometric particles, which constituted the granules, have a diameter within the range of the results presented by the granulometric distribution curves.

In terms of morphology, the micrometric granules show a homogeneous spherical shape. These granules are similar for the different compositions, however for the addition of 0.05 wt% manganese oxide (Figure 54 – K) they are smaller when compared to the others compositions with the same dopant.

In conclusion, it may be verified that all spray dried granules are constituted by nanometric particles, and appear to be suitable packed and hollow granules are not perceptible. The spray drying procedure effectively led to an agglomeration of the particles originated from suspensions, forming dense micrometric granules.

4.1.3.2. Specific Surface Area

The specific surface area values, for both commercial and spray dried doped powders obtained by the B.E.T. isotherm adsorption, are presented in Table 9.

Table 9. Specific surface area (SSA) obtained by B.E.T. isotherm for commercial and doped powders.

		Compositions	Specific Surface Area (B.E.T.) (m^2/g)
Commercial		2 mol% YSZ	23.46
		Ceria	34.19
		Silica	69.05
		Alumina	15.40
		Lanthana	3.66
		Ytterbia	19.00
		Manganese Oxide	84.33
Doped powders	CeO_2	2YSZ + 0.25 wt% CeO_2	23.78
		2YSZ + 0.5 wt% CeO_2	22.97
		2YSZ + 0.75 wt% CeO_2	24.27
	SiO_2	2YSZ + 0.25 wt% SiO_2	22.22
		2YSZ + 0.25 wt% SiO_2 + 0.25 wt%Al_2O_3	22.93
		2YSZ + 0.25 wt% SiO_2 + 1.07 wt%La_2O_3	21.01
	Yb_2O_3	2YSZ + 13.12 wt% Yb_2O_3	19.55
		2YSZ + 19.68 wt% Yb_2O_3	18.60
		2YSZ + 26.24 wt% Yb_2O_3	23.61
	MnO_2	2YSZ + 0.025 wt% MnO_2	21.94
		2YSZ + 0.05 wt% MnO_2	23.36
		2YSZ + 0.25 wt% MnO_2	22.36
		2YSZ + 0.75 wt% MnO_2	20.88

Lanthanais the dopant that present a lower specific surface area (3.66 m^2/g). Contrarily, the silica and manganese oxides are the dopants with higher specific surface areas (69.05 m^2/g and 84.33 m^2/g, respectively). However, the values of the specific surface area of the 2YSZ powders doped with these dopantsdid not present significant differences, due to the small amount of dopant powder used.

4.1.3.3. Crystal Phases Composition

The spray dried powders were analysed by X-ray diffraction in order to identify the crystallographic phases present. The obtained diffractograms for each composition are displayed in Figure 55.

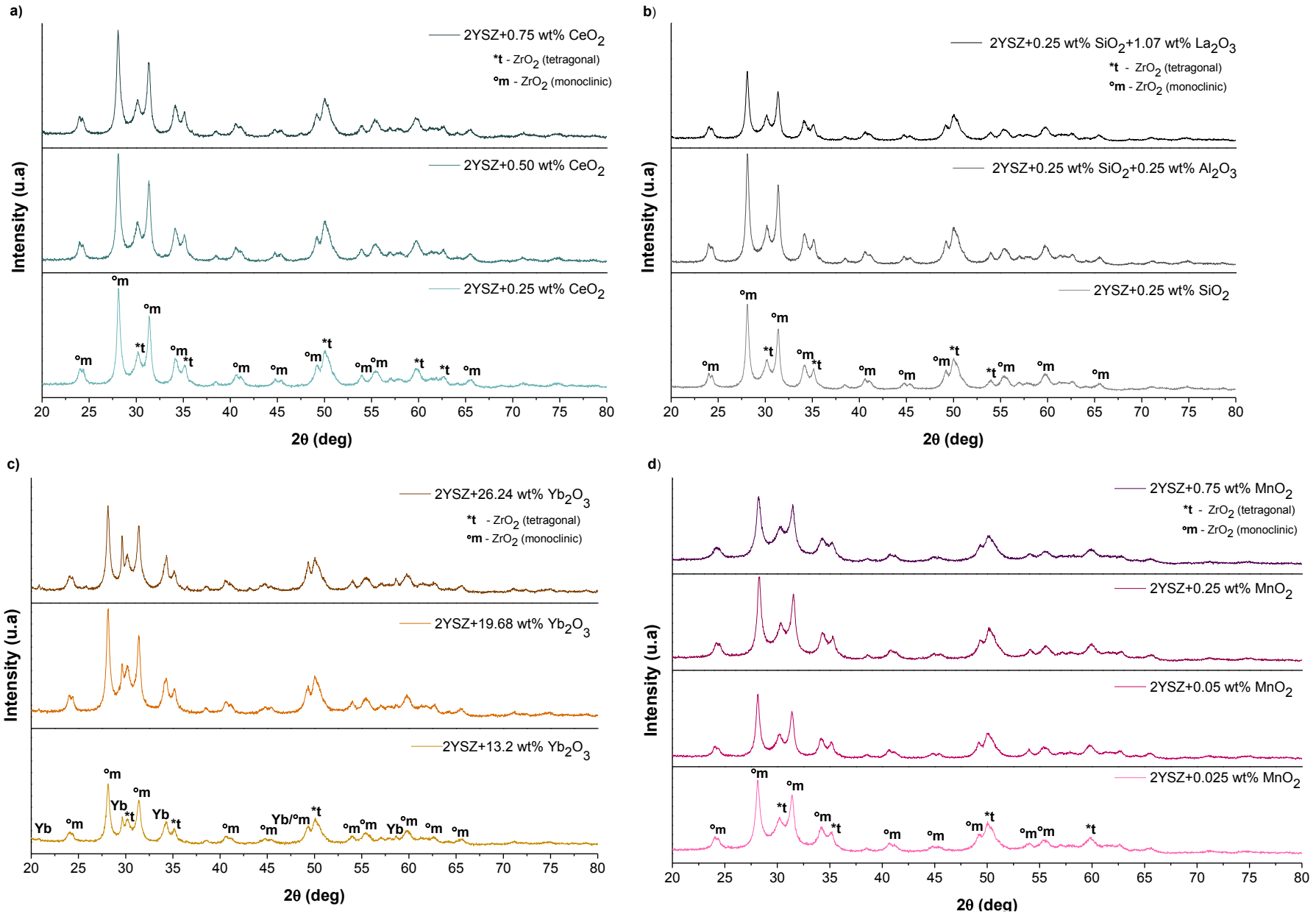

Figure 55. X-ray diffractograms of the powders of 2YSZ doped with different types of oxides and concentrations: **a)** 2YSZ+CeO_2; **b)** 2YSZ+SiO_2 (SiO_2+Al_2O_3; SiO_2+La_2O_3); **c)** 2YSZ+Yb_2O_3; **d)** 2YSZ+MnO_2.

These results evidence the presence of only monoclinic and tetragonal zirconia for all compositions except for 2YSZ doped with ytterbia (Figure 55 – b) where the presence of the dopant was detected. This might be due to the higher dopant amount (13.12 wt% - 26.24 wt%) in the compositions with this oxide, in comparison with the other doped 2YSZ compositions, where the amount of dopant present is very small to be detected by X-ray diffraction.

Phase quantification for all the compositions was performed by Rietveld refinement on Diffract^{Plus}Eva where the peaks and profile data are matched with the information contained in ICDD PDF files. For all compositions, the ICDD PDF file of the monoclinic and tetragonal zirconium oxide used were 00-005-0543 and 01-081-1544, respectively. The quantification of ytterbia was obtained from the ICDD PDF files 00-043-1037 and 00-006-0371. The content of monoclinic and tetragonal zirconia detected in each composition was determined by Diffract^{Plus}Topas and are displayed in Table 10. In general, all compositions of 2YSZ doped with different powders present a phase range between 71 - 79 % of monoclinic zirconia (Table 10), with the remainder being mostly tetragonal zirconia.

Table 10. Phase quantification of zirconia for each composition**.**

	Compositions	**Zirconia phase**	
		ZrO_2 (tetragonal)	**ZrO_2 (monoclinic)**
CeO_2	2YSZ + 0.25 wt% CeO_2	22.15	77.85
	2YSZ + 0.5 wt% CeO_2	21.45	78.55
	2YSZ + 0.75 wt% CeO_2	23.04	76.96
SiO_2	2YSZ + 0.25 wt% SiO_2	24.10	75.90
	2YSZ + 0.25 wt% SiO_2 + 0.25 wt%Al_2O_3	22.81	77.19
	2YSZ + 0.25 wt% SiO_2 + 1.07 wt%La_2O_3	23.77	76.23
Yb_2O_3	2YSZ + 13.12 wt% Yb_2O_3	28.01	71.99
	2YSZ + 19.68 wt% Yb_2O_3	27.50	72.50
	2YSZ + 26.24 wt% Yb_2O_3	28.83	71.17
MnO_2	2YSZ + 0.025 wt% MnO_2	23.48	76.52
	2YSZ + 0.05 wt% MnO_2	24.04	75.96
	2YSZ + 0.25 wt% MnO_2	21.62	78.38
	2YSZ + 0.75 wt% MnO_2	24.38	75.62

The amount of monoclinic zirconia present in these compositions is associated to the transformability of zirconia when in powder phase. The granules of doped zirconia possess a significantly high specific surface area (Table 9) which makes them reactive and

transformable. Therefore, there will be a tendency for zirconia to achieve its stable state at room temperature, i.e., the monoclinic phase. Thus, it will promote the occurrence of the tetragonal to monoclinic transformation. This fact makes the content of monoclinic zirconia to surpass the content of tetragonal zirconia.

4.1.3.4. True density

The particles density of the all powders was measured in a helium pycnometer. Table 11 presents the obtained density values for all commercial and doped 2YSZ powders.

Table 11. Particles density of the all powders measured by helium pycnometry.

		Compositions	Density (g/cm^3)
Commercial		2 mol% YSZ	5.450
		Ceria	7.331
		Silica	2.420
		Alumina	3.971
		Lanthana	5.318
		Ytterbia	6.524
		Manganese Oxide	4.299
Doped powders	CeO_2	2YSZ + 0.25 wt% CeO_2	5.505
		2YSZ + 0.5 wt% CeO_2	5.525
		2YSZ + 0.75 wt% CeO_2	5.502
	SiO_2	2YSZ + 0.25 wt% SiO_2	5.459
		2YSZ + 0.25 wt% SiO_2 + 0.25 wt%Al_2O_3	5.465
		2YSZ + 0.25 wt% SiO_2 + 1.07 wt%La_2O_3	5.484
	Yb_2O_3	2YSZ + 13.12 wt% Yb_2O_3	5.574
		2YSZ + 19.68 wt% Yb_2O_3	5.579
		2YSZ + 26.24 wt% Yb_2O_3	5.228
	MnO_2	2YSZ + 0.025 wt% MnO_2	5.199
		2YSZ + 0.05 wt% MnO_2	5.381
		2YSZ + 0.25 wt% MnO_2	5.265
		2YSZ + 0.75 wt% MnO_2	5.226

The obtained values for each composition are in accordance with the ones of the initial powders (2YSZ and dopants oxides). Ceria presents the highest value of density (7.331

g/cm^3) followed by ytterbia with a density of 6.524 g/cm^3. In contrast, the lowest true density is achieved for silica (2.420 g/cm^3).

In general, all doped 2YSZ powders have similar densities. 2YSZ doped with ceria presents the highest density value, and it can be observed that for different amounts of this dopant the value of density is practically constant (5.511 g/cm^3). In the opposite side, the compositions with manganese oxide exhibit the lowest density value (5.268 g/cm^3). The lower density presented by silica did not influence the final density of the compositions where this dopant is added, since the amount of this oxide is very small.

All defined compositions possess a powder relative density higher than 76 % (considering the theoretical values of each powder dopant element, tetragonal and monoclinic zirconia). Therefore, it can be assumed that the obtained nanometric particles are dense.

4.1.3.5. X-Ray Fluorescence

The chemical composition of each sample obtained by spray-drying was evaluated by x-ray fluorescence analysis. According to ISO 13356:2008 [13] this analysis is required in order to detect impurities in these materials based on Yttria Stabilized Zirconia. The chemical compositions of each composition of doped 2YSZ are presented In Tables 12 - 15.

Table 12. Chemical composition of 2YSZ doped with different amounts of CeO_2.

Composition (%)	**2YSZ + 0.25 wt% CeO_2**	**2YSZ + 0.5 wt% CeO_2**	**2YSZ + 0.75 wt% CeO_2**
ZrO_2	94.29	94.04	93.8
Y_2O_3	3.392	3.383	3.374
HfO_2	1.591	1.587	1.583
Al_2O_3	0.369	0.368	0.366
CeO_2	0.278	0.534	0.793
Other elements	0.08	0.088	0.084

Table 13. Chemical composition of 2YSZ doped with SiO_2; SiO_2 and Al_2O_3 and SiO_2 and La_2O_3.

Composition (%)	2YSZ + 0.25 wt% SiO_2	2YSZ + 0.25 wt% SiO_2 + 0.25 wt% Al_2O_3	2YSZ + 0.25 wt% SiO_2 + 1.07 wt% La_2O_3
ZrO_2	94.29	93.96	93.17
Y_2O_3	3.406	3.41	3.352
HfO_2	1.591	1.601	1.572
Al_2O_3	0.369	0.688	0.362
SiO_2	0.262	0.237	0.224
La_2O_3			1.23
Other elements	0.082	0.104	0.09

Table 14. Chemical composition of 2YSZ doped with different amounts of Yb_2O_3.

Composition (%)	2YSZ + 13.12 wt% Yb_2O_3	2YSZ + 19.68 wt% Yb_2O_3	2YSZ + 26.24 wt% Yb_2O_3
ZrO_2	81.91	76.33	70.71
Yb_2O_3	13.36	19.27	25.21
Y_2O_3	2.943	2.73	2.532
HfO_2	1.37	1.28	1.193
Al_2O_3	0.32	0.299	0.277
Other elements	0.097	0.091	0.078

Table 15. Chemical composition of 2YSZ doped with different amounts of MnO_2.

Composition (%)	2YSZ + 0.025 wt% MnO_2	2YSZ + 0.05 wt% MnO_2	2YSZ + 0.25 wt% MnO_2	2YSZ + 0.75 wt% MnO_2
ZrO_2	94.51	94.49	94.34	93.81
Y_2O_3	3.401	3.398	3.393	3.371
HfO_2	1.611	1.611	1.597	1.593
Al_2O_3	0.369	0.369	0.369	0.367
MnO_2	0.028	0.042	0.225	0.782
Other elements	0.08	0.089	0.076	0.077

Although the mentioned International Standard (ISO 13356:2008) is referred only for ceramic materials based on Yttria Stabilized Tetragonal Zirconia (Y-TZP), it was also considered for the doped compositions. This international standard refers that the hafnia amount must not exceed 5 % and the other minority elements must be below 0.5 %.

Each composition possess a content of hafnia below 5 %, as well as the minority elements do not exceeds the mass fraction of 0.5 %.

From the results of chemical analysis, it is verified that the content of 2YSZ and of all selected dopant are in accordance with the amount previously defined for each compositions.

4.1.3.6. Dilatometric Analysis

In order to investigate the thermal behaviour and densification kinetics of all samples and therefore select a sintering temperature, a dilatometric analysis was performed. The results obtained for all compositions are shown in Figures 59.

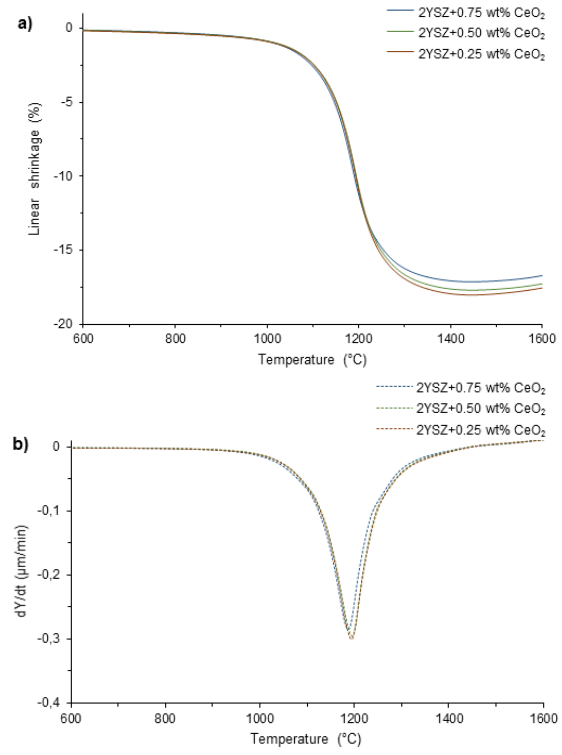

(1) Linear shrinkage and shrinkage rate with the temperature of the composition of 2YSZ doped with CeO_2.

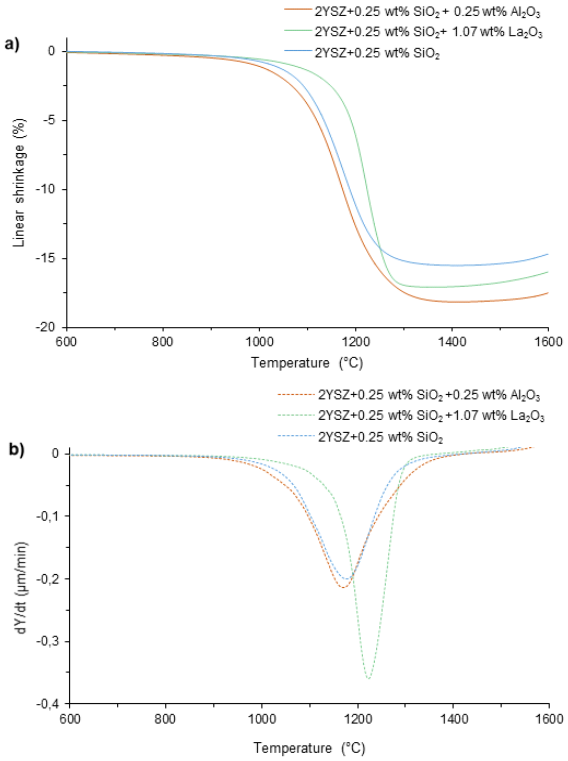

(2) Linear shrinkage and shrinkage rate with the temperature of the composition of 2YSZ doped with SiO_2 alone and SiO_2 with other dopant elements.

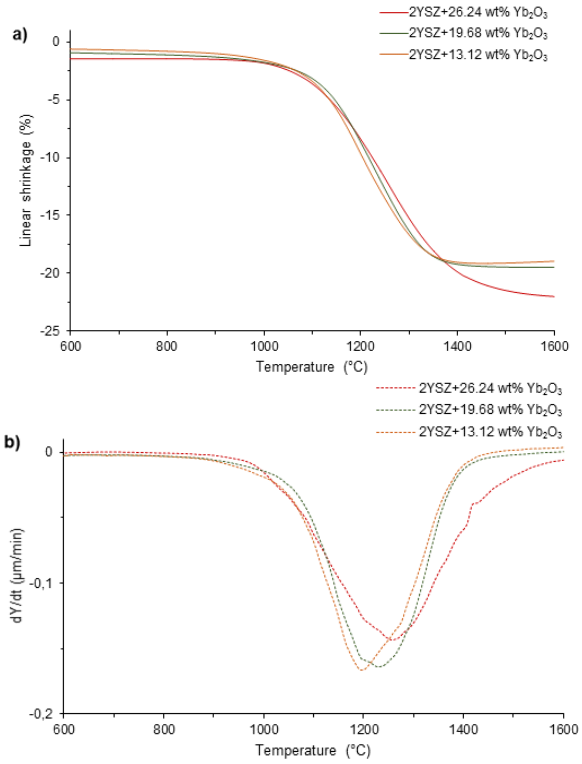

(3) Linear shrinkage and shrinkage rate with the temperature of the composition of 2YSZ doped with Yb_2O_3.

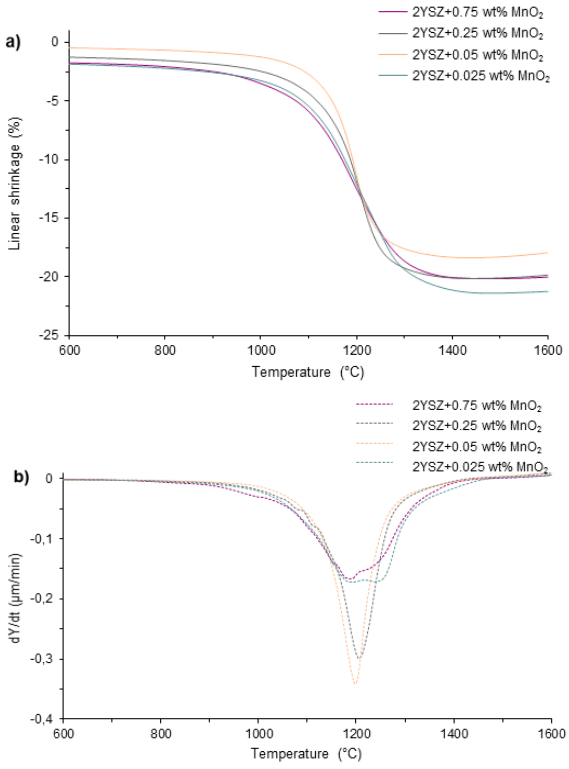

(4) Linear shrinkage and shrinkage rate with the temperature of the composition of 2YSZ doped with MnO_2.

Figure 56. Dilatometric analysis of all compositions in study.

The influence of the green density on linear shrinkage and shrinkage rate of the doped zirconia powders was evaluated, and as it was expected the linear shrinkage decreases for samples prepared with higher green density.

In general, the linear shrinkage curves for all compositions with different dopants and concentrations shows a similarly behaviour of densification (Figure 56 – a). The greater shrinkage rate occurs around at 1200 ºC, with exception of yttria doped zirconia (1350 ºC), as it can be observed in Figure 56 – b.

According to Lange [127], for temperatures below the value of the higher linear shrinkage rate, the sintering kinetics is dominated by densification mechanisms, and above this temperature, nondensification mechanisms namely grain growth will prevail. As mentioned in chapter two, the submicrometric and nanometric grain size is traduced in an improvement of mechanical properties and ageing resistance [25], [29]. In order to avoid an excessive grain growth and the appearance of defects in the microstructure that can cause mechanical failure or degradation, a moderate sintering temperature should be considered [128], [129]. Zirconia is generally sintered at temperatures ranging between 1350 ºC to 1500 ºC for more than two hours [130], where the best properties of zirconia are achieved, namely, the grain size grows slowly, the porosity disappears and the maximum relative density is reached [131]. It has been reported that sintering temperatures ranging between 1350 ºC and 1400 ºC are recommended in order to improve the hydrothermal ageing resistance [28]. Materials sintered at higher temperature tend to initiate this deleterious transformation at earlier stages and their rate of transformation is higher than those sintered at lower temperatures [28].

From these results the sintering conditions of each composition have been selected. In order to ensure that the sintering process occurs correctly, the maximum temperature obtained by dilatometric analysis was slightly increased. The selected sintering cycle for all compositions of doped 2YSZ, except the composition doped with ytterbia, had a maximum of 1350 ºC for three hours with a heating rate of 2 ºC/min and a cooling rate of 5 ºC/min. The three compositions of 2YSZ doped with ytterbia were sintered to a maximum temperature of 1400 ºC for three hours, being the other conditions identical. In Figure 38 is represented the scheme of the sintering cycle.

4.1.4. Characterization of the sintered pieces

4.1.4.1. Density of the sintered pieces

The doped 2YSZ powders were submitted to one uniaxial pressing stage and sintering. The density of the sintered pieces was determined by the Archimedes' Method. The density results obtained for all compositions are shown in Figure 57 and in Table 16.

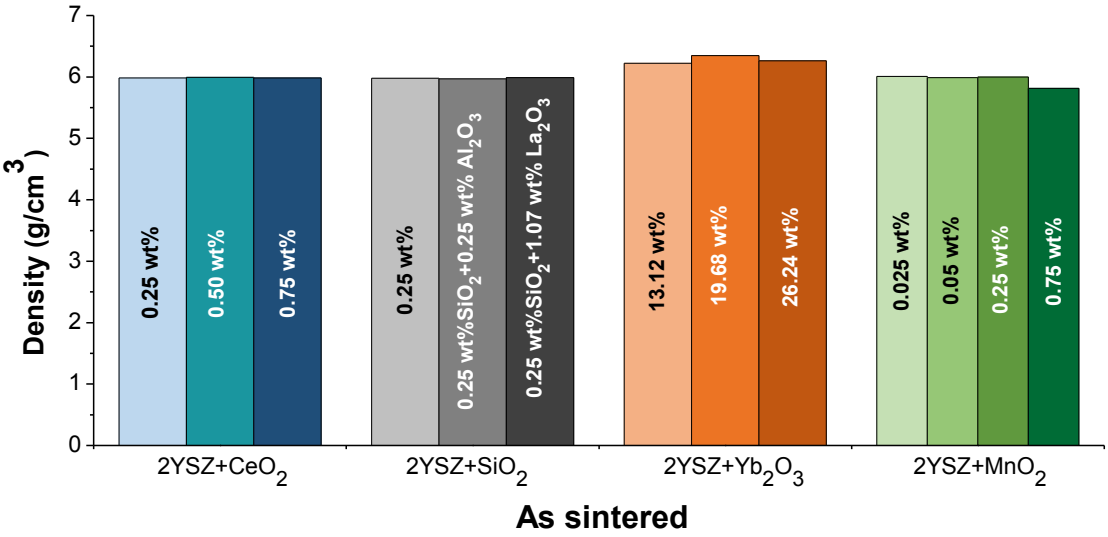

Figure 57. Density of all doped 2YSZ compositions sintered pieces.

Table 16. Densification degree of the sintered compositions of doped 2YSZ.

	Composition	Density (%)
CeO_2	2YSZ + 0.25 wt% CeO_2	98.49
	2YSZ + 0.5 wt% CeO_2	98.65
	2YSZ + 0.75 wt% CeO_2	98.44
SiO_2	2YSZ + 0.25 wt% SiO_2	98.61
	2YSZ + 0.25 wt% SiO_2 + 0.25 wt%Al_2O_3	98.58
	2YSZ + 0.25 wt% SiO_2 + 1.07 wt%La_2O_3	98.73
Yb_2O_3	2YSZ + 13.12 wt% Yb_2O_3	96.57
	2YSZ + 19.68 wt% Yb_2O_3	95.01
	2YSZ + 26.24 wt% Yb_2O_3	90.96
MnO_2	2YSZ + 0.025 wt% MnO_2	98.98
	2YSZ + 0.05 wt% MnO_2	98.67
	2YSZ + 0.25 wt% MnO_2	98.91
	2YSZ + 0.75 wt% MnO_2	95.94

In order to calculate the theoretical density of the obtained doped compositions the mixtures principle was used as described in equation 13,

$$\rho = \rho_{2YSZ} \times (\%\ 2YSZ) + \rho_{Dopant} \times (\%\ Dopant) \quad (13)$$

,where ρ is the density of the final compound, ρ_{2YSZ} is the theoretical density of 2YSZ sample, ρ_{Dopant} is the theoretical density of the added dopant and % 2YSZ and % Dopant are the weight fractions of the 2YSZ and added dopants, respectively. In the case where two dopants are added to the starting 2YSZ, the densities and weight fractions of both them have to be accounted.

The effect of the sintering temperature on the densification of the samples with different dopants was evaluated for all sintered compacts. It can be observed that the sintering stage led to a good densification of all doped 2YSZ pieces (approximately 6 g/cm^3 for all samples, being the Yb_2O_3 doped 2YSZ samples the ones with higher density (higher than 6.23 g/cm^3)). Compared with the theoretical values of density (Table 16), the achieved relative density is superior to 90 %. Considerable higher density at relative low temperature can be attributed to a set of factors such as, spray dried powders (which had a spherical shape, with nanometric particle size and were dense), a good packing of these powders during uniaxial pressing which improved the density of the green bodies and lastly the sintering stage which allowed an increase of the density values.

According to some authors, the spray drying of deflocculated suspensions can result in the production of hollow granules and thus, can give rise to porous ceramics with flaws upon sintering [126], [132]. Nevertheless, the density values obtained for each composition of doped 2YSZ powders are associated to dense particles and not hollow. Thus, in this study it is not verified the same evidence that was previously reported other authors.

4.1.4.2. Crystal phases compositions

In order to confirm the transformation of monoclinic zirconia to the tetragonal phase upon sintering stage, X-ray analysis was performed on the doped 2YSZ samples. The obtained diffractograms for all compositions are show in Figure 58.

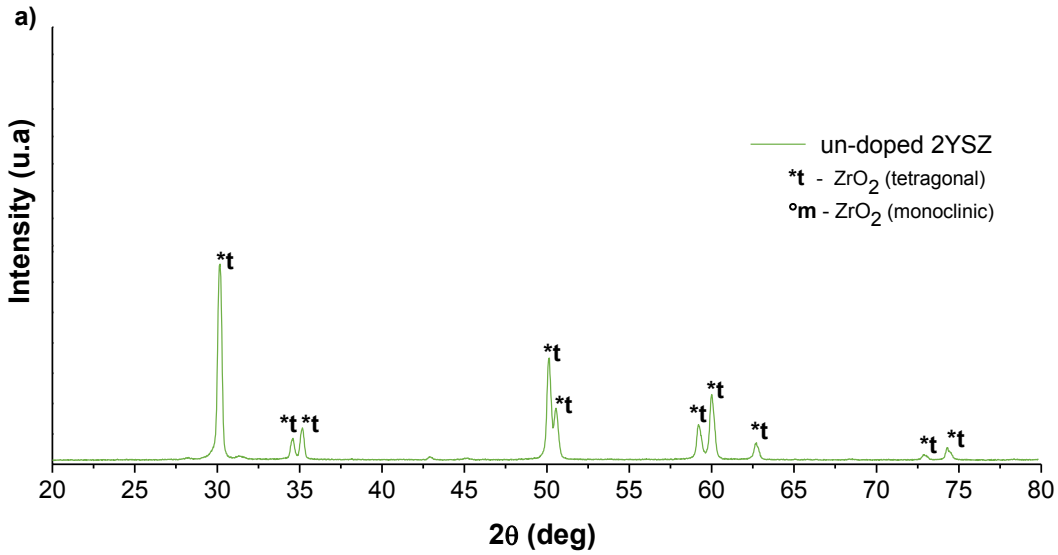

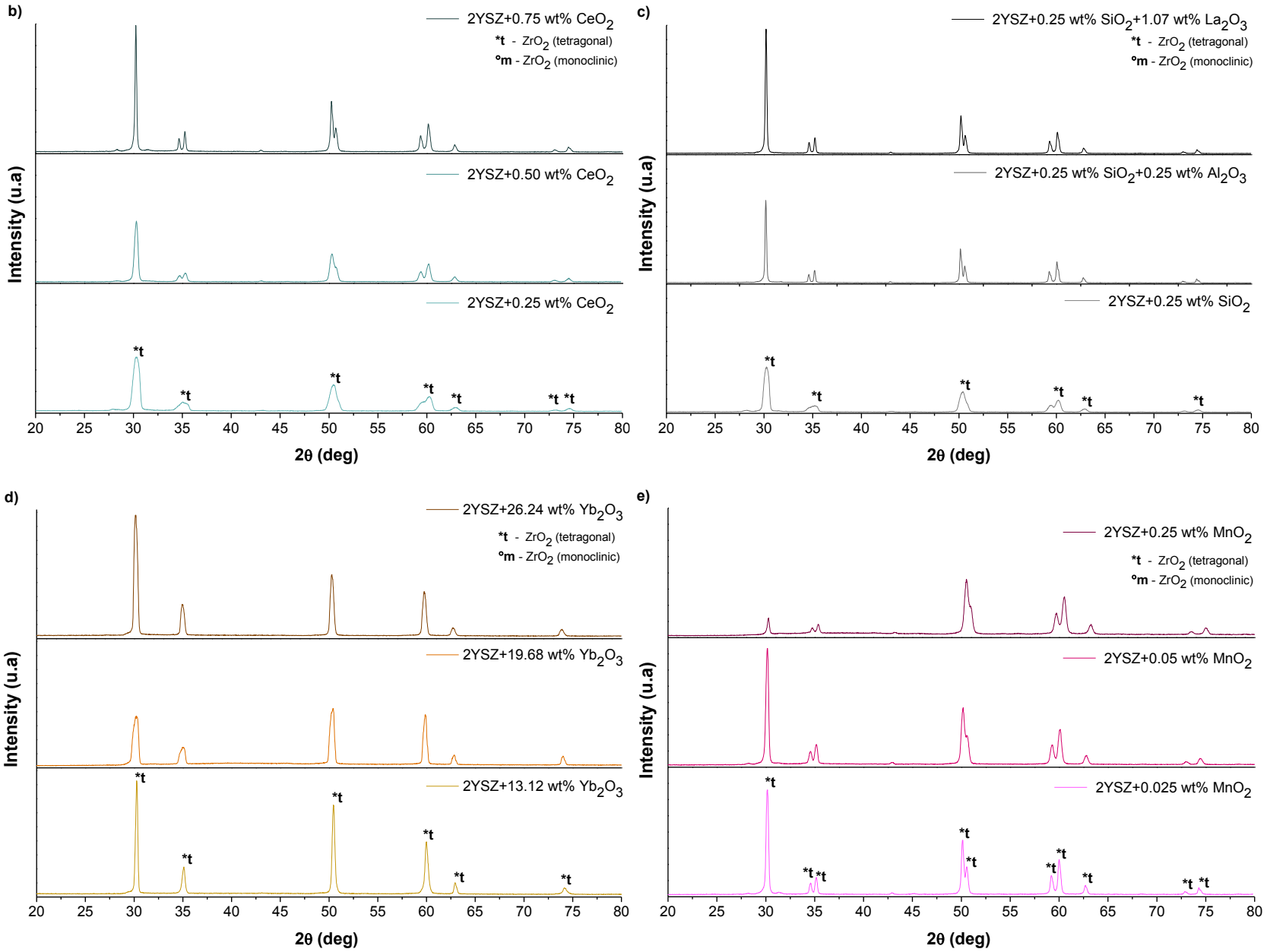

Figure 58. X-ray diffractograms obtained from sintered samples of 2YSZ doped with different types of dopant and concentrations: **a)** un-doped 2YSZ; **b)** 2YSZ+CeO_2; **c)** 2YSZ+SiO_2 (SiO_2+Al_2O_3; SiO_2+La_2O_3); **d)** 2YSZ+Yb_2O_3; **e)** 2YSZ+MnO_2.

The samples sintered at 1350 ºC (un-doped and doped 2YSZ samples) and 1400 ºC (Yb_2O_3 doped zirconia) are mostly constituted by tetragonal zirconia phase. At these sintering temperatures, the most part of the monoclinic zirconia detected in doped 2YSZ powders after spray drying (Figure 55), has been transformed to the beneficial tetragonal zirconia. The sample of 2YSZ doped with an amount of 0.75 wt% MnO_2 (Figure 58 – e) presented a very low mechanical resistance (very fragile) during sintering stage, hence was not in conditions to be characterized in terms of thermal ageing and mechanical resistance tests, so it was excluded. An accentuated decrease of the relative intensity of the peak approximately at 30 º (2θ) can be observed on case of manganese oxide (0.25 wt%) (Figure 58 – e) is associated with the preferred orientation effect due to pellets. A slightly decrease accomplished by an enlargement of the diffraction peaks, mainly at approximately at (2θ) of 30 º, 35 º and 50 º, for2YSZ doped with an intermediate selected amount of ytterbia dopant (19.68 wt%) (Figure 58 – d), occurred due to the XRD equipment not being in spinning mode, which affected the results.

It was observed that for all samples subjected to sintering, the monoclinic phase was transformed into tetragonal zirconia and thus, its detrimental effects would not affect the following tests.

4.1.4.3. Microstructure

To investigate and observe the microstructure of all doped 2YSZ samples, the sintered pieces were thermally etched and observed by scanning electron microscopy. In Figure 59 the micrographs of the obtained microstructures are presented.

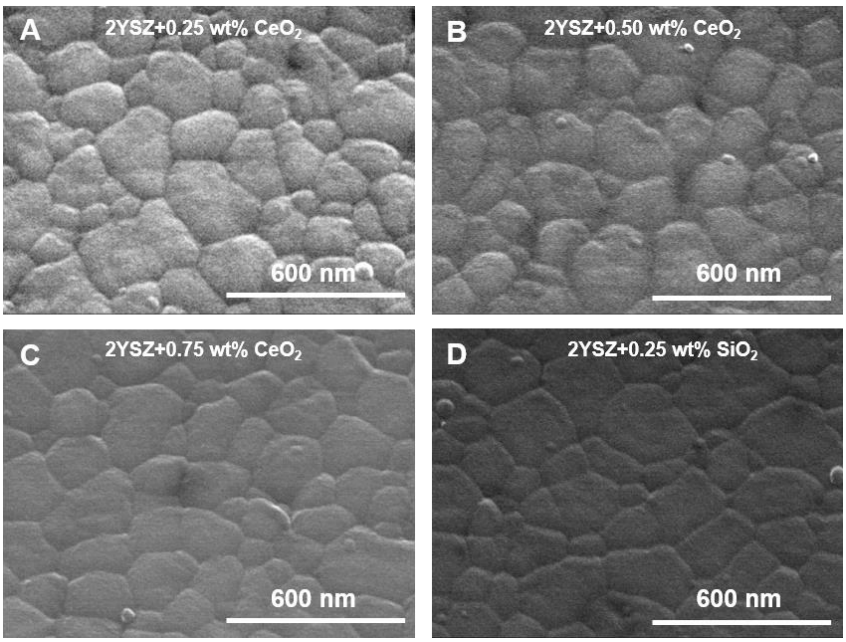

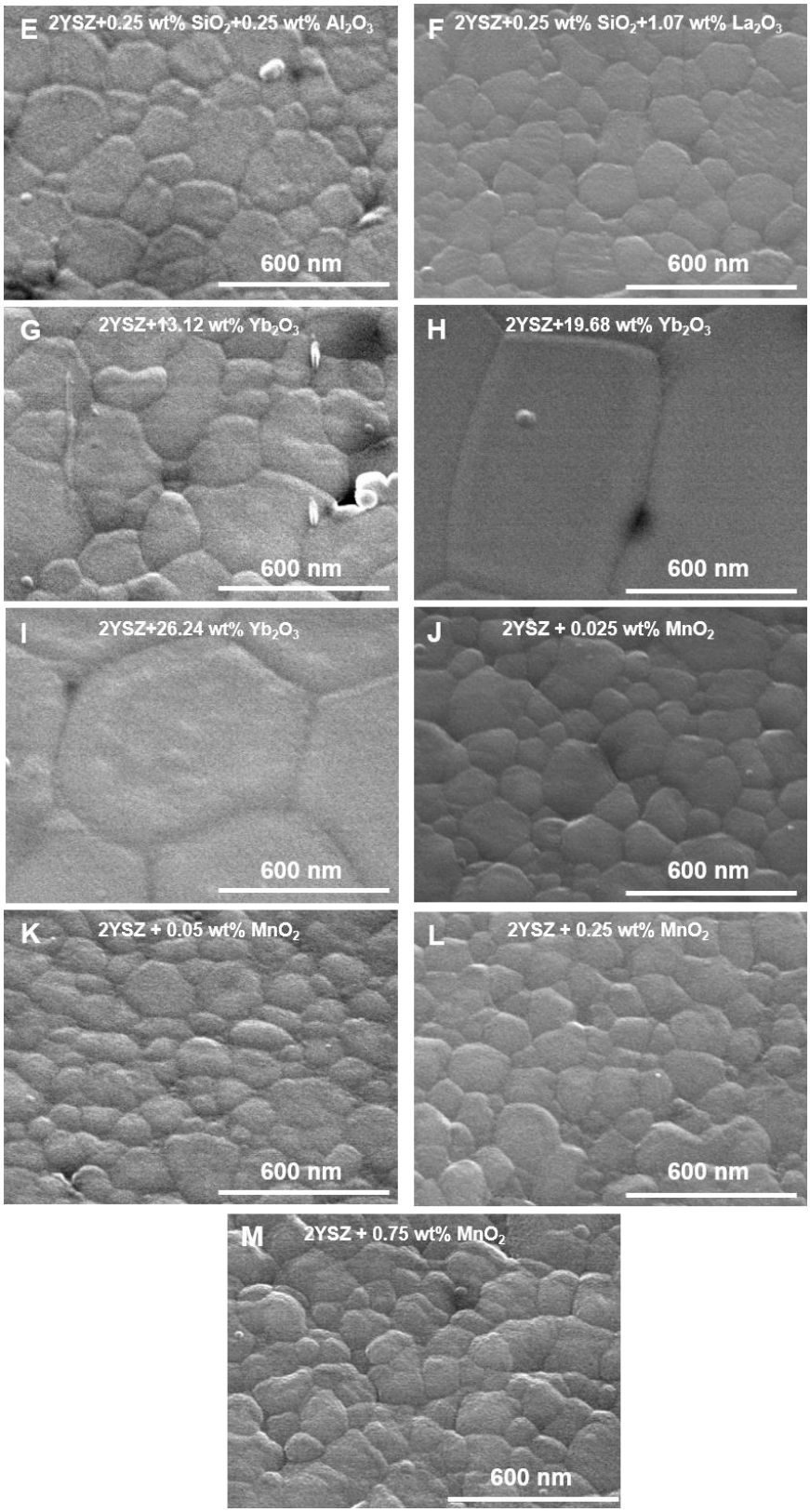

Figure 59. SEM micrographs of the thermal etched doped 2YSZ samples.

As it can be seen by SEM micrographs, a uniform microstructure was accomplished without evident segregation for the doped 2YSZ samples. Although it is possible to detect some small pores in the doped zirconia stabilized samples (generally located at the grain

boundaries), dense sintered samples were obtained, since the achieved density values are all above 90 %, at relative low sintering temperature (1350 ºC and 1400 ºC).

The microstructure presented by every sample of doped zirconia displayed similarities with some published results, in terms of morphology and distribution of the grains of the samples [25], [28], [133], [134].

The mean grain size for each sample was calculated from the SEM micrograph through several measurements, as described in chapter three. Two micrographs were used for each composition (with the same magnification), using the linear interception method. The obtained values are displayed in Table 17.

Table 17. Mean grain size of doped 2YSZ sintered samples calculated by the line interception method.

	Composition	Mean grain size (nm)
CeO_2	2YSZ + 0.25 wt% CeO_2	362±13
	2YSZ + 0.5 wt% CeO_2	345±12
	2YSZ + 0.75 wt% CeO_2	374±13
SiO_2	2YSZ + 0.25 wt% SiO_2	390±16
	2YSZ + 0.25 wt% SiO_2 + 0.25 wt%Al_2O_3	321±13
	2YSZ + 0.25 wt% SiO_2 + 1.07 wt%La_2O_3	297±9
Yb_2O_3	2YSZ + 13.12 wt% Yb_2O_3	432±25
	2YSZ + 19.68 wt% Yb_2O_3	3525±258
	2YSZ + 26.24 wt% Yb_2O_3	1679±246
MnO_2	2YSZ + 0.025 wt% MnO_2	337±12
	2YSZ + 0.05 wt% MnO_2	272±9
	2YSZ + 0.25 wt% MnO_2	591±9
	2YSZ + 0.75 wt% MnO_2	339±12

As it can be observed, the sintering temperature (1350 ºC and 1400 ºC) influenced the grain size of the zirconia stabilized with different types and concentrations of dopants. The samples sintered at 1350 ºC (2YSZ doped with CeO_2, SiO_2, MnO_2) showed similar microstructures and grain sizes. In these samples, it is possible to verify that the mean grain size ranges between 272 to 591 nm and that the concentration and type of the dopants (for each composition) does not significantly affect the mean grain size of these samples. This suggests that the selected sintering temperature did not allow excessive grain growth. In relation to the samples of 2YSZ doped with ytterbia sintered at 1400 ºC, it is possible to verify that higher concentration of this oxide causes an increase of the grain size. For the samples with this dopant, the mean grain size ranges between 432 to 3525 nm. Ytterbia

exhibits a higher grain growth during sintering. Regarding the results published by *Kan et al.* [65], where the sample of zirconia stabilized with 1 mol% Y_2O_3 doped with Yb_2O_3 (13.12 wt%, 19.68 wt% and 26.24 wt%), sintered for 1 hour at 1400 ºC, shows similar homogeneous microstructures (between each dopant content) with average grain sizes of 300 nm, it can be concluded that this excessive grain growth must be related with the difference on the sintering parameters, specifically the holding time (3 hours instead of 1 hour).

4.1.4.4. Thermal ageing tests

X-ray diffraction was performed to confirm the absence of other possible phases that could be formed during the thermal ageing tests, at 200 ºC, after 12 and 36 hours, to verify and quantify the presence of tetragonal and monoclinic zirconia. The obtained diffractograms for each doped 2YSZ composition after 36 hours of treatment are displayed in Figure 60.

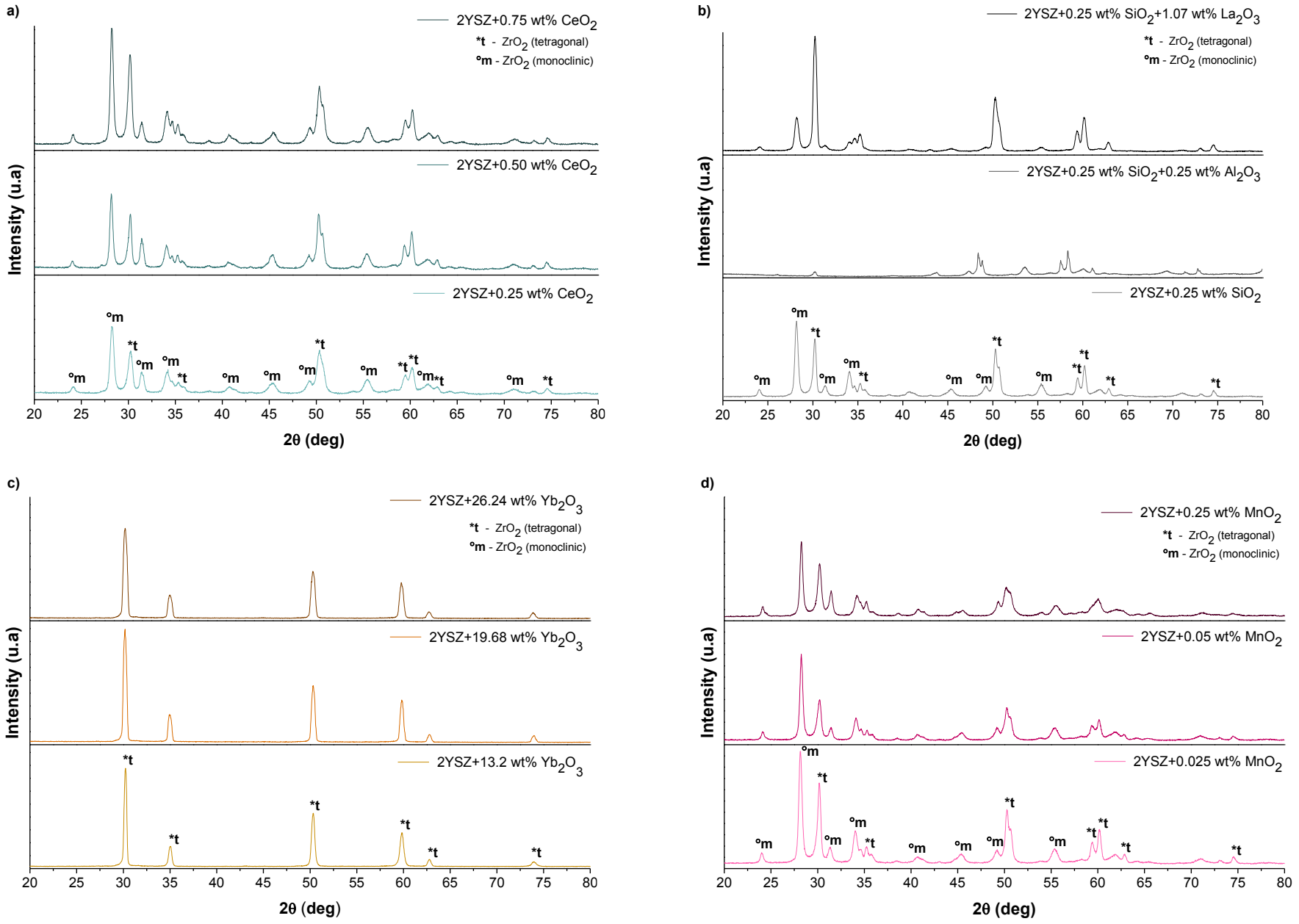

Figure 60. X-ray diffractograms obtained for each composition of doped 2YSZ after 36 hours of thermal ageing tests: **a)** 2YSZ+CeO_2; **b)** 2YSZ+SiO_2 (SiO_2+Al_2O_3; SiO_2+La_2O_3); **c)** 2YSZ+Yb_2O_3; **d)** 2YSZ+MnO_2.

From the acquired results, an increase of the content of monoclinic zirconia is observed in doped 2YSZ samples after being submitted to a degradation environment. Through the diffractograms analyses, it is perceptible that the samples of zirconia doped with ytterbia (Figure 60 – c)) do not show the presence of monoclinic zirconia. Also, it is verified that for aged 2YSZ samples doped with silica and alumina (Figure 60 – b)) some peaks correspondent to monoclinic and tetragonal zirconia were suppressed and others show a decrease of intensity, which suggests a decrease of the crystallinity. Once again, it can be related with the fact of the XRD equipment not being in spinning mode. Nevertheless, the other samples (2YSZ doped with CeO_2, SiO_2, $SiO_2$with La_2O_3, MnO_2) do not exhibit the same behaviour observed for the sample of 2YSZ doped with both oxides, SiO_2 and Al_2O_3.

The ageing phenomenon is the main concern regarding zirconia. In the literature review it was mentioned that the 2YSZ ceramics, since they contain small amounts of stabilizer, are more susceptible to spontaneous phase transformation of zirconia when compared with other samples of zirconia stabilized with a greater amount of yttria (3YSZ for example). Although the greater amount of yttria helps to decrease the spontaneous phase transformation, the same behaviour can be obtained by doping the 2YSZ with different oxides (as mentioned earlier in this document). In order to compare the degree of degradation of the selected 2YSZ doped samples through the time of exposition (12 and 36 hours) at low temperature (200 ºC), the quantification of the zirconia phases was calculated with the purpose of investigating their vulnerability to thermal ageing (Table 18).

Table 18. Phase quantification of 2YSZ doped samples after thermal ageing tests.

	Compositions	0 hours		12hours		36 hours	
		ZrO_2_m	ZrO_2_t	ZrO_2_m	ZrO_2_t	ZrO_2_m	ZrO_2_t
CeO_2	2YSZ+0.25 wt% CeO_2	0.09	99.91	52.09	47.91	62.07	37.93
	2YSZ+0.5 wt% CeO_2	1.61	98.39	31.35	68.65	62.44	37.56
	2YSZ+0.75 wt% CeO_2	3.62	96.38	49.35	50.65	56.20	43.80
SiO_2	2YSZ+0.25 wt% SiO_2	2.67	97.33	41.27	58.73	58.30	41.7
	2YSZ+0.25 wt% SiO_2+0.25 wt% Al_2O_3	0.72	99.28	43.05	56.95	-	-
	2YSZ+0.25 wt% SiO_2+1.07 wt% La_2O_3	0.22	99.78	15.06	84.94	24.49	71.51
Yb_2O_3	2YSZ+13.12 wt% Yb_2O_3	0	100	0.13	99.87	0.04	99.96
	2YSZ+19.68 wt% Yb_2O_3	1.34	98.66	0.84	99.16	0.06	99.94
	2YSZ+26.24 wt% Yb_2O_3	0.03	99.97	0.46	99.54	0.06	99.94
MnO_2	2YSZ+0.025 wt% MnO_2	2.08	97.92	38.8	61.20	59.62	40.38
	2YSZ+0.05 wt% MnO_2	1.19	98.81	44.71	55.26	61.20	38.80
	2YSZ+0.25 wt% MnO_2	19.76	80.24	36.08	63.92	62.19	37.81
	2YSZ+0.75 wt% MnO_2	--	--	--	--	--	--

From the results presented in Table 18, it can be observed that for some doped 2YSZ samples the deleterious transformation of zirconia was prevented. There was no evidence of degradation in all samples of zirconia doped with different amounts of ytterbia, since more than 99.9 % is constituted by tetragonal zirconia. Comparing with the other samples, the best results in terms of prevention of degradation were achieved by these samples.

The 2YSZ doped with SiO_2 and La_2O_3presented a small amount of monoclinic phase after 36 hours of degradation (24.49 %). These improvements on ageing resistance were somehow expected, since the published studies [53]–[60], [65], reported that theses dopants (ytterbia, silica and lanthana) stabilize the tetragonal phase of zirconia and they can promote an effective deceleration of the transformability of zirconia, resulting in an improvement of degradation resistance.

In relation to zirconia doped with manganese oxide samples, an increase of monoclinic zirconia occurs with the increase of this dopant (Table 18). An enhancement of the ageing resistance would also be expected, since it has been reported that this dopant improves the resistance to degradation [50], [51]. *Ramesh et al*. [51] verified that by the addition of MnO_2 to zirconia, a slow decrease on the ageing kinetics phenomenon occurs.

As previously mentioned, the aged samples doped with silica and alumina led to the suppression and decreasing of intensity of the peaks correspondent to the phases of zirconia, resulting in a decrease of the sample's crystallinity (Figure 60 – b). For this reason, the quantifications of zirconia phases' correspondent to this doped sample after 36 hours of thermal ageing test were not measured (Table 18).

Comparing the aged doped samples at intermediate time stage (12 hours of procedure of the thermal ageing treatment), the sample of zirconia doped with 0.50 wt% of ceria achieved the lowest value of monoclinic phase (31.35 %) in relation to the other samples in the same period of time (except when compared with zirconia doped with Yb_2O_3 and zirconia doped with both oxides, SiO_2 and La_2O_3). For the concentrations smaller and higher than this value (0.50 wt% of CeO_2), the amount of tetragonal zirconia decreases.

In order to investigate if the degradation expands to the bulk, the cross-section of the samples after 36 hours of ageing was observed by SEM. A method which consists in measuring the thickness of the monoclinic layer, from the distance of the sharp uneven line from the surface until transformed zone of the bulk,allows to study the extension of the degradation and it is a method used by several authors [8], [28], [135]. The obtained micrographs of cross-section surfaces of doped samples are displayed in Figure 61.

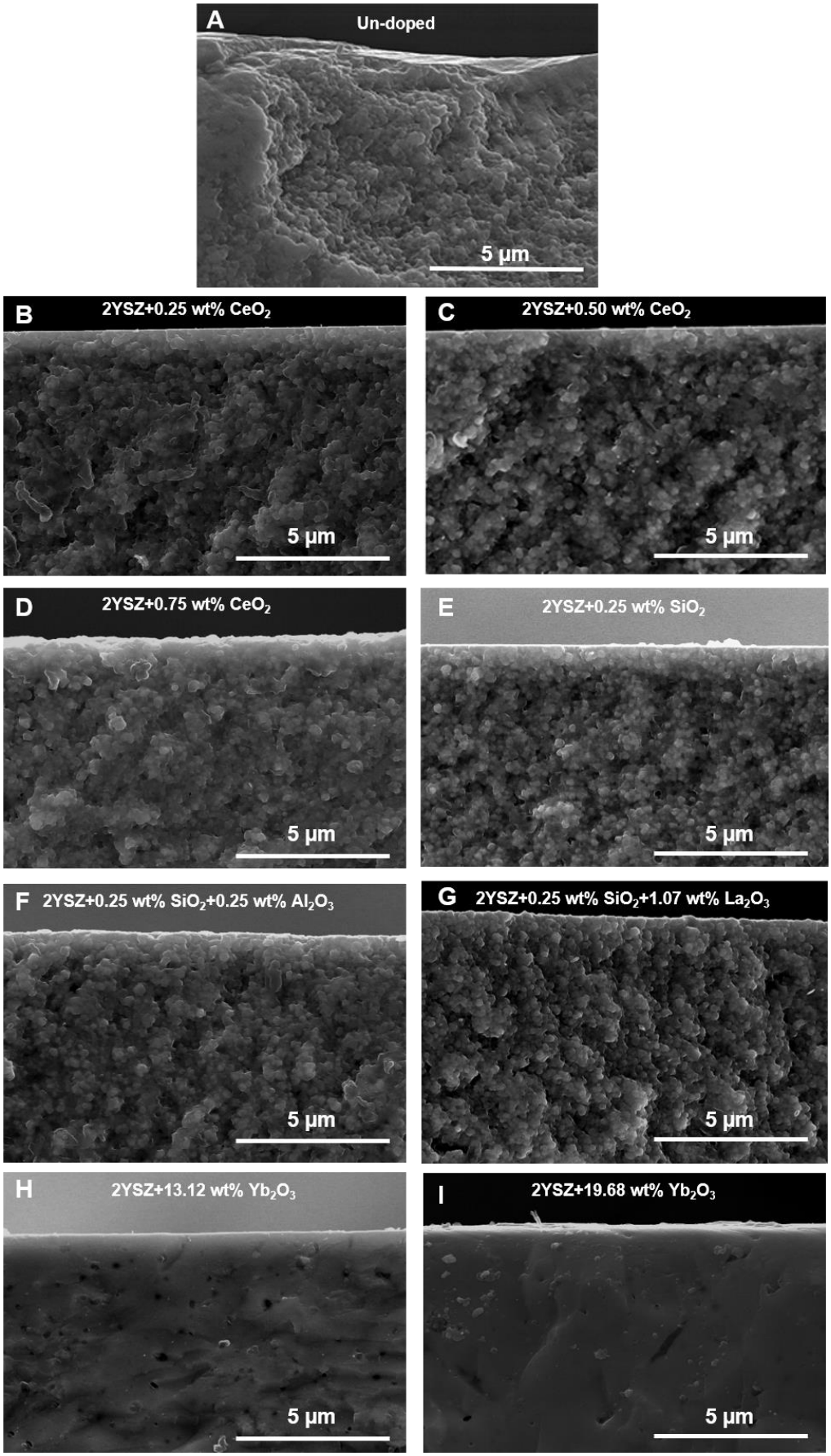
A
Un-doped
5 µm
B
2YSZ+0.25 wt% CeO_2
5 µm
C
2YSZ+0.50 wt% CeO_2
5 µm
D
2YSZ+0.75 wt% CeO_2
5 µm
E
2YSZ+0.25 wt% SiO_2
5 µm
F
2YSZ+0.25 wt% SiO_2+0.25 wt% Al_2O_3
5 µm
G
2YSZ+0.25 wt% SiO_2+1.07 wt% La_2O_3
5 µm
H
2YSZ+13.12 wt% Yb_2O_3
5 µm
I
2YSZ+19.68 wt% Yb_2O_3
5 µm

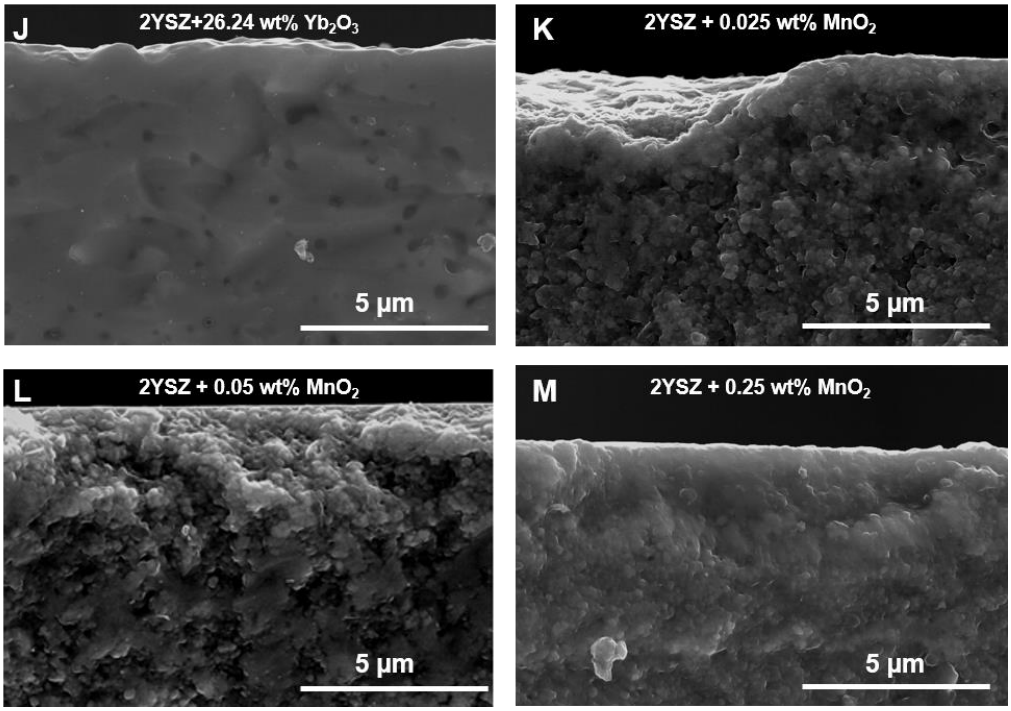

Figure 61. SEM images of the cross-section of the surface of the doped 2YSZ samples after 36 hours of thermal ageing tests.

Figure 61 - A corresponds to a 2YSZ sample without the addition of dopants, provided by INNOVNANO, which was used as a reference sample after ageing, for comparison with the doped samples. From the micrographs it can be seen that the reference sample is degraded, since it presents an extensive grain pull-out at the surface and a porous structure. The monoclinic transformed region is characterized by the presence of porosity, grain pull-out and intergranular fracture [28], [53]. In terms of structure, monoclinic fraction presents a porous and disorganized structure. On the other hand the tetragonal region is dense, and presents a continuous, smooth surface.

As it can be observed, the 2YSZ doped with CeO_2 (B, C, D), SiO_2 (E) and SiO_2 with alumina and lanthana (F, G, respectively), and Yb_2O_3 (G, I) samples present a continuous surface of the cross-section, with no evident layer of porosity and grain pull-out, which is also a characteristic of the tetragonal fraction.

In the sample with higher grain size, the cracking tends to cross through the grains of the sample. In this case, the samples demonstrate a smoother superficial fracture which suggests a transgranular fracture. An example of this effect is presented in the sample of 2YSZ doped with Yb_2O_3 (Figure 61 – H, I, J), with a mean grain size range of 432 - 3525 nm. In contrast, for the samples with a smaller grain size, the crack has to pass between the grains, i.e., it has to circumvent the grain boundary, resulting in a more intergranular cracking and therefore a slightly rougher surface. As an example, the 2YSZ doped with

an amount of 0.05 wt% of MnO_2, which have a smaller mean grain size (272 nm), presents a slightly rougher surface.

In general, for all mentioned samples, the obtained grain size, the partially uniform microstructure with no evident agglomeration and the appropriated sintering temperature contributed to these beneficial results of thermal ageing resistance. As confirmed by some authors, the application of a relative low sintering temperature (1350 ºC and 1400 ºC) may enhance the ageing resistance [28]. An obtained nanometric grain size (Table 17) and no visible agglomeration of the grains (Figure 59) leads to an adequate stabilization of the zirconia. Samples of 2YSZ with finer and smaller grain sizes are ideal to achieve better mechanical properties and ageing resistance [1]. For these reasons, it will be expected that the surface layer of monoclinic zirconia would not cause a decay of the mechanical properties (fracture toughness) of the aged sample.

In terms of thermal ageing resistance, the behaviour observed by ytterbia doped 2YSZ samples is related with their grain size. In the samples doped with ytterbia that present higher value of grain size, corresponding to the samples with higher concentration of ytterbia (2YSZ+19.68 wt% Yb_2O_3 and 2YSZ+26.24 wt% Yb_2O_3), a decrease of the mechanical properties will be expected. Thus, a slightly lower sintering temperature would be beneficial for the samples doped with this oxide in order to obtain a smaller grain size, which would consequently lead to an improvement of the mechanical properties.

From all doped samples, the 2YSZ doped with manganese oxide samples are the most affected by the thermal ageing (Figure 61 - K, L, M). From these micrographs it can be observed that the surface of these samples were degraded with the exposure to low temperature during the established period of time of this ageing tests. In these samples, the thickness of this degraded layer is large enough to be measured by the distance of the sharp uneven line from the surface until the point into the bulk of the sample where this degradation ends. It is important to acknowledge that these values should be regarded as rough estimates providing useful additional information rather than exact thickness of surface layers degraded after exposure to thermal ageing. The results of these measurements of monoclinic fraction are presented in Table 19.

Table 19. Thickness of the monoclinic fraction layer after ageing.

	Compositions	36 hours
		SEM (μm)
Reference	2YSZ	10.84
MnO_2	2YSZ+0.025 wt% MnO_2	2.9
	2YSZ+0.05 wt% MnO_2	3.1
	2YSZ+0.25 wt% MnO_2	3.5

Through the measurement carried out in MnO_2 doped 2YSZ, it is verified that with the increase of the amount of dopant (Table 18), the thickness of transformed zone also increases (Table 19). In terms of the grain size, the samples of 2YSZ doped with 0.25 wt% of manganese oxide show the highest value (591 nm). As previously mentioned, bigger grains of zirconia lead to a reduction of the mechanical properties [4], [21].The sintering temperature (1350 ºC) selected from the dilatometric analysis (Figure 56), for this doped samples allows a slightly increase of the grain size. A decay of the fracture toughness for the 2YSZ doped with this highest amount of MnO_2 (0.25 wt%) due to the monoclinic content present in this sample and its grain size, will be expected.

4.1.4.5. Mechanical Properties

One of the most important characteristics of zirconia ceramics is their excellent mechanical properties. The densification upon sintering process is a fundamental factor that benefits the mechanical properties of these materials. It is known that the final density of the sintered samples and grain size have a strong influence in the mechanical properties, since high density ceramic materials with a reduced grain size leads to the improvement of the mechanical properties [1].

The fracture toughness for all 2YSZ doped samples, after the thermal ageing test was studied. Through this mechanical parameter it is possible to investigate the capacity of the doped samples to resist crack propagation, avoiding catastrophic fracture. The mechanical test was carried out as described in the procedures presented in chapter three, and the results obtained are displayed in Figure 62.

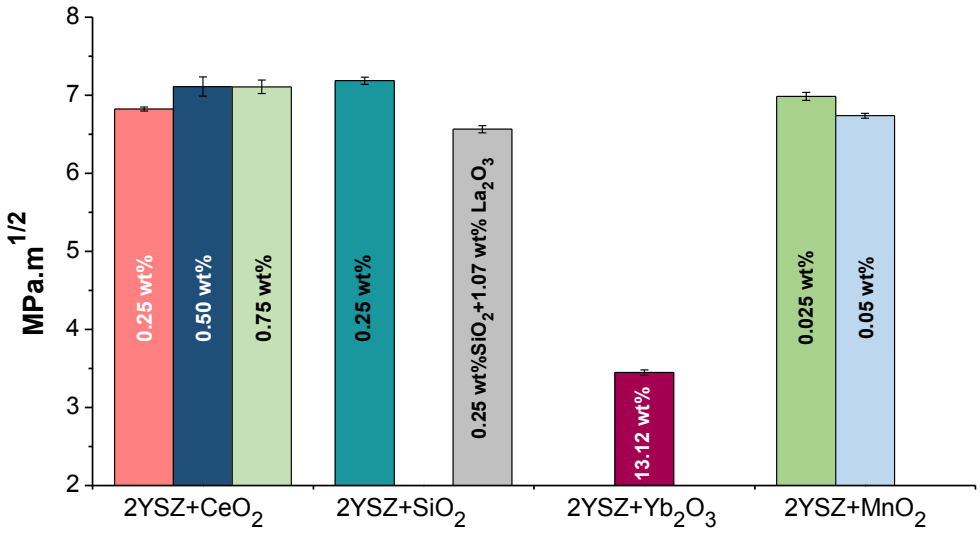

Figure 62. Results obtained for fracture toughness of the doped 2YSZ samples.

Since zirconia with lower amount of yttria (2YSZ) is more susceptible to the tetragonal to monoclinic transformation, the fracture toughness was greatly influenced by this stabilizer content and by the addition of the dopant oxides. The toughening enhancement is proportional to the amount of transformable zirconia present in doped 2YSZ samples. This phenomenon is related with the martensitic transformation of zirconia. From the obtained results, it can be verified that 2YSZ doped samples present a similar value of fracture toughness after being submitted to ageing tests during a period of 36 hours, except zirconia doped with ytterbia where that parameter decreases significantly.

As previously mentioned, although ytterbia doped 2YSZ samples present the higher ageing resistance when compared to the other doped samples, they present a microstructure with a larger grain size (432 – 3525 nm). From the results, it was confirmed that with the increase of the content of this dopant, which led to a higher growth of the grains, the indentations of the cracks were too large and it was not possible to be measured (19.68 wt% Yb_2O_3 and 26.24 wt% Yb_2O_3). This behaviour can be related to the higher grain size which makes the propagation of the crack to occur inside the grains, since in this case the contribution of the grain boundary effect is lower, because the lower amount of grain boundary does not contribute to dissipate the energy in order to stop the crack more rapidly. Among the samples doped with ytterbia the one with a lower content of dopant (13.12 wt% Yb_2O_3), presented the lower grain size and achieved the lowest value of fracture toughness when compared with the other samples, 3.45 $MPa.m^{1/2}$.

The sample of zirconia doped with a higher amount of manganese oxide (0.25 wt% of MnO_2) showed a higher extension of degradation in comparison with all of the other doped samples, which could be confirmed by SEM micrographs and by the values of

monoclinic fraction (3.4 μm) measurements. The higher grain size of this sample (591 nm) and the amount of monoclinic zirconia (62.19 %), makes that propagation of crack to occur in the inside of samples, making them more fragile samples in terms of mechanical resistance.

In relation to the other samples (2YSZ doped with CeO_2, SiO_2, SiO_2 with La_2O_3), it is possible to confirm that the degradation occurs only at the surface of the doped samples. A densification above 90 % of the sintered doped samples allowed to obtain good fracture toughness results, as can be seen in Table 16. Regarding the doped 2YSZ samples, the highest value of fracture toughness was achieved for silica doped 2YSZ sample, 7.19 $MPa.m^{1/2}$. Thus, it can be concluded that the different dopants do not show relevant differences in the fracture toughness of the doped 2YSZ samples. In parallel, it is visible that for each dopant, at different concentrations, the fracture toughness is not influenced, since the achieved values are very similar. Thus, it may be concluded that for these samples, the amount of monoclinic zirconia present at the surface layer was not deleterious to fracture toughness.

4.1.4.6. Conclusion of the preliminary study

Throughout this preliminary study and in order to verify the ageing resistance and fracture toughness behaviour, thermal ageing tests and mechanical tests were carried out to the defined doped samples and the selection of the best type and concentration of doped oxide of zirconia was accomplished. It was verified that some of the selected samples did not present the important characteristics of zirconia stabilized ceramics: improved ageing resistance and fracture toughness. However, from the obtained results, it can be confirmed that some of the selected doped 2YSZ samples played an important role in improving the resistance to ageing and mechanical properties of the less stable zirconia. From the results obtained for the amount of monoclinic zirconia and for the fracture toughness it can be concluded that an improvement of the ageing resistance and mechanical properties was achieved when ceria (0.50 wt%) and, silica with lanthana (2YSZ+0.25 wt% SiO_2+ 1.07 wt% La_2O_3) were added to 2YSZ.

The sample of 2YSZ doped with CeO_2 showed an improvement of the ageing resistance and a good value of fracture toughness, 7.11 $MPa.m^{1/2}$. Ceria improves the mechanical properties of YSZ, namely, the addition of this dopant promotes the increasing of the fracture toughness [46]. The 2YSZ doped with this oxide, sintered at 1350 ºC,

presented a homogeneous morphology with a mean grain size of 297 nm and a density of 5.99 g/cm^3.

On other hand, in order to protect the tetragonal phase against the degradation, silica (SiO_2) and lanthana (La_2O_3) oxide were tested. Both these dopants have proven to decelerate the tetragonal to monoclinic transformation [53], [54], [56]–[59]. These oxides retain the mechanical properties of 2YSZ, which means that although the ageing resistance increases, it has no deleterious effect in mechanical properties [53], [60]. The amount of each dopant was selected accordingly to the published results (0.25 wt% SiO_2 and 1.07 wt% La_2O_3) [55], [60]. The 2YSZ doped with both these oxides was sintered at 1350 ºC, reaching a density of 5.99 g/cm^3. This sample presented a homogenous morphology with a mean grain size of 297 nm. Although, a slightly lower fracture toughness value was obtained after the sample being submitted to thermal ageing, 6.56 MPa.m$^{1/2}$.

Hence, a study of the resistance to hydrothermal ageing tests was performed with these two selected samples.

4.2. Study of the selected doped 2YSZ samples

After the initial characterization (thermal ageing resistance and fracture toughness) of all doped 2 mol% Yttria Stabilized Zirconia (2YSZ) samples, the best ones were selected for comparison with the un-doped 2YSZ samples commercialized by INNOVNANO. This comparison was done in order to evaluate the ageing resistance by hydrothermal ageing tests and mechanical properties (before and after the hydrothermal ageing tests).

A schematization related with the selected doped zirconia compositions is presented in Figure 63. The further study of these selected samples was carried out and the achieved results are presented in the following sections.

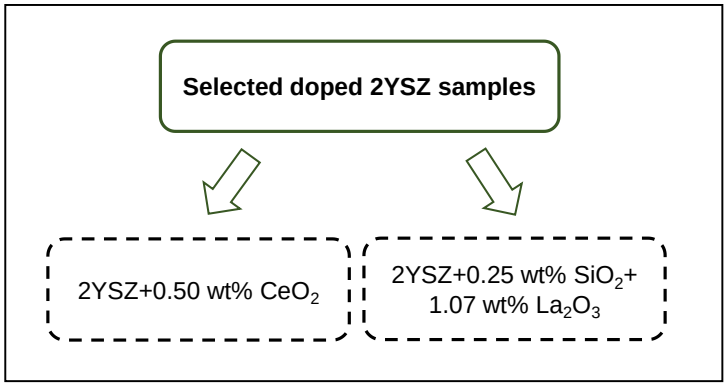

Figure 63. Selected doped 2YSZ compositions derived from the results previously analyzed.

4.2.1. Characterization of the selected doped 2YSZ spray dried powders

Since it was not possible to use the same ball milling that was used for the first samples, available at INNOVNANO (Figure 31), the best selected compositions were submitted to a deagglomeration process in another milling equipment (available at the University of Aveiro). A Teflon jar with micrometric balls of zirconia was used in a planetary milling equipment (Retsch PM400) in order to achieve a controlled particle size distribution. The operating conditions (time and velocity) of this equipment were previously adjusted and controlled, to obtain similar results (in terms of the grain size distribution) than those presented in the previous preliminary study.

4.2.1.1. Specific Surface Area

The specific surface area (SSA) of the two selected doped spray dried powders was measured by the B.E.T. adsorption isotherm. In Table 20, the obtained SSA values are presented.

Table 20. Specific surface area of each doped 2YSZ composition powders.

Composition	Specific Surface Area (B.E.T.) (m^2/g)
2YSZ+0.50 wt% CeO_2	22.23
2YSZ+0.25 wt% SiO_2+1.07 wt% La_2O_3	21.34

As expected, the obtained values for these compositions are identical to the values achieved in the preliminary study (22.97 m^2/g for CeO_2 doped 2YSZ and 21.01 m^2/g for 2YSZ doped with SiO_2 and La_2O_3). The specific surface areas of both the selected composition powders are very similar. Comparing these results with the value obtained for the un-doped 2YSZ (23.46 m^2/g), it is noticed that the addition of dopants (CeO_2, SiO_2, La_2O_3) did not significantly affect the specific surface area.

4.2.1.2. Powder density

The obtained value of the powder density determined by helium pycnometer for the doped 2YSZ with ceria was 5.556 g/cm^3. This value is similar to the value obtained for the 2YSZ doped with silica and lanthana oxide (5.524 g/cm^3), and they are in accordance with the previous values obtained in a preliminary study (5.525 g/cm^3 for CeO_2 doped 2YSZ and 5.484 g/cm^3 for SiO_2 with La_2O_3 doped 2YSZ). From the obtained values it can be considered that the nanometric particles, which constitute the granules of doped 2YSZ, are dense nanoparticles.

4.2.1.3. X-Ray Fluorescence

The chemical composition of each doped 2YSZ powders was analyzed through X-ray fluorescence. This characterization is important because it allows to confirm the presence of the dopants used in each sample, and assures the absence of any contamination. The result contents of each oxide are summarized in Table 21.

Table 21. Chemical composition for each doped 2YSZ composition powders.

Composition (%)	2YSZ+0.50 wt% CeO_2	2YSZ+0.25 wt% SiO_2+1.07 wt% La_2O_3
ZrO_2	92.727	92.230
Y_2O_3	3.969	3.931
HfO_2	2.096	2.170
Al_2O_3	0.371	0.301
CeO_2	0.560	-
SiO_2	-	0.269
La_2O_3	-	1.035
Other elements	0.277	0.064

From the obtained results of chemical compositions, the presence of each added dopant (CeO_2, SiO_2, La_2O_3) to 2YSZ is confirmed.

As previously observed for the compositions of the preliminary study, no contaminations were noticed. As specified on ISO 13356:2008 [13], it was verified that the content of hafnia is below 5% and the other minority elements are below 0.5%, for each selected doped zirconia powder.

Also, the content of zirconia, yttria and selected dopants, are in agreement with the defined composition for each doped 2YSZ composition.

4.2.3. Characterization of selected doped 2YSZ sintered samples

4.2.3.1. Density of the green and sintered pieces

The stages of powder pressing significantly affect the densification and physical properties of the sintered materials [136], [137]. The effect of the green density on the sintering behaviour of ceramics materials has been a widely studied topic. *Krell et al.* [137], compared the effect of the final density (after sintering) of submicron alumina prepared by uniaxial pressing (UP) and cold isostatic pressing (CIP) in addition to the uniaxial pressing. The study confirmed that a reduction of the sintering temperature occurs for the samples subjected to UP and CIP, as well as an increase in the final density of the sintered samples for compacts with higher green density. This occurs due to the enhancement on the particles' densification of the samples that were submitted to both pressing stages.

Uniaxial pressing presents some limitations which are mainly associated with unsymmetrical density due to non-uniform pressure inside the sample which lead to

deformities and cracking of the samples during the sintering process [138]. Contrarily to UP, cold isostatic pressing allows the achievement of a more uniform distribution of density in the samples. It also decreases the number of free defects (pores), since the samples are submitted to equal and simultaneous pressures over all their surface. Thus, it allows a maximum of uniformity of the density and, as a consequence, more uniform microstructures [139].

Well densified samples are an indicator of good mechanical properties. Since a good degree of densification was already achieved with uniaxial pressing for all samples, in the preliminary study, the addition of one more pressing stage (CIP) is expected to improve the densification of the selected samples, before sintering. The densities of the green and sintered bodies were measured geometrically and by the Archimedes' Method, respectively. The values obtained for each doped composition, after each stage of pressing and sintering, are presented in Figure 64. The densification degree related with the theoretical values of each element was determined and presented in Table 22.

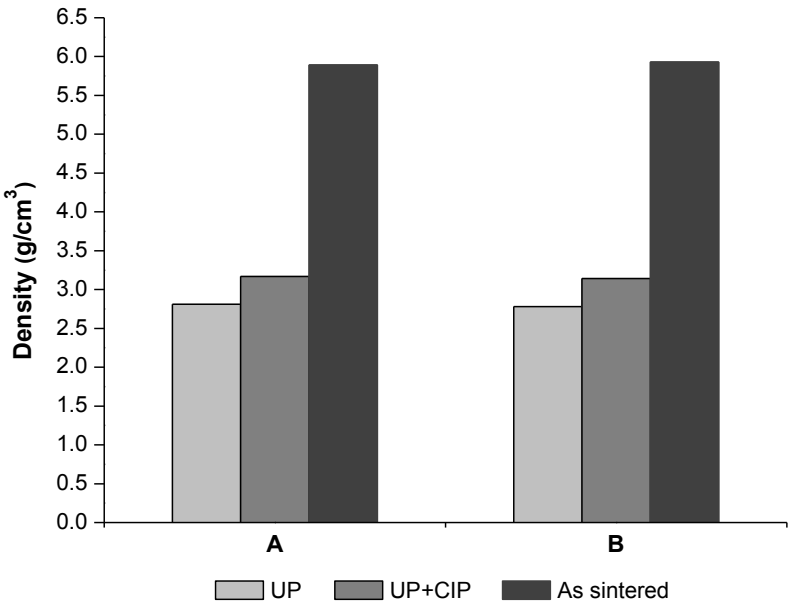

Figure 64. Density values achieved for different stages of pressing (UP and CIP) and sintering for best doped 2YSZ samples: **A)** 2YSZ+0.5 wt% CeO_2; **B)** 2YSZ+0.25 wt% SiO_2+1.07 wt% La_2O_3.

Table 22. Density degree of each doped 2YSZ composition after sintering.

Composition	Density (%)
2YSZ+0.5 wt% CeO_2	96.94
2YSZ+0.25 wt% SiO_2+1.07 wt% La_2O_3	97.76

From the obtained results it can be confirmed that the density of the green bodies increases with the additional stage of cold isostatic pressing. A slight improvement of approximately 0.4 g/cm^3 was obtained.

The sintering process led to a densification of the doped 2YSZ samples of approximately 2.80 g/cm^3, when compared to their values of green density (after the Cold Isostatic Pressing). Both selected doped 2YSZ sintered samples present very close density values (5.89 g/cm^3 and 5.93 g/cm^3 for 2YSZ+0.5 wt% CeO_2 and 2YSZ+0.25 wt% SiO_2+1.07 wt% La_2O_3, respectively), demonstrating similarities between these samples. Once more, the sintering process highly contributed to the increase of the densification degree reaching values of approximately 97 %, relatively to the theoretical values. These values are the result of a good packing of the nanometric particles during the pressing stages and the homogeneity of green bodies. These factors are important for the sintering of ceramics at relatively low temperature (1350 ºC) with higher density. However, the density degree, relatively to the theoretical values, is slightly lower when compared with the same compositions prepared in the preliminary study, where both samples achieved a value of density higher than 98.65 %. This decrease of density can be correlated with the modification of the milling equipment. Due to this modification, aspects such as time and velocity were controlled and defined, in order to obtain a particle size distribution of these compositions to be coherent with the results obtained before (with INNOVNANO's ball mill). From this control, the results and differences on the particle size distribution are presented in Figure 65.

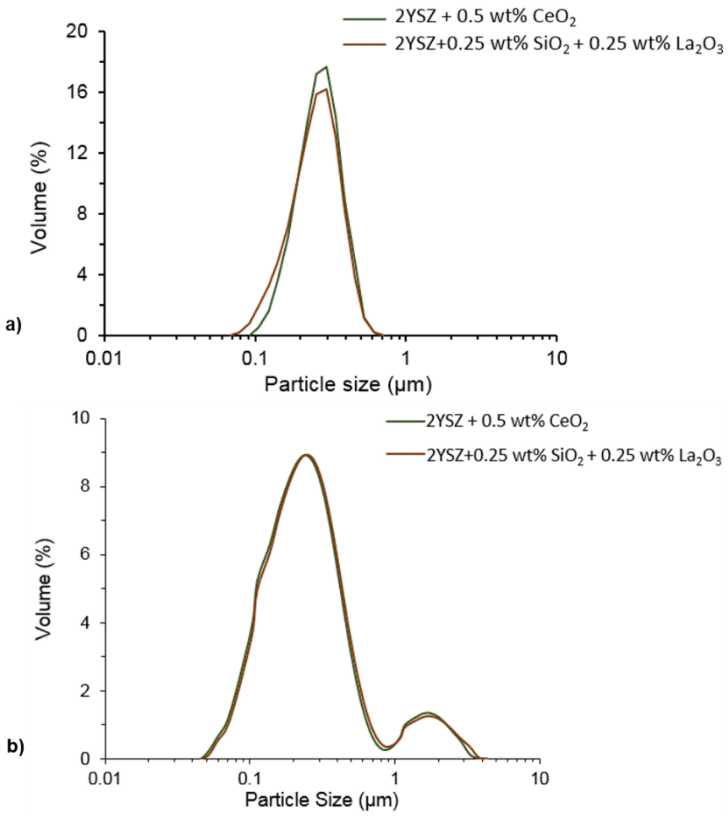

Figure 65. Particle size distribution of the selected doped 2YSZ samples: **a)** process performed at University of Aveiro; **b)** process performed at INNOVNANO.

The powders were subjected to a deagglomeration process during 30 min for 2YSZ+0.5 wt% CeO_2 and 1 and a half hour for 2YSZ+0.25 wt% SiO_2+1.07 wt% La_2O_3 at 250 rpm. From the analysis of the obtained graphic, slight differences are observed in terms of the particle size distribution behaviour of both selected samples when compared with the same compositions, in the preliminary study (Figure 65 – b). It can be possible to verify that these selected samples exhibit a unimodal distribution of the particles, while previously, a bimodal distribution was obtain for all samples.

Also, by the presented results, it can be confirmed that a higher peak volume fraction of sub micrometric particles (around 16 %) is obtained for the ball milling process at the University of Aveiro (Figure 65 - a) while on the samples milled at INNOVNANO the bimodal distribution resulted in lower values of volume fraction of the same type of particles (close to 9 %). The values of the mean diameter obtained for the selected compositions are displayed in Table 23.

Table 23. Mean diameter of the selected doped 2YSZ compositions.

Composition	Mean diameter (d50) (μm)
2YSZ+0.5 wt% CeO_2	0.253
2YSZ+0.25 wt% SiO_2+1.07 wt% La_2O_3	0.233

Comparing the obtained values of the selected compositions with those of the samples milled at INNOVANO, it is possible to conclude that the working parameters (time and velocity) were well defined, since the mean diameter values are similar (0.221 μm and 0.228 μm for the first samples - 2YSZ+0.5 wt% CeO_2 and 2YSZ+0.25 wt% SiO_2+1.07 wt% La_2O_3, respectively) for both milling processes.

Nevertheless, problems associated with the use of the Teflon jars were observed. A slightly amount of Teflon particles were visible in aqueous suspensions of these compositions. Although, these aqueous suspensions have been sieved (sieve of 80 μm), some of these particles passed to the suspension of each composition. Whilst the cold isostatic pressing have contributed to increase the green density of the samples (when compared with the samples uniaxially pressed), their final density was not benefited by this additional pressing stage, due to the presence of the Teflon impurities. From the obtained density values, it can be seen that the density decreased about 1.71 % for 2YSZ doped with CeO_2 and 0.97% for 2YSZ doped SiO_2 and La_2O_3 samples, relatively to the theoretical values, in comparison with the prepared sintered samples in the preliminary study with these dopants. Since the density of the samples is influenced by the last stage (sintering), this is the process that will define the final density of the samples. The burn (on the sintering process) of the Teflon particles present in the spray dried powders

promoted the creation of some porosity in the sintered samples, which consequently led to the decrease of the density for both sintered samples.

The value of approximately 97 % is still an indicator of good densification, but this value is not sufficient to guarantee the required mechanical properties. Due to this density decrease of the sintered doped samples, a slight decrease of mechanical and ageing resistances, in relation to un-doped zirconia samples that have not passed through the same milling process, will be expected.

4.2.3.2. Crystal Phases Composition

X-ray diffraction was carried out for the sintered doped samples in order to verify the presence of zirconia phases (tetragonal and monoclinic zirconia) and confirm the absence of new crystalline phases that could be formed during the sintering stage. The obtained diffractograms of each doped 2YSZ sintered sample are presented in Figure 66.

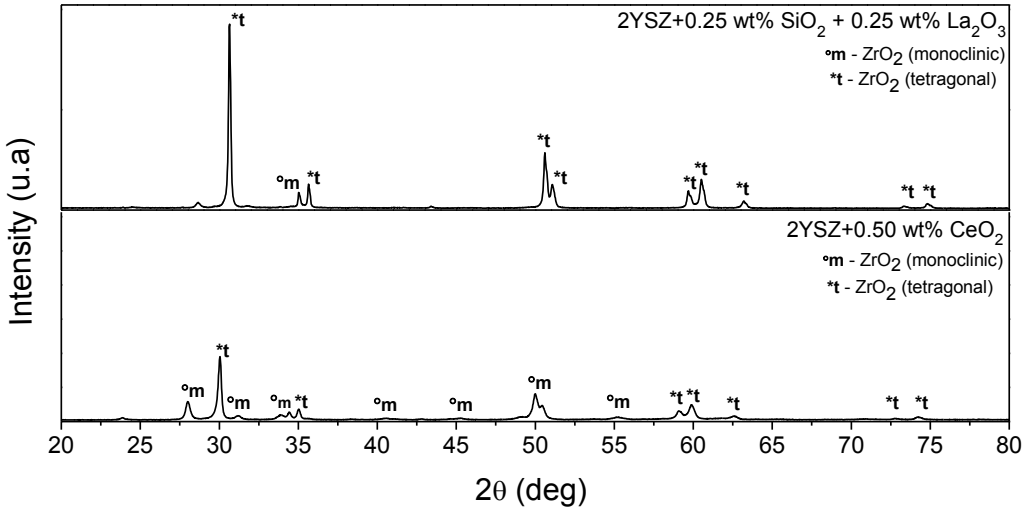

Figure 66. X-ray diffractogram obtained for each selected doped 2YSZ sample after sintering.

From the diffractograms analysis, it can be confirmed that the only phases present in the doped 2YSZ samples are monoclinic and tetragonal ZrO_2. It was expected that the sintering stage carried at 1350 ºC would not allow the presence of monoclinic zirconia (this phase is only stable until 1170 ºC) and also because, by the dilatometric studies it was possible to verify that this is the temperature where a higher densification of the samples is achieved. However, some amount of monoclinic zirconia was detected by Diffrac^{Plus}Topas. The content of every detected phase of zirconia is displayed in Table 24.

Table 24. Phase quantification of each selected doped sintered sample.

Composition	$ZrO_{2\ (tetragonal)}$ (%)	$ZrO_{2\ (monoclinic)}$ (%)
2YSZ+0.5 wt% CeO_2	72.51	27.49
2YSZ+0.25 wt% SiO_2+1.07 wt% La_2O_3	90.63	9.37

The sintering temperature applied in these samples did not allow all the monoclinic zirconia to transform into the benefic tetragonal phase of zirconia. The higher value of monoclinic phase in sintered samples was observed for the sample doped with ceria. For 2YSZ doped with both oxides (SiO_2 and La_2O_3), a lower amount of monoclinic zirconia (9.37 %) is verified. The higher amount of monoclinic phase in the sample of 2YSZ doped with ceria explains its lower verified density (96.94 %) whilst the sample doped with both oxides presents lower amount of monoclinic zirconia (9.37 %) making this sample somewhat denser.

Due to the confirmed presence of some monoclinic zirconia after sintering in the samples, it can be expected a slight deleterious effect that will affect the following tests.

4.2.3.3. Microstructure

The selected doped sintered samples were thermally etched and observed by scanning electron microscopy. The obtained micrographs were used to evaluate the microstructure and determine their grain size. The obtained images for each doped 2YSZ composition are exhibited in Figure 67.

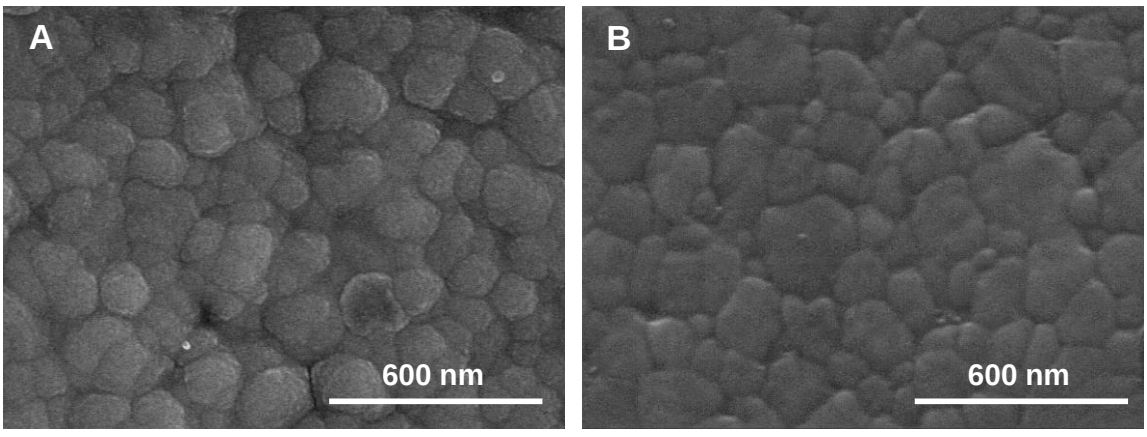

Figure 67. SEM micrographs obtained from the thermal etched doped samples: **A)** 2YSZ+0.5 wt% CeO_2; **B)** 2YSZ+0.25 wt% SiO_2+1.07 wt% La_2O_3.

From the obtained images, a different microstructure can be clearly noticed. In relation to the sample doped with ceria (Figure 67 – A), an segregation of the granules is noticed while in the sample doped with both oxides (silica and lanthana), Figure 67 - B, a

well dispersed microstructure and without segregation of the granules was observed. The density of CeO_2 doped 2YSZ samples reached slightly lower values (around 97 %) in comparison with the 2YSZ doped with both oxides (approximately 98 %). From these density values, it is possible to assume that this visible porosity, appear only at the surface of the material.

The mean grain size of the both selected doped samples was also determined from SEM micrographs. This procedure was performed in the same conditions as the other samples in the preliminary study (two micrographs for each composition, with the same magnification), using the linear interception method. The obtained results for the mean grain sizes are summarized in Table 25.

Table 25. Mean grain size of each composition determined by line interception method.

Composition	Mean grain size (nm)
2YSZ+0.5 wt% CeO_2	275±9
2YSZ+0.25 wt% SiO_2+1.07 wt% La_2O_3	308±8

Regarding Table 25, it can be noticed that a similar mean grain size was achieved for both samples when compared with the mean grain sizes obtained for the starting samples (345 and 297 nm for 2YSZ+0.5 wt% CeO_2 and2YSZ+0.25 wt% SiO_2+1.07 wt% La_2O_3, respectively). A less stabilized zirconia (2 mol% yttria) is beneficiated by the presence of smaller grain size, while larger grains make the sample more vulnerable to spontaneous phase transformation of zirconia [4], [21]. Considering that relatively small mean grain sizes were achieved, good results regarding ageing resistance for both selected samples would be expected.

As previously mentioned, in the work published by *Ragurajan et al.* [47], the sample doped with CeO_2 presented a homogenous microstructure and a small grain size. In the present experimental work, the sample doped with CeO_2 (0.50 wt%) also presented a smaller grain size (275 nm). However an irregular surface is observed.

In relation to the composition doped with SiO_2 and La_2O_3 oxides, it was reported in literature that, such as density, the addition of these dopants do not cause significant variation of the grain size [53], [60]. As a dopant, lanthana does not cause a significant variation of the grain size [53] neither causes a decrease in the zirconia grain size. This is associated with the segregation of La^{3+} cation at the zirconia grain boundary [55]. A slightly higher value of the mean grain size was observed for the composition doped with both oxides (SiO_2 and La_2O_3), 308 nm, comparing to the zirconia doped with CeO_2 (275 nm).

4.2.3.4. Mechanical properties

Mechanical tests of doped 2YSZ sintered samples were carried out in order to evaluate the effect of the addition of the selected dopants to 2YSZ on their hardness, fracture toughness and flexural strength. The outcome for each doped sample was compared between each one and with un-doped sample of 2YSZ commercialized by INNOVNANO. In Figure 68, the results of mechanical tests performed for doped zirconia samples are presented.

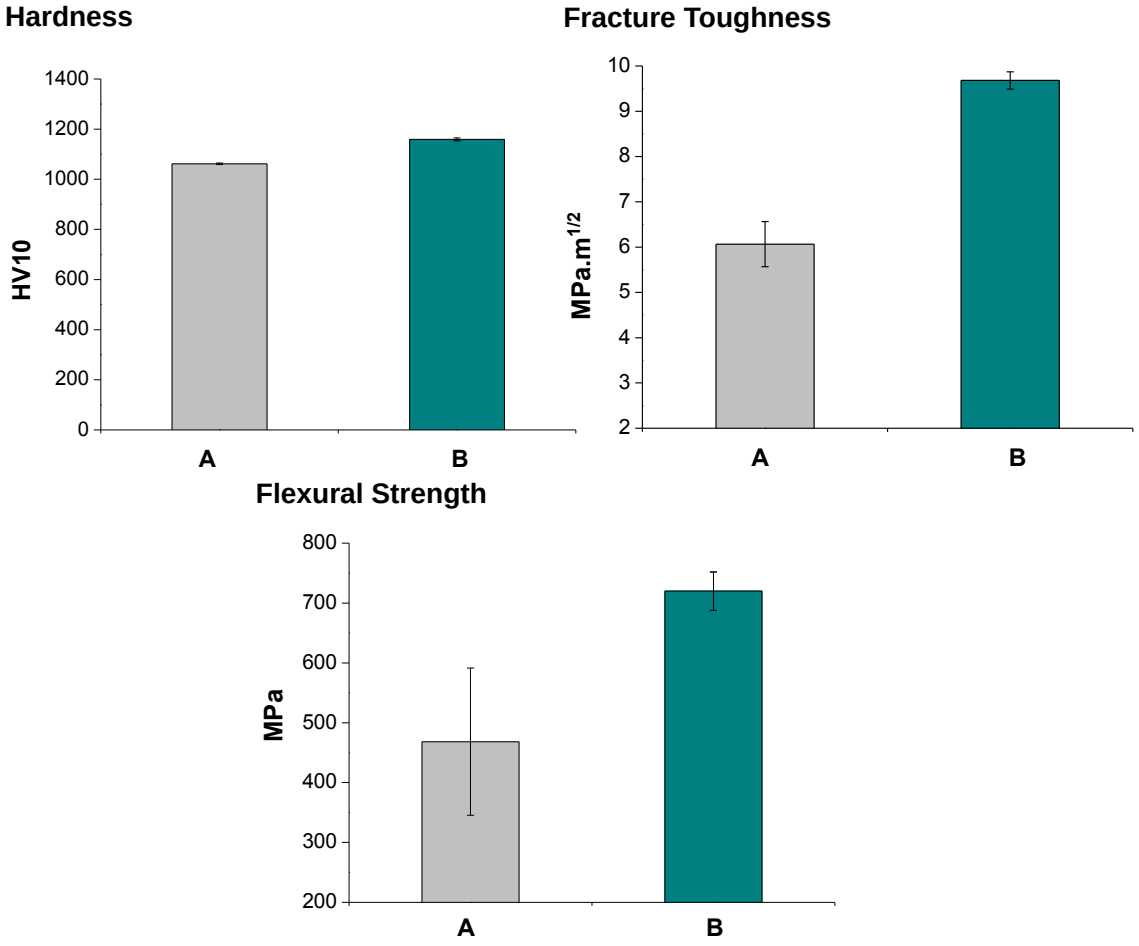

Figure 68. Results obtained for Vickers Hardness, fracture toughness and flexural strength of the samples: **A)** 2YSZ+0.5 wt% CeO_2; **B)** 2YSZ+0.25 wt% SiO_2+1.07 wt% La_2O_3.

Regarding the obtained results of the mechanical properties, higher values were obtained for the sintered 2YSZdoped with both oxides samples (SiO_2 and La_2O_3) in comparison to the CeO_2 doped zirconia sample.

Nevertheless, an enhancement of the mechanical properties would be expected for the sample doped with ceria since it has been reported that this dopant improves the mechanical properties of stabilized zirconia, principally the fracture toughness [47], [48]. However, regarding the mechanical properties, this effect was not visible in the sample

prepared for the present study. Comparing the achieved results with the results obtained by *Ragurajan et al.* [47], it was noticed that similar values of fracture toughness were achieved (6.07 MPa.$m^{1/2}$ against 6.4 MPa.$m^{1/2}$, respectively) while a slight decrease of the Vickers hardness (again, 1061 HV against 1346 HV) was observed. The obtained result of flexural strength for this sample was 468.4 MPa. Thus, the obtained results are not in conformity with results from previous studies that reported the increase of the fracture toughness and hardness. However, in terms of mechanical properties, this decrease might be related with the lower density obtained by this sample (around 97 %). Some of the porosity observed in the CeO_2 doped zirconia microstructure (caused by burning of Teflon particles) led to a density decrease, which is not favorable for the mechanical properties.

In relation to zirconia doped with silica and lanthana, it was reported that these two dopants play an important role on enhancing the ageing resistance [53], [60], but do not have a considerable effect on the mechanical properties [53], [60]. For this reason, the obtained values of mechanical properties of this doped sample are comparable, although slightly lower, to the reached results for the un-doped zirconia. Similarly to the fracture toughness parameter, the flexural strength is also a parameter influenced by spontaneous transformability phase of zirconia. This sample doped with both oxides present a higher value of fracture toughness when compared to the un-doped zirconia sample (9.68 compared to 8.92 MPa.$m^{1/2}$, respectively). Regarding the other mechanical parameters (hardness and flexural strength) a decrease in relation to un-doped 2YSZ is verified. A slight decrease of hardness is verified (1159 against 1299 HV of the un-doped sample), being this difference rather higher in the case of the flexural strength (again, 700 to 1215 MPa).

Although a decrease in the mechanical properties of both doped samples compared to the un-doped zirconia sample is observed, the greatest decrease is noticeable for flexural strength (468.4 MPa for CeO_2 doped 2YSZ, 700 MPa for SiO_2 with La_2O_3 doped 2YSZ and 1215 MPa for un-doped sample). The presence of porosity in both selected samples is the key factor to the higher decrease of this mechanical parameter.

Regarding the fracture toughness, it is verified that the 2YSZ doped with both oxides, SiO_2 and La_2O_3, obtained an higher result of this mechanical parameter in relation to the sample prepared in the prelaminar study, after being submitted a test of thermal ageing resistance during a period of 36 hours, (9.68 to 6.56 MPa.$m^{1/2}$, after the treatment), as would be expected. On the other hand, CeO_2 doped zirconia sample, which was milled at the University of Aveiro presented a lower value of fracture toughness comparatively to the identical sample prepared for the preliminary study, after being submitted to thermal degradation. This effect evidenced for this sample can be related to the lower density

presented by this sample (96.94 %), since the porosity make this sample less resistant to mechanical properties.

Better values of mechanical properties would be expected if there was no influence by the ball mill process. If the density of these samples would have been better, higher values of mechanical properties should be attained.

Also, the samples could have been pre calcinated until a certain temperature (given by a Thermogravimetric analysis – where the temperature of the Teflon decomposition would be defined) in order to decompose all the Teflon particles that were present on the powder suspensions, thus eliminate the porosity of the prepared samples. This way, it would be expected that the samples' densities would increase, thus enhancing the mechanical properties of both selected samples.

4.2.4. Accelerated Ageing Test

The ageing resistance of zirconia was expected to be affected by the addition of the selected dopants. The presence of the monoclinic phase zirconia in the samples after being submitted to degradation tests is an ageing indicator. As mentioned, the grains of stabilized zirconia only with 2 mol% of stabilizer (Y_2O_3) are more susceptible to spontaneous transformation of tetragonal to monoclinic zirconia and for this reason, the dopants addition are important to slow down this transformability.

In the literature it is referred that ceria presents an important role on the enhancement of YSZ mechanical properties (in particular the fracture toughness) [46]. Since the addition of CeO_2 increases the transformability of zirconia, a slight increase in the monoclinic zirconia would be expected. On the other hand, the silica and lanthana oxides are reported to improve the Low Temperature Degradation (LTD) of YSZ ceramic. Therefore, the ageing resistance of the samples was expected to be improved, by slowing down the tetragonal to monoclinic transformation during the ageing hydrothermal tests.

In order to investigate the behaviour of doped 2YSZ samples to hydrothermal ageing resistance, the samples were placed in a suitable autoclave and exposed to water steam at 134 ºC ± 2 ºC under a pressure of 0.2 MPa during a period of time of 5 hours. These tests were performed according to the ISO 13358:2008 [13] standard. The monoclinic content of each doped sample was quantified by X-ray diffraction after being submitted to an ageing environment. The obtained amount of monoclinic phase of zirconia was compared between each doped sample. The obtained results for each doped composition are presented in Figure 69.

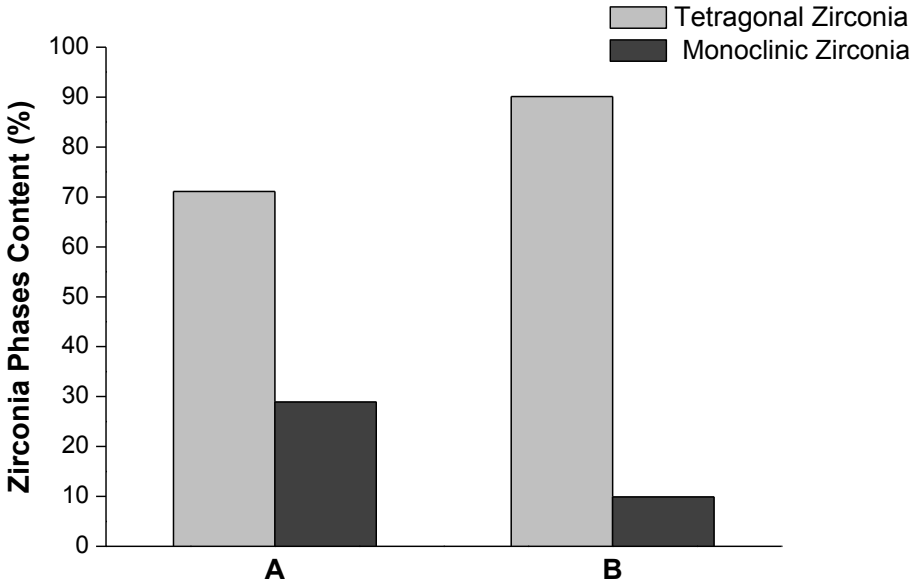

Figure 69. Zirconia phases content (%) present for each aged doped 2YSZ sample: **A)** 2YSZ+0.5 wt% CeO_2; **B)** 2YSZ+0.25 wt% SiO_2+1.07 wt% La_2O_3.

Regarding the results obtained for the aged doped 2YSZ, it can be verified that the 2YSZ doped with ceria is the sample with greater amount of monoclinic zirconia (28.9 %). This was expected because this dopant oxide is more vulnerable to ageing since it is reported that this quaternary oxide, Ce^{4+}, does not produce oxygen vacancies, therefore causing an increase of transformability of zirconia. This fact explains the reinforcement of the mechanical properties, mainly of the fracture toughness. However, it was also reported that doping zirconia with CeO_2 leads to an increase of both tetragonality and stability [46], [49].

As mentioned, the obtained SEM image, Figure 67 – A, presented some porosity at the surface. One plausible explanation for the detection of monoclinic zirconia in higher amounts after the hydrothermal ageing test (28.9 %) can be related with an easier infiltration of the water species through the pores, into the sample. Thus, the doped 2YSZ grains present on the surface were more easily destabilized and transformed to the monoclinic phase of zirconia. Figure 70 compares the extension of the degradation between un-doped (commercialized by INNOVANANO) and doped 2YSZ samples, after their exposure to hydrothermal ageing test, during a period of five hours. In Figure 70 – B it is possible to observe the extension of the tetragonal to monoclinic transformation of the grains of zirconia.

As expected, the 2YSZ doped with SiO_2 (0.25 wt%) and La_2O_3 (1.07 wt%) does not present the same behaviour. It can be observed that both dopants successfully delayed the deleterious transformation upon hydrothermal ageing. This sample did not suffer a

significant degradation since it presented less than 9.87 % of monoclinic zirconia after 5 hours of ageing tests, while the un-doped 2YSZ presented an amount of monoclinic zirconia above 15 %. This was the reason why these dopants were selected. Through addition of the ternary oxide, La^{3+}(such as Y^{3+}), a deceleration of transformability of tetragonal zirconia is promoted, because these cations have a lower valence than zirconia (Zr^{4+}) which produces oxygen vacancies that maintain the charge balance [53], [54]. The achieved values for the sample of 2YSZ doped with SiO_2 and La_2O_3 oxides are in agreement with the ones specified by the ISO 13356:2008 standard which refers that the fraction of monoclinic zirconia after 5 hours in autoclave at 134ºC ± 2 ºC under a pressure of 0.2 MPa must be below or equal to 25 %.

As mentioned, these dopants, SiO_2 and La_2O_3, enhance the tetragonal zirconia resistance to degradation, since they have a stabilizing function of zirconia. For this reason, the behaviour that was observed for CeO_2 doped 2YSZ sample, is not observed for this sample. The monoclinic phase of zirconia remained insignificant despite the surface porosity present (Figure 67 - B). Therefore, it is possible to confirm that the addition of these oxides enhances the ageing resistance of the stabilized zirconia, even in the presence of surface porosity. In Figure 70 – C it is possible to observe that no significant degree of degradation was detected in SiO_2 and La_2O_3 doped 2YSZ sample, which allowed to its successful stabilization.

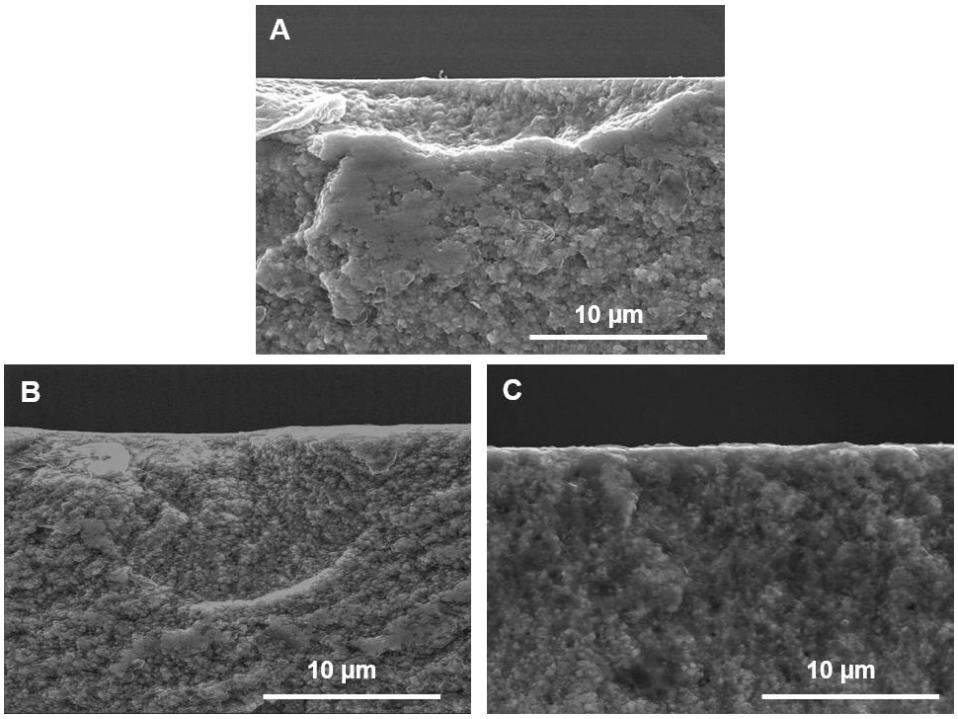

Figure 70. SEM images of the cross-sections of the surfaces of the samples after 5 hours of hydrothermal ageing test: **(A)** un-doped sample (commercialized by INNOVNANO), **(B)** CeO_2 doped 2YSZ, **(C)** SiO_2 and La_2O_3 doped 2YSZ.

From the obtained SEM micrographs of the samples' cross-sections, it is possible to observe that the degradation expands into the bulk of the un-doped sample. The same behaviour was observed for the ceria doped zirconia samples. In both mentioned samples it is perceptible the existence of porosity, grain pull-out and a disorganized structure, being these characteristics predominant of a monoclinic transformed region. Perceptible changes in volume occur during the phase transformations of zirconia. When expansion of grains' volume occurs, stresses are created in the surroundings of the tetragonal grains, leading them to transform too. A grain removal induced by the stress applied in the grains, creates a crater on the surface of the material (Figure 70 – A, B). On the other hand, the cross-section of both oxides (SiO_2 and La_2O_3) doped 2YSZ confirms that the degradation did not expand into the bulk. In contrast to the un-doped and CeO_2 doped zirconia samples, in this sample it is evidenced a smooth and continuous surface, without the presence of grain pull-out, characteristic of a tetragonal fraction. Hence, it is possible to confirm that the SiO_2 and La_2O_3 dopants in fact increased the ageing resistance, in comparison with the un-doped zirconia sample.

For both doped 2YSZ samples it is possible to verify the presence of porosity on the bulk of these samples (Figure 70 – B, C). This effect, once again, is related with the burn of the Teflon particles during the sintering stage.

The thickness of the degraded layer of the most affected samples (un-doped and CeO_2 doped 2YSZ sample) by hydrothermal tests is large enough to be measured. It was evaluated by the distance of the sharp uneven line from the surface until the transformed zone of the bulk for each of these aged samples (Table 24).

Table 26. Evaluation by SEM micrographs of the transformed zone depth of the monoclinic fraction layer after hydrothermal tests.

	Compositions	**5 hours**
		SEM (μm)
Control	2YSZ	5.521
Doped	2YSZ+0.50 wt% CeO_2	12.638

From those results, it can be verified that the transformed zone has greatly extended into the doped sample (CeO_2). A higher amount of monoclinic phase of zirconia, more than the required for the ISO standard (≤ 25 %), and the extension of the transformed zone (12.638 μm) was obtained for the CeO_2 doped 2YSZ sample. For these reasons, a decay of the mechanical properties of this sample was expected. In order to investigate the extension of the degradation, the mechanical properties of the doped samples after the exposition to ageing environmental tests were analyzed. In Table 27 it is possible to verify the difference of both the amount of monoclinic phase of zirconia and the evolution of the mechanical properties before and after of the hydrothermal ageing tests.

Table 27. Results of the mechanical tests for doped and un-doped 2YSZ samples before and after hydrothermal ageing.

Samples		**$ZrO_{2(monoclinic)}$ (%)**	**Hardness (HV)**	**Fracture Toughness ($MPa.m^{1/2}$)**	**Flexural Strength (MPa)**
Un-doped	Un-aged	< 5	1299	8.92	1215
	Aged	>15	>1280	~ 7.50	~ 1250
2YSZ+0.50 wt% CeO_2	Un-aged	27.49	1061	6.07	468.4
	Aged	28.9	1048.2	5.47	52.95
2YSZ+0.25 wt% SiO_2+1.07 wt% La_2O_3	Un-aged	9.37	1159	9.68	700
	Aged	9.87	1141	9.15	698

In general, a decrease of the mechanical properties of both selected samples after being submitted to environmental degradations (5 hours) was observed.

There is a clear evidence that the extension of the surface porosity into the bulk compromises the integrity of the material. In CeO_2 doped 2YSZ sample, the superficial degradation was prolonged to the inside of the bulk, leading to a substantial decline of the mechanical properties (Figure 70). These results support the previous interpretation, since a significant decrease in these properties was expected, if the degradation is prolonged into the sample's bulk.

After the ageing, there is a decay in the mechanical resistance (hardness and fracture toughness parameters) of the 2YSZ doped with ceria samples, in relation to their behaviour before this treatment (this decay was approximately 1.23 % for hardness and 9.85 % for fracture toughness, respectively), which is related with the transformability of zirconia during the period of exposition to degradation environment. It was expected that the CeO_2 dopant would lead to the improvement of the mechanical tests results, and would also provide some ageing resistance to YSZ, due the published results [46], [47]. However, due to the observed porosity in the microstructure, a density of approximately of 97 % and an amount of 27.49 % of monoclinic zirconia after sintering, makes this sample fragile. Therefore, an increase of the monoclinic zirconia occurred when this sample was submitted to a degradation environment (hydrothermal ageing test), being possible to observe that the degradation was prolonged into the sample. Due to these facts, a decrease of the mechanical resistance (hardness, fracture toughness and flexural strength) was observed. The higher decrease in flexural strength (468.39 MPa before the hydrothermal ageing to 52.95 MPa after the degradation treatment) observed for this aged sample is related with the presence of porosity and the amount of monoclinic phase of zirconia formed during the hydrothermal ageing test. The higher amount of monoclinic zirconia (28.9 %) and the porosity, made this sample more fragile. Therefore, the force required to fracture this sample is relatively lower. Several authors have mentioned that the reduction of this mechanical parameter is associated with the degradation of the sample due to the spontaneous phenomenon of transformation phases of the grains of zirconia [2], [7]. In Figure 71 an illustration of the crack indentation method carried out to a CeO_2 doped zirconia stabilized sample is presented. It is perceptible how degraded this sample is, since this sample developed more micro-cracks than it would be expected (only at the corners of the indentation), which is a characteristic of an aged sample. The poor capacity to resist to crack propagation by this doped 2YSZ sample is noticed, which is related with the low obtained values of the mechanical properties.

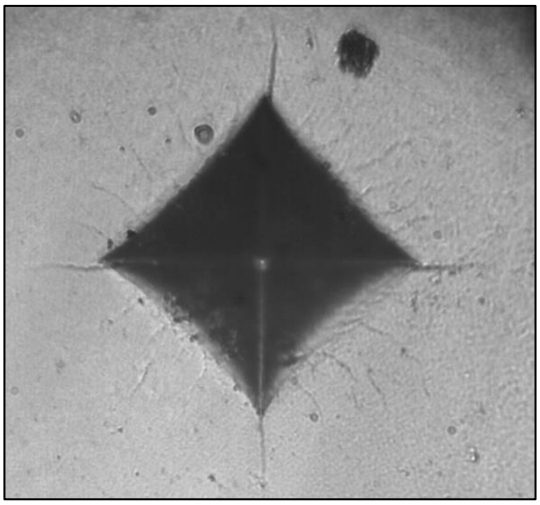

Figure 71. Illustration of crack indentation method performed at CeO_2 doped yttria stabilized zirconia.

The ageing resistance of zirconia was enhanced with the addition of both dopants (SiO_2 and La_2O_3). After hydrothermal ageing, a slight decrease of the mechanical resistance, in relation to the results obtained before degradation was observed. This slight decrease is related with the small amount of monoclinic phase of zirconia (9.87 %) formed during hydrothermal tests. Comparing all the mechanical properties presented by this sintered sample of SiO_2 with La_2O_3 doped 2YSZ before ageing, a decay of less than 5.5 % after five hours of hydrothermal tests was observed and a value higher than 500 MPa of flexural strength was obtained. Therefore, these results are also in agreement with the requirements of the ISO standard (13356:2008). In contrast, ceria doped 2YSZ sample does not satisfy the conditions required by the mentioned ISO standard. Firstly, this sample has an amount of monoclinic zirconia higher (28.9 %) than the specified by standard (≤ 25 %), a decay of mechanical resistance higher that 20 % and a flexural strength widely lower than that mentioned by referred ISO standard (≥ 500 MPa).

The sample of 2YSZ doped with both oxides, SiO_2 and La_2O_3, obtained an amount of monoclinic zirconia much lower that the un-doped zirconia (9.87 % to higher than 15 %). For this sample, a maximum value of fracture toughness of 9.15 $MPa.m^{1/2}$ was obtained while the un-doped zirconia achieved a value above 7.50 $MPa.m^{1/2}$. In relation to other mechanical parameters, such as hardness and flexural strength, a decrease was observed, which was higher for the latter parameter (698 MPa for doped sample and approximately 1250 MPa for the un-doped sample). The hardness value obtained was of 1141 HV while the und-doped sample presented a value above 1280 HV.

Throughout the hydrothermal test of silica with lanthana doped 2YSZ samples, the degradation did not progress into the bulk, which prevented the decay of the mechanical properties. Thus, the material's integrity was successfully maintained since the

degradation was restricted only at surface of this sample. Therefore, it can be assumed that the small monoclinic fraction detected by X-ray analysis is only present on the polished surface of the sample, and after five hours of ageing, no signal of serious degradation was observed. By doping 2YSZ with SiO_2 and La_2O_3, an improvement of the ageing resistance was achieved when compared with the un-doped 2YSZ sample. With this dopants implementation, the sample's mechanical properties, after 5 hours of ageing tests, were practically kept the same in relation to sample before ageing. Hence, thanks to a set of characteristics and the used preparation methods, namely, the spray dried powders, pressing and sintering, the mechanical properties after the testing time, showed only a slight decrease.

Chapter 5

Conclusion and Future Work

5. Conclusions and Future Work

The identification of the mechanism of the toughening transformation presented by zirconia brought advantages when compared with others ceramic materials. The tetragonal to monoclinic transformation presented by zirconia is the key issue for the use of zirconia bioceramics in biomedical applications (arthroplasty and dental devices). However, the disastrous happenings of Prozyr® femoral heads implants of zirconia (Saint Gobain Desmarquest) caused by their high fracture rates *in vivo,* led to various studies regarding the behaviour of zirconia ceramics, accomplished by the scientific and orthopedic communities, where a special emphasis has been given to the critical issue of zirconia's degradation. The ageing phenomenon causes an undesirable impact to biomedical devices, which compromise the implants' functionality after prolonged exposure to wet environments, in a process denominated as Low Temperature Degradation (LTD). In order to answer to this deleterious degradability of zirconia, the addition of small amounts of dopants oxides on YSZ powders, present a clear benefit for preventing ageing, while preserving its outstanding toughness and strength. Therefore, the biomedical devices require a full control of their characteristics upon the producing stages in order to maximize their mechanical properties, ageing resistance and reliability *in vivo*, to guarantee to humans a better quality of life.

In this work several dopant oxides (CeO_2, SiO_2, Al_2O_3, La_2O_3, Yb_2O_3, MnO_2), with different concentrations were used to dope the 2YSZ ceramic with the purpose to enhance its thermal ageing resistance and/or mechanical properties.

Nanostructured raw powders with a narrow particle size distribution allied to a milling and optimized spray-drying stage allowed the achievement of micrometric dense doped 2YSZ granules. One stage of pressing (uniaxial pressing) and relatively low sintering temperatures (1350 ºC and 1400 ºC (for ytterbia doped 2YSZ)) were applied and allowed the effective achievement of high density doped samples (higher than 90 % until near 99 %, regarding the theoretical values, for doped 2YSZ sintered samples). Thermal ageing tests were carried out and the amount of monoclinic zirconia (indicator of degradation) was determined after 12 and 36 hours in a laboratory furnace (at 200 ºC). A good ageing resistance for 2YSZ doped with ceria (0.50 wt%) at intermediate time of procedure of treatment was achieved. A suitable thermal ageing resistance was obtained for 2YSZ ceramics doped with ytterbia, and silica with lanthana. Although 2YSZ doped with CeO_2, SiO_2 and MnO_2 (0.025 wt% and 0.05 wt%) showed higher amounts of monoclinic zirconia, it was demonstrated that the degradation caused by ageing tests did not progressed into

the bulk. However, for the samples of zirconia doped with a higher amount of MnO_2 (0.25 wt%) it was observed that the degradation penetrates into the bulk. In addition, for the doped samples with a small grain size, good mechanical properties, specifically fracture toughness, were achieved. Although an enhancement of the ageing resistance of ytterbia doped zirconia was achieved, a decay of the mechanical properties of these samples was verified, which is related with their higher grain size (432 – 3525 nm). Relatively to the sample of zirconia doped with manganese oxide (0.25 wt%), a progression of the degradation into the bulk was observed, which led to a decrease of the sample's mechanical resistance.

The samples 2YSZ+0.50 wt% CeO_2 and 2YSZ+0.25 wt% SiO_2+1.07 wt% La_2O_3 were further selected in order to study their hydrothermal ageing resistance and mechanical properties comparatively to the un-doped 2YSZ. The spray-drying parameters were maintained and two stages of pressing (uniaxial and cold isostatic pressing) were applied, in order to attain a higher densification of these sintered doped samples. The sintering conditions were the same as the previous ones. However, a decay of the final density of both sintered doped samples, when compared with the theoretical values, was observed. This decay was related with the milling procedure of the particles, in which Teflon particles from the milling jar passed to the aqueous suspension of both compositions, causing a decrease of the samples' final density after sintering (1.71 % for 2YSZ doped with CeO_2 and 0.97 % for SiO_2 with La_2O_3, relatively to the previous prepared samples of the preliminary study). For both selected doped samples, different microstructures were observed in terms of segregation of the grains. For the sample doped with ceria the lowest density was obtained due to the presence of some surface porosity and, therefore the most accentuated decrease of the mechanical resistance was observed for this sample.

Accordingly to the literature, with the addition of CeO_2 to 2YSZ material, an enhancement of the mechanical properties, especially the fracture toughness, would be expected. However, due to the sample's surface porosity and consequent lower density combined with the higher amount of monoclinic zirconia obtained after the sintering stage (27.49 %) a decrease of the mechanical parameters was verified. A maximum of fracture toughness of 6.07 $MPa.m^{1/2}$ was obtained for CeO_2 doped 2YSZ, while the 2YSZ doped with SiO_2 and La_2O_3 achieved a value of 9.68 $MPa.m^{1/2}$.

A 5 hours hydrothermal ageing treatment was carried out for both selected doped 2YSZ samples, according with the specifications of ISO 13356:2008 (134 ± 2ºC, and 0.2 MPa).

The cross-section of the doped and un-doped samples, after this treatment, were observed by SEM. The presence of grain pull-out on the bulk of both un-doped and ceria doped 2YSZ samples was observed. The hydrothermal ageing tests demonstrated the vulnerability of these samples to Low Temperature Degradation, since a higher amount of monoclinic zirconia was detected (28.9 % for CeO_2 doped 2YSZ and a value higher than 15 % for un-doped sample), which makes that degradation to progress into the bulk. The same behaviour was not observed for the sample of zirconia doped with silica and lanthana. This sample presented a lower amount of monoclinic zirconia (9.87 %) after being submitted to a degradation environment. From this evidence it can be assumed that this doped sample successfully hindered the degradation and compelled it to the material's surface.

Concurrently, a deleterious effect on the mechanical properties of the aged ceria doped 2YSZ sample was observed. Once again, this confirmed that the sample's surface porosity and resulting lower density along with a higher amount of monoclinic phase of zirconia obtained after ageing test, makes this sample to be more fragile. The amount of monoclinic phase of zirconia and the obtained result of flexural strength (52.95 MPa) are not in accordance with the requirements reported by ISO 13356:2008, since this standard specifies that the amount of monoclinic zirconia should be equal or below 25 %, and the residual biaxial and bending strength of the aged composites should not decrease more than 20 % after this test. Nevertheless, by the obtained results of the mechanical tests on the aged samples, it was verified that the mechanical properties were practically maintained for the composition that demonstrated a good ageing resistance (SiO_2 with La_2O_3 doped 2YSZ). These results were somehow expected, since these dopants should not influence the mechanical properties, but only decelerate the tetragonal to monoclinic transformation, resulting in an improvement of the ageing resistance. These samples achieved an amount of monoclinic phase of zirconia of 9.87 %, which is much lower that the obtained for un-doped 2YSZ (higher than 15 %). For this sample, a maximum value of fracture toughness of 9.15 $MPa.m^{1/2}$ was obtained while the un-doped zirconia achieved a value above of 7.50 $MPa.m^{1/2}$. In relation to other mechanical parameters, such as hardness and flexural strength, a decrease was observed, being this decrease higher in the latter parameter (698 MPa to approximately 1250 MPa). However, between the sintering and ageing (5 hours) stages, there was a decay of less than 5.5 % on the sample's mechanical properties (hardness, fracture toughness and flexural strength). Hence, the obtained results of mechanical properties and the amount of monoclinic zirconia presented by this doped sample are in conformity to the specifications of ISO standard.

Finally it can be concluded that samples of doped 2YSZ with improved thermal ageing resistance and mechanical properties (fracture toughness) were achieved. A further study (with the doped 2YSZ samples that demonstrated the best mechanical and ageing performances) was performed in order to evaluate their hydrothermal ageing resistance and mechanical behaviour. A decrease of the mechanical properties was observed for both selected doped samples. The most promising result was obtained for the Low Temperature Degradation resistance of 2YSZ doped with SiO_2 and La_2O_3, with good density values and a fine microstructure that completely hindered the degradation. The sample's mechanical properties, after 5 hours of ageing tests, were practically kept the same in relation to the sintered sample (before ageing). By doping the zirconia sample with SiO_2 and La_2O_3, it was possible to attain a lower content of the monoclinic phase when compared with the un-doped stabilized zirconia samples.

Future Work

The obtained results throughout this study lead to a few suggestions for the continuation of this work. A continuation of this study will allow the unveiling of certain aspects that would clarify certain results and behaviour of determined samples. Therefore, some future work is suggested:

- The samples of 2YSZ doped with ytterbia exhibited a significant improvement of ageing resistance when compared with the un-doped, however the mechanical properties, due to the higher grain size, significantly decay. It is then suggested the production of this doped 2YSZ sintered at a slightly lower temperature in order to improve the mechanical properties, but maintaining the excellent ageing resistance;
- In order to guarantee the excellent characteristic of the doped 2YSZ materials, an efficient deagglomeration process must be ensured. If the selected compositions have been deagglomerated in the same equipment used with the initial samples, the problems with Teflon particles would not occur and better densifications and enhancement of the characteristics of this doped ceramics would be obtained;
- An additional stage of hot isostatic pressing is also proposed to optimize the results, by improving the densification (suppressing some remaining porosity) and in particular, to enhance the characteristics of the 2YSZ samples such as their ageing and mechanical resistances.

References

[1] C. Piconi and G. Maccauro, “Zirconia as a ceramic biomaterial,” *Biomaterials*, vol. 20, pp. 1–25, 1999.

[2] S. Deville, J. Chevalier, G. Fantozzi, J. F. Bartolomé, J. Requena, J. S. Moya, R. Torrecillas, and L. A. Díaz, “Low-temperature ageing of zirconia-toughened alumina ceramics and its implication in biomedical implants,” *J. Eur. Ceram. Soc.*, vol. 23, no. 15, pp. 2975–2982, 2003.

[3] P. Palmero, L. Montanaro, H. Reveron, and J. Chevalier, “Surface Coating of Oxide Powders: A New Synthesis Method to Process Biomedical Grade Nano-Composites,” *Materials (Basel).*, vol. 7, no. 7, pp. 5012–5037, 2014.

[4] J. Chevalier, “What future for zirconia as a biomaterial?,” *Biomaterials*, vol. 27, no. 4, pp. 535–43, 2006.

[5] J. Chevalier and L. Gremillard, “Ceramics for medical applications: A picture for the next 20 years,” *J. Eur. Ceram. Soc.*, vol. 29, no. 7, pp. 1245–1255, 2009.

[6] S. M. Kurtz, S. Kocagöz, C. Arnholt, R. Huet, M. Ueno, and W. L. Walter, “Advances in zirconia toughened alumina biomaterials for total joint replacement.,” *J. Mech. Behav. Biomed. Mater.*, vol. 31, pp. 107–16, 2014.

[7] J. Chevalier, L. Gremillard, and S. Deville, “Low-Temperature Degradation of Zirconia and Implications for Biomedical Implants,” *Annu. Rev. Mater. Res.*, vol. 37, no. 1, pp. 1–32, 2007.

[8] J. Chevalier, L. Gremillard, A. V. Virkar, and D. R. Clarke, “The Tetragonal-Monoclinic Transformation in Zirconia: Lessons Learned and Future Trends,” *J. Am. Ceram. Soc.*, vol. 92, no. 9, pp. 1901–1920, 2009.

[9] S. Lawson, “Environmental degradation of zirconia ceramics,” *J. Eur. Ceram. Soc.*, vol. 15, no. 6, pp. 485–502, 1995.

[10] C. Piconi, G. Maccauro, L. Pilloni, W. Burger, F. Muratori, and H. G. Richter, “On the fracture of a zirconia ball head,” *J. Mater. Sci. Mater. Med.*, vol. 7, pp. 289–300, 2006.

[11] M. Ferrari, A. Vichi, and F. Zarone, “Zirconia abutments and restorations: from laboratory to clinical investigations.,” *Dent. Mater.*, vol. 31, no. 3, pp. 63–76, 2015.

[12] B. and G. Gallions Reach Dental Clinic Thamesmead, “Gallions Reach Dental Clinic Thamesmead, Bexleyheath and Greenwich,” *“Category Archives: Restorative Dentistry” [online]. Availabe: http://gallionsreachdentalclinic.co.uk/dental-advice/category/restorative-dentistry/.* .

[13] “International Standard Organization No: 13356 - Ceramic materials based on yttria-stabilized tetragonal zirconia (Y-TZP),” vol. 2008. 2008.

[14] S. Saridag, O. Tak, and G. Alniacik, “Basic properties and types of zirconia: An overview,” *World J. Stomatol.*, vol. 2, no. 3, pp. 40–47, 2013.

[15] M. Mamivand, M. A. Zaeem, and H. El Kadiri, “Phase field modeling of the tetragonal-to-monoclinic phase transformation in zirconia,” *Acta Mater.*, vol. 61, pp. 5223–5235, 2013.

[16] T. Miyazaki, T. Nakamura, H. Matsumura, S. Ban, and T. Kobayashi, “Current status of zirconia restoration.,” *J. Prosthodont. Res.*, vol. 57, no. 4, pp. 236–261, 2013.

[17] P. F. Manicone, P. Rossi Iommetti, and L. Raffaelli, “An overview of zirconia ceramics: Basic properties and clinical applications,” *J. Dent.*, vol. 35, no. 11, pp. 819–826, 2007.

[18] H. Schubert and F. Frey, “Stability of Y-TZP during hydrothermal treatment: neutron experiments and stability considerations.,” *J. Eur. Ceram. Soc.*, vol. 25, no. 9, pp. 1597–1602, 2005.

[19] L. Borchers, M. Stiesch, F. W. Bach, J. C. Buhl, C. Hübsch, T. Kellner, P. Kohorst, and M. Jendras, “Influence of hydrothermal and mechanical conditions on the strength of zirconia,” *Acta Biomater.*, vol. 6, no. 12, pp. 4547–4552, 2010.

[20] S. Fabris, A. T. Paxton, and M. W. Finnis, “A stabilization mechanism of zirconia based on oxygen vacancies only,” *Acta Mater.*, vol. 50, no. 20, pp. 5171–5178, 2002.

[21] S. Deville, J. Chevalier, and L. Gremillard, “Influence of surface finish and residual stresses on the ageing sensitivity of biomedical grade zirconia,” *Biomaterials*, vol. 27, no. 10, pp. 2186–2192, 2006.

[22] E. Camposilvan and M. Anglada, “Micropillar compression inside zirconia degraded layer,” *J. Eur. Ceram. Soc.*, vol. 35, no. 14, pp. 4051–4058, 2015.

[23] C. Sanon, J. Chevalier, T. Douillard, M. Cattani-Lorente, S. S. Scherrer, and L. Gremillard, “A new testing protocol for zirconia dental implants,” *Dent. Mater.*, vol. 31, no. 1, pp. 15–25, 2015.

[24] S. Deville, H. El Attaoui, and J. Chevalier, “Atomic force microscopy of transformation toughening in ceria-stabilized zirconia,” *J. Eur. Ceram. Soc.*, vol. 25, no. 13, pp. 3089–3096, 2005.

[25] Z. K. Wu, N. Li, C. Jian, W. Q. Zhao, and J. Z. Yan, “Low temperature degradation of Al2O3-doped 3Y-TZP sintered at various temperatures,” *Ceram. Int.*, vol. 39, no. 6, pp. 7199–7204, 2013.

[26] Y. Kawai, M. Uo, Y. Wang, S. Kono, S. Ohnuki, and F. Watari, “Phase transformation of zirconia ceramics by hydrothermal degradation.,” *Dent. Mater. J.*, vol. 30, no. 3, pp. 286–292, 2011.

[27] F. Zhang, K. Vanmeensel, M. Inokoshi, M. Batuk, J. Hadermann, B. Van Meerbeek, I. Naert, and J. Vleugels, “Critical influence of alumina content on the low temperature degradation of 2-3mol% yttria-stabilized TZP for dental restorations,” *J. Eur. Ceram. Soc.*, vol. 35, no. 2, pp. 741–750, 2015.

[28] T. Kosmač and A. Kocjan, “Ageing of dental zirconia ceramics,” *J. Eur. Ceram. Soc.*, vol. 32, no. 11, pp. 2613–2622, 2012.

[29] F. Zhang, K. Vanmeensel, M. Inokoshi, M. Batuk, J. Hadermann, B. Van Meerbeek, I. Naert, and J. Vleugels, “3Y-TZP ceramics with improved hydrothermal degradation resistance and fracture toughness,” *J. Eur. Ceram. Soc.*, vol. 34, no. 10, pp. 2453–2463, 2014.

[30] J. Chevalier, B. Cales, and J. M. Drouin, “Low-Temperature Aging of Y-TZP Ceramics,” *J. Am. Ceram. Soc.*, vol. 82, no. 8, pp. 2150–2154, 1999.

[31] L. Gremillard, J. Chevalier, T. Epicier, S. Deville, and G. Fantozzi, “Modeling the aging kinetics of zirconia ceramics,” *J. Eur. Ceram. Soc.*, vol. 24, no. 13, pp. 3483–3489, 2004.

[32] Y. Takigawa, T. Shibano, Y. Kanzawa, and K. Higashi, “Effect of Small Amount of Insoluble Dopant on Tetragonal to Monoclinic Phase Transformation in Tetragonal Zirconia Polycrystal,” *Mater. Trans.*, vol. 50, no. 5, pp. 1091–1095, 2009.

[33] X. Liu, G. Lu, and Z. Yan, “Preliminary synthesis and characterization of mesoporous nanocrystalline zirconia,” *J. Nat. Gas Chem.*, vol. 12, pp. 161–166, 2003.

[34] M. Arita, Y. Takahashi, G. Pezzotti, T. Shishido, T. Masaoka, K. Sano, and K. Yamamoto, “Environmental Stability and Residual Stresses in Zirconia Femoral Head for Total Hip Arthroplasty: In Vitro Aging versus Retrieval Studies,” *Biomed Res. Int.*, vol. 2015, pp. 1–9, 2015.

[35] J. W. Christian, “The Theory of Transformations in Metals and Alloys,” *J. W. B. T.-T. of T. in. M. and A. Christian, Ed. Oxford Pergamon*, pp. 1–22, 1965.

[36] J. Schneider, S. Begand, R. Kriegel, C. Kaps, W. Glien, and T. Oberbach, “Low-Temperature Aging Behavior of Alumina-Toughened Zirconia,” *J. Am. Ceram. Soc.*, vol. 91, no. 11, pp. 3613–3618, 2008.

[37] B. Cales and J. M. Drouin, “Low-Temperature Aging of Y-TZP Ceramics,” vol. 54, pp. 2150–2154, 1999.

[38] M. Keuper, K. Eder, C. Berthold, and K. G. Nickel, “Direct evidence for continuous linear kinetics in the low-temperature degradation of Y-TZP,” *Acta Biomater.*, vol. 9, no. 1, pp. 4826–4835, 2013.

[39] F. Sommer, R. Landfried, F. Kern, and R. Gadow, “Mechanical properties of zirconia toughened alumina with 10-24vol.% 1Y-TZP reinforcement,” *J. Eur. Ceram. Soc.*, vol. 32, no. 16, pp. 4177–4184, 2012.

[40] R. C. Garvie, R. H. Hannink, and R. T. Pascoe, “Ceramic steel?,” *Nature*, vol. 258, no. 5537, pp. 703–704, 1975.

[41] I. Denry and J. R. Kelly, “State of the art of zirconia for dental applications,” *Dent. Mater.*, vol. 24, no. 3, pp. 299–307, 2008.

[42] D. J. Kim, H. J. Jung, J. W. Jang, and H. L. Lee, “Fracture Toughness, Ionic Conductivity, and Low-Temperature Phase Stability of Tetragonal Zirconia Codoped with Yttria and Niobium Oxide,” *J. Am. Ceram. Soc.*, vol. 14, pp. 2309–2314, 1998.

[43] J.W.Martin, *Concise Encyclopedia of the Structure of Materials, 1st Edition*. Amsterdam, 2007.

[44] G. Witz, V. Shklover, W. Steurer, S. Bachegowda, and H. P. Bossmann, “Phase Evolution in Yttria-Stabilized Zirconia Thermal Barrier Coatings Studied by Rietveld Refinement of X-Ray Powder Diffraction Patterns,” *J. Am. Ceram. Soc.*, vol. 90, no. 9, pp. 2935–2940, 2007.

[45] L. Li, O. Van Der Biest, P. Wang, J. Vleugels, W. W. Chen, and S. Huang, “Estimation of the phase diagram for the ZrO2 – Y2O3 – CeO2 system,” *J. Eur. Ceram. Soc.*, vol. 21, pp. 2903–2910, 2001.

[46] N. A. Rejab, A. Z. A. Azhar, M. M. Ratnam, and Z. A. Ahmad, “The effects of CeO2 addition on the physical, microstructural and mechanical properties of yttria stabilized zirconia toughened alumina (ZTA),” *Int. J. Refract. Met. Hard Mater.*, vol. 36, pp. 162–166, 2013.

[47] D. Ragurajan, M. Satgunam, and M. Golieskardi, “The Effect of Cerium Oxide Addition on the Properties and Behavior of Y-TZP,” *Int. Sch. Res. Not.*, vol. 2014, pp. 1–5, 2014.

[48] R. V. Mangalaraja, B. K. Chandrasekhar, and P. Manohar, “Effect of ceria on the physical, mechanical and thermal properties of yttria stabilized zirconia toughened alumina,” *Mater. Sci. Eng. A*, vol. 343, no. 1–2, pp. 71–75, 2003.

[49] M. T. Hernandez, J. R. Jurado, P. Duran, and J. L. G. Fierro, “Subeutectoid degradation of yttriastabilized tetragonal zirconia polycrystal and ceria-doped yttria-stabilized tetragonal zirconia polycrystal ceramics,” *J Am Ceram Soc*, vol. 74, no. 6, pp. 1254–8, 1991.

[50] S. Ramesh, W. J. K. Chew, C. Y. Tan, J. Purbolaksono, A. M. Noor, M. A. Hassan, U. Sutharsini, M. Satgunam, W. D. Teng, M. Oxide, and M. Properties, “Influence of Manganese on the sintering properties of tetragonal zirconia,” *Ceram. - Silikaty*, vol. 57, no. 1, pp. 28–32, 2013.

[51] S. Ramesh, S. Meenaloshini, C. Y. Tan, W. J. K. Chew, and W. D. Teng, “Effect of manganese oxide on the sintered properties and low temperature degradation of Y-TZP ceramics,” *Ceram. Int.*, vol. 34, no. 7, pp. 1603–1608, 2008.

[52] H. Zhou, J. Li, D. Yi, and L. Xiao, “Effect of manganese oxide on the sintered properties of 8YSZ,” *Phys. Procedia*, vol. 22, pp. 14–19, 2011.

[53] A. A. Nogiwa-Valdez, W. M. Rainforth, P. Zeng, and I. M. Ross, “Deceleration of hydrothermal degradation of 3Y-TZP by alumina and lanthana co-doping,” *Acta Biomater.*, vol. 9, no. 4, pp. 6226–6235, 2013.

[54] S.-L. Hwang and I. W. Chen, “Grain Size Control of Tetragonal Zirconia Polycrystals Using the Space Charge Concept,” *J. Am. Ceram. Soc.*, vol. 73, no. 11, pp. 3269–3277, 1990.

[55] F. Zhang, K. Vanmeensel, M. Batuk, J. Hadermann, M. Inokoshi, B. Van Meerbeek, I. Naert, and J. Vleugels, “Highly-translucent, strong and aging-resistant 3Y-TZP ceramics for dental restoration by grain boundary segregation,” *Acta Biomater.*, vol. 16, pp. 215–222, 2015.

[56] T. Nakamura, H. Usami, H. Ohnishi, M. Takeuchi, H. Nishida, T. Sekino, and H. Yatani, “The effect of adding silica to zirconia to counteract zirconia’s tendency to degrade at low temperatures.,” *Dent. Mater. J.*, vol. 30, no. 3, pp. 330–335, 2011.

[57] L. Gremillard, J. Chevalier, T. Epicier, and G. Fantozzi, “Improving the Durability of a Biomedical-Grade Zirconia Ceramic by the Addition of Silica,” *J. Am. Ceram. Soc.*, vol. 85, no. 2, pp. 401–7, 2002.

[58] Y. J. Lin, P. Angelini, and M. L. Mecartney, “Microstructural and Chemical Influences of Silicate Grain-Boundary Phases in Yttria-Stabilized Zirconia,” *J. Am. Ceram. Soc.*, vol. 73, no. 9, pp. 2728–2735, 1990.

[59] L. Gremillard, T. Epicier, J. Chevalier, and G. Fantozzi, “Microstructural study of silica-doped zirconia ceramics,” *Acta Mater.*, vol. 48, no. 18–19, pp. 4647–4652, 2000.

[60] A. Samodurova, A. Kocjan, M. V. Swain, and T. Kosmač, “The combined effect of alumina and silica co-doping on the ageing resistance of 3Y-TZP bioceramics,” *Acta Biomater.*, vol. 11, pp. 477–487, 2015.

[61] S. N. B. Hodgson and J. Cawley, “The effect of titanium oxide additions on the properties and behaviour of Y-TZP,” *J. Mater. Process. Technol.*, vol. 119, no. 1–3, pp. 112–116, 2001.

[62] M. Zhao, X. Ren, and W. Pan, “Effect of Lattice Distortion and Disordering on the Mechanical Properties of Titania-Doped Yttria-Stabilized Zirconia,” *J. Am. Ceram. Soc.*, vol. 97, no. 5, pp. 1566–1571, 2014.

[63] S. Lawson, C. Gill, and G. P. Dransfield, “The effects of copper and iron oxide additions on the sintering and properties of Y-TZP,” *J. Mater. Sci.*, vol. 30, no. 12, pp. 3057–3060, 1995.

[64] S. Ramesh, J. Purbolaksono, M. Hamdi, I. Sopyan, R. Tolouei, M. Amiriyan, F. Tarlochan, and W. D. Teng, “Low-temperature degradation (LTD) behaviour of CuO-doped tetragonal zirconia ceramic,” *Ceram. - Silikaty*, vol. 56, no. 1, pp. 15–19, 2012.

[65] Y. Kan, G. Zhang, P. Wang, O. Van der Biest, and J. Vleugels, “Yb2O3 and Y2O3 co-doped zirconia ceramics,” *J. Eur. Ceram. Soc.*, vol. 26, pp. 3607–3612, 2006.

[66] Y. D. Cho, J. C. Shin, H. L. Kim, M. Gerelmaa, H. I. Yoon, H. M. Ryoo, D. J. Kim, and J. S. Han, “Comparison of the osteogenic potential of titanium and modified zirconia-based bioceramics,” *J. Int. Mol. Sci.*, vol. 15, no. 3, pp. 4442–4452, 2014.

[67] M. Golieskardi, M. Satgunamb, D. Ragurajanc, and D. Namasivayamd, “Sintering and Densification Behavior of Nb2O5-doped Y-TZP Ceramics,” 2014, pp. 26–30.

[68] H. Zhao, X. Li, F. Ju, and U. Pal, “Effects of particle size of 8mol% Y2O3 stabilized ZrO2 (YSZ) and additive Ta2O5 on the phase composition and the microstructure of sintered YSZ electrolyte,” *J. Mater. Process. Technol.*, vol. 200, no. 1–3, pp. 199–204, 2008.

[69] H. Kawahara, S. Ochi, K. Tanetani, K. Kato, M. Isogai, Y. Mizuno, H. Yamamoto, and A. Yamagami, “Biological test of dental biomaterials, effect of pure metals upon the mouse subcutaneous fibroblast, strain L cell in tissue cultura,” *Japan Soc. Dent. Appar. Mater*, no. 4, pp. 65–85, 1963.

[70] S. G. Steinemann, “Corrosion of Surgical Implants—In vivo and in vitro Tests, Evaluation of Biomaterials,” *Wiley New York, NY, USA,* pp. 1–34, 1980.

[71] R. Olivares-Navarrete, J. J. Olaya, C. Ramírez, and S. E. Rodil, “Biocompatibility of Niobium Coatings,” *Coatings*, vol. 1, no. 1, pp. 72–87, 2011.

[72] D. M. Findlay, K. Welldon, G. J. Atkins, D. W. Howie, A. C. W. Zannettino, and D. Bobyn, “The proliferation and phenotypic expression of human osteoblasts on tantalum metal,” *Biomaterials*, vol. 25, no. 12, pp. 2215–2227, 2004.

[73] J. D. Bobyn, K. K. Toh, S. A. Hacking, M. Tanzer, and J. J. Krygier, “Tissue response to porous tantalum acetabular cups: A canine model,” *J. Arthroplasty*, vol. 14, no. 3, pp. 347–354, 1999.

[74] U. Sankar, S. Meenaloshini, A. Mahdi, S. Ramesh, and W. D. Teng, “Mechanical Properties of Niobium Oxide Doped Y-TZP for Biomedical Applications,” *Solid State Sci. Technol.*, vol. 19, no. 2, pp. 232–241, 2011.

[75] S. Kanchana and S. Hussain, “Zirconia a Bio-inert Implant Material,” *J. Dent. Med. Sci.*, vol. 12, no. 6, pp. 66–67, 2013.

[76] V. Covacci, N. Bruzzese, G. Maccauro, C. Andreassi, G. A. Ricci, C. Piconi, E. Marmo, W. Burger, and A. Cittadini, “In vitro evaluation of the mutagenic and carcinogenic power of high purity zirconia ceramic,” *Biomaterials*, vol. 20, pp. 371–376, 1999.

[77] H. Warashina, S. Sakano, S. Kitamura, K. I. Yamauchi, J. Yamaguchi, N. Ishiguro, and Y. Hasegawa, “Biological reaction to alumina, zirconia, titanium and polyethylene particles implanted onto murine calvaria,” *Biomaterials*, vol. 24, no. 21, pp. 3655–3661, 2003.

[78] E. Kobayashi, S. Matsumoto, H. Doi, T. Yoneyama, and H. Hamanaka, “Mechanical properties of the binary titanium-zirconium alloys and their potential for biomedical materials,” *J. Biomed. Mater. Res.*, vol. 29, no. 8, pp. 943–950, 1995.

[79] I. Dion, L. Bordenave, and F. Lefebre, “Physico-chemistry and cytotoxicity of ceramics Part II Cytotoxicity of ceramics,” *J. Mater. Sci. Mater. Med.*, vol. 5, pp. 18–24, 1994.

[80] J. Li, Y. Liu, L. Hermansson, and R. Soremark, “Evaluation o biocompatibility of various ceramic powders with human fibroblasts in vitro,” *Clin. Mater.*, vol. 12, no. 4, pp. 197–201, 1993.

[81] R. J. Kohal, W. Att, M. Bächle, and F. Butz, “Ceramic abutments and ceramic oral implants. An update,” *Periodontol. 2000*, vol. 47, no. 1, pp. 224–243, 2008.

[82] O. Roualdes, M. E. Duclos, D. Gutknecht, L. Frappart, J. Chevalier, and D. J. Hartmann, “In vitro and in vivo evaluation of an alumina-zirconia composite for arthroplasty applications,” *Biomaterials*, vol. 31, no. 8, pp. 2043–2054, 2010.

[83] M. Kuntz, “Live-Time Prediction of BIOLOX® delta,” *Bioceramics Alternative Bearings in Joint. Arthroplasty SE - 39, J.-D. Chang K. Billau, Eds. Steinkopff.*, pp. 281–288, 2007.

[84] C. Vermes, K. A. Roebuck, R. Chandrasekaran, J. G. Dobai, J. J. Jacobs, and T. T. Glant, “Particulate wear debris activates protein tyrosine kinases and nuclear factor kappaB, which down-regulates type I collagen synthesis in human osteoblasts.,” *J. Bone Miner. Res.*, vol. 15, no. 9, pp. 1756–1765, 2000.

[85] C. Vermes, R. Chandrasekaran, J. J. Jacobs, J. O. Galante, K. A. Roebuck, and T. T. Glant, “The Effects of Particulate Wear Debris, Cytokines, and Growth Factors on the Functions of MG-63 Osteoblasts.,” *J. Bone Jt. Surgery.*, vol. 83, no. 2, p. 201, 2001.

[86] J. Chevalier, J. M. Drouin, and B. Cales, “Low temperature ageing behavior of zirconia hip joint heads,” *Bioceram. Int. Symp. Ceram. Med., 10th*, pp. 135–138, 1997.

[87] A. H. De Azaa, J. Chevaliera, G. Fantozzia, M. Schehlb, and R. Torrecillas, “Crack growth resistance of alumina, zirconia and zirconia toughened alumina ceramics for joint prostheses,” *Biomaterials*, vol. 23, no. 3, pp. 937–945, 2002.

[88] R. Depprich, H. Zipprich, M. Ommerborn, C. Naujoks, H.-P. Wiesmann, S. Kiattavorncharoen, H.-C. Lauer, U. Meyer, N. R. Kübler, and J. Handschel, “Osseointegration of zirconia implants compared with titanium: an in vivo study.,” *Head Face Med.*, vol. 4, no. 1, p. 30, 2008.

[89] S. G. Steinemann, “Titanium—the material of choice?,” *Periodontol 2000*, no. 17, pp. 7–21, 1998.

[90] Z. Özkurt and E. Kazazoğlu, “Zirconia Dental Implants: A Literature Review,” *J. Oral Implantol.*, vol. 37, no. 3, pp. 367–76, 2011.

[91] Y. Ji, X. D. Zhang, X. C. Wang, Z. C. Che, X. M. Yu, and H. Z. Yang, “Zirconia bioceramics as all-ceramics crowns material: A review,” *Rev. Adv. Mater. Sci.*, vol. 34, pp. 72–78, 2013.

[92] Y. Ichikawa, Y. Akagawa, H. Nikai, and H. Tsuru, “Tissue compatibility and stability of a new zirconia ceramic in vivo,” *J. Prosthet. Dent.*, vol. 68, no. 2, pp. 322–326, 1992.

[93] L. Sennerby, A. Dasmah, B. Larsson, and M. Iverhed, “Bone Tissue Responses to Surface-Modified Zirconia Implants: A Histomorphometric and Removal Torque Study in the Rabbit,” *Clin. Implant Dent. Relat. Res.*, vol. 7, Suppl 1, pp. S13–S20, 2005.

[94] T. Albrektsson, P.-I. Brånemark, H.-A. Hansson, and J. Lindström, “Osseointegrated Titanium Implants: *Requirements for Ensuring a Long-Lasting, Direct Bone-to-Implant Anchorage in Man*,” *Acta Orthop. Scand.*, vol. 52, no. 2, pp. 155–170, 1981.

[95] T. R. Ramesh, M. Gangaiah, P. V. Harish, U. Krishnakumar, and B. Nandakishore, “Zirconia Ceramics as a Dental Biomaterial - An Over view,” *Trends Biomater. Artif. Organs*, vol. 26, no. 3, pp. 154–160, 2012.

[96] L. Rimondini, L. Cerroni, A. Carrassi, and P. Torricelli, “Bacterial Colonization of Zirconia Ceramic Surfaces: An in Vitro and in Vivo Study,” *Int. J. Oral Maxillofac. Implants*, vol. 17, no. 6, pp. 793–8, 2002.

[97] S. C. Singhal, “Zirconia Electrolyte Based Fuel Cells,” 2001.

[98] S. C. Singhal, “Solid Oxide Fuel Cells,” *Electrochem. Soc. Interface*, pp. 41–44, 2007.

[99] C. Zuo, M. Liu, and M. Liu, *Sol-Gel Processing for Conventional and Alternative Energy, Advances in Sol-Gel Derived Materials and Technologies. Chapter 2 - Solid Oxide Fuel Cells*. 2012.

[100] R. Krishnamurthy and D. J. Srolovitz, “Sintering and microstructure evolution in columnar thermal barrier coatings,” *Acta Mater.*, vol. 57, no. 4, pp. 1035–1048, 2009.

[101] M. Instruments, “Zeta potential: An Introduction in 30 minutes,” *Zetasizer Nano Serles Technical Note. MRK654-01*, vol. 2, pp. 1–6, 2011.

[102] Malvern Instruments Ltd, “ZETASIZER Nano Series brochure.” pp. 1–20, 2011.

[103] A. Sosnik and K. P. Seremeta, “Advantages and challenges of the spray-drying technology for the production of pure drug particles and drug-loaded polymeric carriers,” *Adv. Colloid Interface Sci.*, vol. 223, pp. 40–54, 2015.

[104] R. Wisniewski, “Spray Drying Technology Review,” 2015, July, pp. 1–46.

[105] C. Arpagaus, N. Schafroth, and M. Meuri, “Laboratory Scale Spray Drying of Lactose: A Review,” *Information Bulletin Büchi Switzerland*, no. 57. pp. 1–12, 2010.

[106] Büchi Labortechnik AG, “Training Papers Spray Drying,” *Training papers*. pp. 1–19, 2002.

[107] T. Sato and M. Shimada, “Crystal Phase Change in Yttria-Partially-Stabilized Zirconia by Low-Temperature Annealing,” *J. Am. Ceram. Soc.*, vol. 67, no. 10, p. C-212--C-213, 1984.

[108] T. Sato and M. Shimada, “Transformation of Yttria-Doped Tetragonal Zr02 Polycrystals by Annealing in Water,” *J. Am. Ceram. Soc.*, vol. 68, no. 6, pp. 356–359, 1985.

[109] T. Sato and M. Shimada, “Control of the Tetragonal-to-Monoclinic Phase Transformation of Yttria Partially Stabilized Zirconia in Hot Water,” *J. Mater. Sci.*, vol. 20, no. 11, pp. 3988–3992, 1985.

[110] T. Vagkopoulou, S. O. Koutayas, P. Koidis, and J. R. Strub, “Zirconia in dentistry: Part 1. Discovering the nature of an upcoming bioceramic.,” *Eur. J. Esthet. Dent.*, vol. 4, no. 2, pp. 130–151, 2009.

[111] J. Cotič, P. Jevnikar, A. Kocjan, and T. Kosmač, “Complexity of the relationships between the sintering-temperature-dependent grain size, airborne-particle abrasion, ageing and strength of 3Y-TZP ceramics,” *Dent. Mater.*, vol. 32, no. 4, pp. 510–518, 2016.

[112] G. Maccauro, P. Iommetti, L. Raffaelli, and P. Manicone, *Alumina and Zirconia Ceramic for Orthopaedic and Dental Devices*, Chapter 15. 2011.

[113] Masaki T., Int J High Technol Ceram., no. 2, pp. 85–98, 1986.

[114] K. Niihara, “A fracture mechanics analysis of indentation-induced Palmqvist crack in ceramics,” *J. Mater. Sci. Lett.*, vol. 2, no. 5, pp. 221–223, 1983.

[115] Malvern Instruments Ltd, “Sample dispersion and refractive index guide Reference manual.” 2000.

[116] S. R. Cullity, B. D. and Stock, *Elements of X-Ray Diffraction. Third edition*, 1986.

[117] William D. Callister, *FUNDAMENTALS OF MATERIALS SCIENCE AND ENGINEERING: An Integrated Approach. International 3rd Edition. John Wiley & Sons Inc*. 2008.

[118] D. K. Schroder, *Semiconductor Material and Device Characterization. Third edition*.

[119] S. Brunauer, P. H. Emmett, and E. Teller, “Adsorption of Gases in Multimolecular Layers,” *J. Am. Chem. Soc.*, vol. 60, no. 2, pp. 309–319, 1938.

[120] P. A. Webb, *Analytical methods in fine particle technology. First edition.* Published 1997 by Micromeritics Instrument Corporation.

[121] E.Y.H. Keng, “Air and helium pycnometer,” *Powder Tecnol.*, vol. 3, no. 3, pp. 179–180, 1969.

[122] D. K. Schroder, *MATERIAL AND DEVICE SEMICONDUCTOR MATERIAL AND DEVICE Third Edition*, vol. 44, no. 4. 2006.

[123] P. Brouwer, *Theory of XRF*. 2010.

[124] R. L. Fullman, “Measurement of particle size in opaque bodies,” *Trans. Met. Soc. AIME*, vol. 197, p. 447, 1953.

[125] S. S. Scherrer, I. L. Denry, and H. W. Wiskott, “Comparison of three fracture toughness testing techniques using a dental glass and a dental ceramic.,” *Dent. Mater.*, vol. 14, no. 4, pp. 246–255, 1998.

[126] G. Bertrand, P. Roy, C. Filiatre, and C. Coddet, “Spray-dried ceramic powders: A quantitative correlation between slurry characteristics and shapes of the granules,” *Chem. Eng. Sci.*, vol. 60, no. 1, pp. 95–102, 2005.

[127] F. F. Lange, “Powder processing science and technology for increased reliability,” *J. Am. Ceram. Soc.*, vol. 72, no. 1, pp. 3–15, 1989.

[128] Marx, D. and Murphy, R., “Sputtering targets: Challenges for the 1990s.,” *Solid State technol.*, vol. 33, no. 3, p. S11, 1990.

[129] Friz, M. and Waibel, F., “Coating Materials,” *Opt. Interf. Coatings*, vol. 88, pp. 105–130.

[130] J. Cotič, P. Jevnikar, A. Kocjan, and T. Kosmač, “Complexity of the relationships between the sintering-temperature-dependent grain size, airborne-particle abrasion, ageing and strength of 3Y-TZP ceramics.,” *Dent. Mater.*, vol. 32, no. 4, pp. 510–518, 2016.

[131] J. Li, Z. Tang, Z. Zhang, and S. Luo, “Study of factors influencing the microstructure and phase content of ultrafine Y-TZP,” *Mater. Sci. Eng. B Solid-State Mater. Adv. Technol.*, vol. 99, no. 1–3, pp. 321–324, 2003.

[132] V. Naglieri, D. Gutknecht, V. Garnier, P. Palmero, J. Chevalier, and L. Montanaro, “Optimized Slurries for Spray Drying: Different Approaches to Obtain Homogeneous and Deformable Alumina-Zirconia Granules,” *Materials (Basel).*, vol. 6, no. 11, pp. 5382–5397, 2013.

[133] C. L. Yang, H. I. Hsiang, and C. C. Chen, “Characteristics of yttria stabilized tetragonal zirconia powder used in optical fiber connector ferrule,” *Ceram. Int.*, vol. 31, no. 2, pp. 297–303, 2005.

[134] S.-D. Kim and K.-S. Hwang, “Crystallinity, Microstructure and Mechanical Strength of Yttria-Stabilized Tetragonal Zirconia Ceramics for Optical Ferrule,” *Mater. Sci. Appl.*, vol. 2, no. 1, pp. 1–5, 2011.

[135] P. Kohorst, L. Borchers, J. Strempel, M. Stiesch, T. Hassel, F. W. Bach, and C. Hübsch, “Low-temperature degradation of different zirconia ceramics for dental applications,” *Acta Biomater.*, vol. 8, no. 3, pp. 1213–1220, 2012.

[136] M. J. Mayo, “Processing of nanocrystalline ceramics from ultrafine particles,” *Int. Mater. Rev.*, vol. 41, no. 3, pp. 85–115, 1996.

[137] A. Krell and J. Klimke, “Effects of the homogeneity of particle coordination on solid-state sintering of transparent alumina,” *J. Am. Ceram. Soc.*, vol. 89, no. 6, pp. 1985–1992, 2006.

[138] D. W. Richerson, *Modern ceramic engineering – properties, processing and use in design.* Third Edition. Chaper 13. Published 2006 by CRC Press – Taylor & Francis group.

[139] R. Riedel and I.-W. Chen, *Ceramics science and technology: Volume 3: Synthesis and processing. First edition*.